UNIVERSITA' DEGLI STUDI DI VERONA

DEPARTMENT OF
NEUROSCIENCE, BIOMEDICINE AND MOVEMENT SCIENCES

GRADUATE SCHOOL OF
LIFE AND HEATH SCIENCES

DOCTORAL PROGRAM IN
NEUROSCIENCE, PSYCHOLOGICAL AND PSYCHIATRIC SCEINCES,
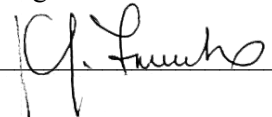*AND MOVEMENT SCIENCES*

With the financial contribution of
University of Verona

Cycle XXXIII / Year 2017

NEUROPSYCHOLOGICAL AND BEHAVIORAL STUDIES ON

OBJECT GRASPING IN HUMANS WITH AND WITHOUT VISION

S.S.D. M-PSI/02

Coordinator: Prof. Gianluigi Zanusso

Signature _____

Tutor: Prof. Luigi Cattaneo

Signature _____

Doctoral Student: Dott.ssa Martina Pirruccio

Signature _____

TABLE OF CONTENTS

List of figures

Chapter 4:   Gaze direction influences grasping actions towards unseen, haptically explored, objects

List of tables

x

Chapter 1

Sensorimotor transformations for actions

When we interact with our surroundings in everyday life, we rely on sensory information that are continuously encoded in our brain and used to plan our own actions and control them online. Basically, we can say that interactions with the external environment are allowed by perception. For example, if we think of the movement necessary to grasp and manipulate a full bottle, a glass or a pen, we know that for each object we are used to execute specific motor plans which differ in grip configuration and grip force, as well as the force employed by the whole arm. Despite we carry out several motor plans in a continuous and automatic way, the brain does not passively process sensory inputs; instead, it implements the so-called sensorimotor transformations necessary to provide the motor output suited to the goal of the movement. Therefore, sensory information is re-coded and translated in further reference systems along cortical dynamic networks in order to create internal models as a substrate for actions, as well as to orchestrate and update sensory-based movements. In other words, the brain uses sensorimotor transformations to translate sensory inputs from the outside to motor instructions towards the outside (Cisek, 2007; Cisek & Kalaska, 2010; Huda et al., 2019;

Rizzolatti & Luppino, 2001). Here we focus on the cortical underpinning of these sensorimotor transformations and how they modulate the motor behavior.

1.1. The organization of parietal and premotor areas in monkeys

Decades of research highlighted that sensorimotor transformations involve complex, specific and reciprocal connections between parietal and motor areas (Borra et al., 2017; Rizzolatti & Matelli, 2003; Turella & Lingnau, 2014). The key evidence on this parieto-frontal network arise from investigations conducted in monkey, that is the experimental subject phylogenetically closest to humans and allows to provide reliable cortical maps adaptable to human models (Caminiti et al., 2015; Mantini et al., 2012; Orban, 2016; Sereno & Tootell, 2005). For monkeys, research mostly adopted the single cell recording technique, an electrophysiological technique able to detect the activation of single neuronal cells, allowing to clearly identify neurons activated during specific motor tasks (Criado et al., 2008).

The posterior parietal cortex (PPC) of monkey is subdivided in superior (SPL) and inferior parietal lobule (IPL) and intraparietal area (IP), and it is considered the associative area by definition, crucial for multisensorial integration for space perception and processing, as well as body schema representation (Andersen, 1997; Sakata et al., 1995). Indeed, each parietal sector is organized in several anatomically and functionally distinct areas containing specific maps of the personal, peripersonal and extrapersonal space relative to the control of specific effectors (Borra & Luppino, 2017; Bracci & Peelen, 2013; Rizzolatti & Luppino, 2001; Rizzolatti et al., 1998; Rozzi et al., 2008). In reach-to-grasp movements, the spatial processing of PPC is the main carrier of the guidance of motor behavior, as it is responsible for the coordination of hand and translation of sensory information into coordinate systems in which

these movements can be performed (Caminiti et al., 2015; Crawford et al., 2011; Gail & Andersen, 2006; Rizzolatti et al., 1998). Indeed, several lesion and single cell recording studies proved that neurons of PPC are activated during reaching and that a parietal damage leads to deficits of spatial coding (optic ataxia, neglect), as well as marked inaccuracy on the directing the limb and the grasping performing (Balan & Gottlieb, 2009; Battaglini et al., 2002; Faugier-Grimaud et al., 1985; Padberg et al., 2010).

Similarly to PPC, also the premotor cortex (PMC) is organized in several structurally and functionally independent areas, such as the dorsal (PMd) and the ventral premotor cortex (PMv) and the supplementary motor area (SMA). Altogether, the main aim of PMC is to elaborate motor instructions (e.g., information about the effector that need to be used for action and the geometric properties of the target object) to be sent to the primary motor cortex (M1) using body-centered frames of reference (Beurze et al., 2007; Hoshi & Tanji, 2000; Nakayama et al., 2008; Schubotz & Von Cramon, 2003). As regards the reach-to-grasp movements, some authors pointed out that the reaching and the grasping components are differentially coded by PMd and PMv respectively. In fact, activation of PMd (area F2vr) is linked to arm movements directed towards specific space locations, while PMv, in particular area F5, seems to code specific types of hand shaping for grasping (e.g., precision grip, whole-hand prehension) and, generally, specific actions. Indeed, F5 has been proposed as the center of the "motor vocabulary", namely a storage of the motor acts known by the monkey (Hepp-Reymond et al., 1994; Hoshi & Tanji, 2000; Jeannerod et al., 1995; Rizzolatti et al., 1988; Rizzolatti & Luppino, 2001; Rizzolatti et al., 1998).
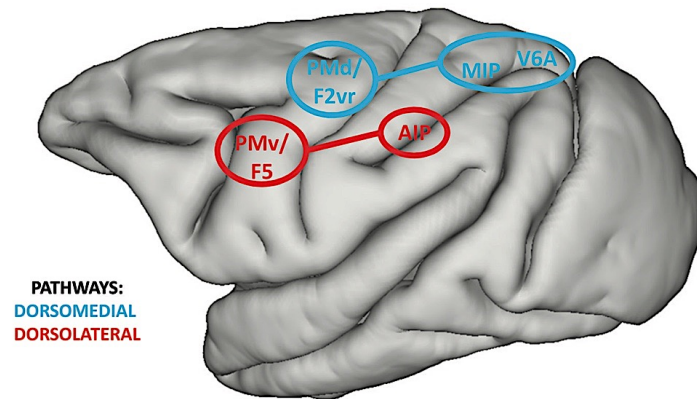
Figure 1. Schematic representation of the two dorsal pathways in monkey (adapted from Turella & Lingnau, 2014)
Parieto-frontal connections are topographically determined, so that regions within IPL (AIP) target ventral premotor areas (PMv/F5) and portions of SPL (MIP and V6A) interact with dorsal premotor areas (PMd/F2vr). The dorsomedial (blue) and the dorsolateral (red) pathways mediate the reaching and the grasping component respectively.

1.1.1. Parieto-frontal connections in monkeys

It is well known that sensorimotor transformations are mediated by reciprocal parieto-frontal connections with the aim to send sensory information to the premotor region in order to provide the ideal motor command to interact with the external. Actually, these networks are part of the visual dorsal stream projecting from visual striate cortices to PPC, crucial for the spatial coding of the target object; (N. R. Cohen et al., 2009; Milner & Goodale, 2008). Once the structural and functional subdivision of PPC and PMC was studied, it became clear that parieto-frontal connections are topographically organized so that parietal areas are connected to premotor regions with similar properties; hence, SPL is mostly linked to PMd and IPL to PMv (Borra et al., 2008; Borra & Luppino, 2017; Caminiti et al., 1998, 2015; Davare et al., 2011; Johnson et al., 1996; Rizzolatti & Luppino, 2001; Wise et al., 1997). For this reason, a subdivision of the visual dorsal stream in a dorsomedial (including visual area V6A, the medial part of the intraparietal sulcus (MIP) and PMd) and a dorsolateral (connecting the anterior part

of the intraparietal sulcus (AIP) with PMv) pathway has been proposed (Figure 1). The dorsomedial connection contains maps of the space around us, associated with reaching movements for controlling the upper limb position in the space. On the other hand, the dorsolateral network subserves the grasping component and it's responsible of the transformation of object intrinsic properties (e.g., shape, size, orientation) into the appropriate motor commands for the hand pre-shaping (Brochier & Umiltà, 2007; Fluet et al., 2010; Gail & Andersen, 2006; Galletti & Fattori, 2018; Karl & Whishaw, 2013; Rizzolatti & Matelli, 2003; Santandrea et al., 2018; Turella & Lingnau, 2014). As a matter of fact, the neural underpinnings of the sensorimotor transformations could be located in visuomotor neurons of both AIP and PMv, showing selective responses for geometric properties of target objects, such as size (Bonini et al., 2014a; Murata et al., 2000; Rizzolatti & Matelli, 2003; Verhagen et al., 2008). In support of this, Gallese and collogues (1994) demonstrated that the pharmacological inactivation of AIP in monkey leads to grasping impairments resulting in a mismatch between hand pre-shaping and the real size of the target object. Crucially, deficit of hand configuration was observed during precision grasping, which is supposed to demand more elaborate sensorimotor conversions, but not during whole-hand prehension. Analogously, inactivation of area F5 leads to similar deficits in hand shaping that are more evident for smaller objects (Fogassi et al., 2001; Matsumura et al., 1991). Altogether, these data suggest that neurons of these areas are active when more precise and accurate sensorimotor transformations are required. Actually, it is plausible that reaching and grasping rely on different neural bases, since only grasping requires specific processing of sensory information to pre-shape the hand. Moreover, these data support the idea that the efficiency of the sensorimotor processes mediated by AIP-PMv connections is reflected on the observable and measurable motor behavior, namely hand kinematics during reaching. In this view, hand shaping during movements and eventual

5

configuration errors are the direct expression of the shift from sensory inputs to body-centered motor instructions, namely sensorimotor transformations.

1.2. Sensorimotor transformation in humans

Despite the gap between monkey and human due to 30 million years of independent evolution, many comparative investigations confirm that monkey and human brains share common anatomical and functional maps of sensory, motor and associative functions (Caminiti et al., 2015; Mantini et al., 2012; Orban, 2016; Sereno & Tootell, 2005). Clearly, given its invasive nature, the use of the single cell recording is not viable way in research in humans; consequently, more indirect measures have been adopted, such as electrophysiological indexes (electroencephalography or electromyography), neuroimaging (structural and functional MRI, PET, DTI) or non-invasive transcranial stimulation techniques (tDCS, TMS).

Human PPC shows similar subdivision to monkey parietal region, hence it consists of SPL, IPL and IP. Crucially, human parietal activity has been linked to spatial coding and control of the movement in the three-dimensional environment; such parietal involvement has been largely confirmed by lesional data. For instance, patients with parietal lesions, especially IPL, show hemispatial neglect symptoms consisting of spatial attention disorders which, according to the damaged parietal subregion, concern personal, peripersonal or extrapersonal space and egocentric or allocentric frames of reference (Husain & Nachev, 2006; Mesulam, 1999; Shinoura et al., 2009; Vuilleumier, 2013). Optic ataxia (also called misreaching) is a deficit following lesions of medial parieto-occipital cortex which affects reaching and grasping movements performed with upper limb towards a given spatial direction (Jakobson et al., 1991; Karnath & Perenin, 2005). In line with this, virtual lesions induced by transcranial magnetic stimulation (TMS) applied over the medial PPC containing the putative human homolog of

macaque area V6A caused deviation of the upper limb's direction (Civarro et al., 2013; Van Donkelaar & Adams, 2005; Vesia et al., 2010) and depth (Breveglieri et al., 2020) during reaching movements similarly to patients with optic ataxia. Finally, PPC lesions could led to topographical disorientation, a neuropsychological disorder in which patient are not able to orient and find their way in familiar environments (Aguirre & D'Esposito, 1999; Wilson et al., 2005). It is well clear that all these syndromes are characterized by spatial coding and motor control disorders, with no hint of perceptual deficit: patients with parietal lesions are able to recognize objects, but they can't include them in their spatial maps (in neglect), they fail in the motor coordination necessary to reach them (in optic ataxia), and they can't localize them into an environment (in topographical disorientation).
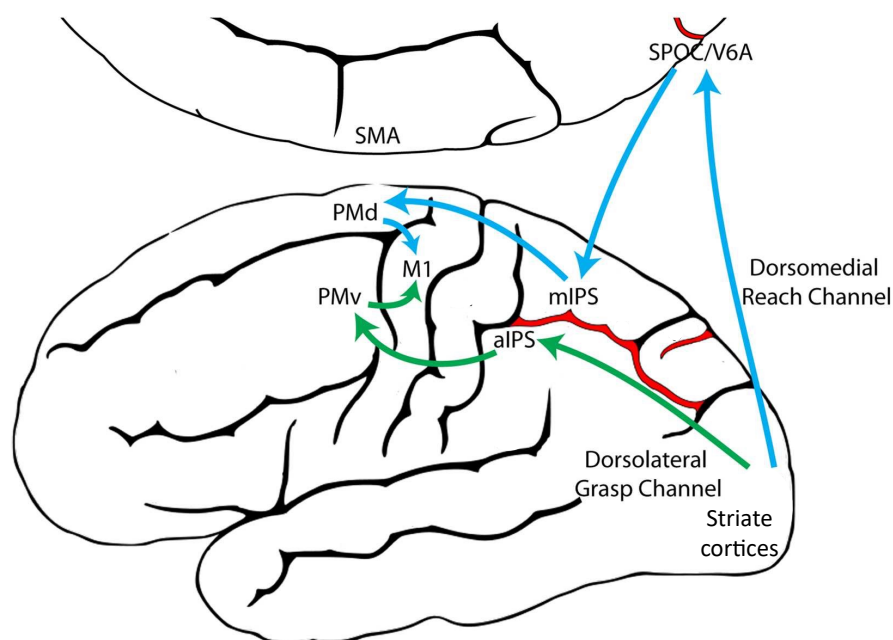
Figure 2. Schematic figure of the two dorsal pathways in humans (adapted from Karl & Whishaw, 2013)
The dorsomedial reaching pathway (blue), including SPOC, mIPS and PMd, encoded maps of the surrounding space to control the upper limb position during reaching. The dorsolateral grasping pathway (green), including aIPS and PMv, implements sensorimotor transformations to encode object's intrinsic properties and convert them in the motor command to properly pre-shape the hand during grasping.

Like in monkeys, each sector of PPC is reciprocally and topographically connected to regions of PMv and PMd, which are in turn connected to M1. In particular, a subdivision of the dorsal stream analogue to the one already described for monkey has been revealed in humans as well. A large amount of evidence highlighted the existence of a dorsomedial pathway, which seems to be involved in online motor control of the upper limb during reaching, and a dorsolateral pathway responsible of the shift from sensory information to motor commands, namely sensorimotor transformations (Figure 2; for reviews see Binkofski & Buxbaum 2013; Culham et al., 2006; Culham and Valyear, 2006; Davare et al., 2011; Filimon, 2010; Galletti & Fattori, 2018; Grafton, 2010; Karl and Whishaw, 2013; Olivier et al., 2007; Turella & Lingnau 2014). Specifically, functional neuroimaging studies identified the human dorsomedial pathway in the superior parieto-occipital cortex (SPOC, the putative homolog of macaque area V6A; Connolly et al., 2003; Prado et al., 2005), the medial intraparietal sulcus (mIPS, Beurze et al., 2007; Filimon et al., 2009; Prado et al., 2005) and PMd (Beurze et al., 2007; Filimon et al., 2007, 2009; Prado et al., 2005), which sowed selective activation during reaching. On the other hand, human dorsolateral grasping pathway has been localized mostly in the anterior intraparietal sulcus (aIPS, the homologue of monkey's AIP) and PMv. For instance, a fMRI study by Culham and colleagues (2003) reported stronger activity of AIP for grasping than reaching. An interesting fMRI study conducted by Cavina-Pratesi and colleagues (2010) compared the activity of the two dorsal visual streams during reaching (i.e., subjects transported their limb toward a given object and touched it with their knuckles without grasping it) and grasping (i.e., participants grasped the object with a thumb-index precision grip) of objects located adjacent to the hand of far, but still within the peripersonal space. They observed activity of SPOC and SPL during hand transportation and activity of aIPS and PMv for object prehension, thus confirming the dissociation between reaching and grasping. Crucially, activity of areas of the dorsolateral stream was observed also when no hand transportation was required

(i.e., the object was placed adjacent to the hand). Anyway, if on the one hand we need to consider that one of the major drawbacks of the functional neuroimaging is the impossibility to causally determine the exact contribution of each area to reaching and grasping components, on the other hand it has been largely confirmed by neuropsychological and non-invasive brain stimulation evidence. Indeed, lesion studies described patients with lesions on aIPS with inaccuracy of coordination of fingers to grip objects despite a relatively preserved reaching movement. On the contrary, it has been observed that patients with parietal lesions sparing aIPS did not impair the grasping component (Binkofski et al., 1998). Besides, TMS approaches allow not only to causally investigate the contribution of these areas to grasping, but also to determine the temporal dynamics of their involvement. For instance, Bartoli and collogues (2014) adopted TMS to highlight a muscle-specific cortico-spinal facilitation during the observation of tools with different affordances (i.e., properties of the object which relates to the possible hand-object interactions) 150 ms after stimuli presentation. This evidence suggests that sensorimotor transformations occur early in the brain. With specific regard to sensorimotor network, virtual lesions induced by TMS applied over aIPS disrupts hand pre-shaping during grasping (Davare et al., 2007), as well as the grip adjustment during online correction of grasping movement when target size or orientation changed unexpectedly after movement initiation, but still maintaining correct reaching motion (Glover et al., 2005). Moreover, perturbation of aIPS activity caused impairment of grasping only when applied within 65 ms after object orientation changing and not later, suggesting an early involvement of aIPS in online control motion (Tunik et al., 2005). Crucially, the same TMS protocol applied over more caudal parietal regions (mIPS, parieto-occipital complex) or the hand representation in M1 showed no consequence on reach-to-grasp movements (Rice et al., 2006; Tunik et al., 2005). Causal investigation with TMS have been conducted also to establish the crucial involvement of PMC in grasping; for instance, Davare and colleagues (2006) induced transient lesion to PMv and PMd during a grip-

lift task to dissociate their involvement in precision grasping. Here, TMS over PMv during movement preparation impaired hand pre-shaping to grasp the object, while the virtual lesion of PMd altered the coupling between the grip and lift components of grasping movements. Altogether, the mentioned neuroimaging, neuropsychological and TMS studies confirm the role of aIPS and PMv in the grasping component, which is given by conversion of sensory information on intrinsic properties of the target object onto motor instructions to pre-shape the hand (namely, sensorimotor transformations).

Besides the activation of singular parietal and frontal areas, activity of aIPS-PMv (dorsolateral pathway) and SPOC-PMd (dorsomedial pathway) connections has been examined during grasping of small and large objects with dynamic causal modeling of fMRI, a technique which determines the effective connectivity between cortical areas (Friston et al., 2003). Using this approach, it has been found that grasping smaller object activates aIPS-PMv connectivity, while grasping larger objects activates SPOC-PMd connectivity (Grol et al., 2007). Clearly, when we have to grasp small objects, we need to elaborate more precise motor instructions compared to when we grasp larger objects; this means that the brain needs to implement more accurate sensorimotor transformations. Activation of aIPS-PMv effective connectivity during grasping requiring more definite hand pre-shaping corroborates the idea that sensorimotor transformations could actually rely on the dorsolateral pathway. Dorsolateral connectivity has been indirectly examined also with a TMS causal approach inducing transient lesion on aIPS and mIPS as control site, and subsequently evaluating the PMv-M1 connectivity with electromyographic measurement (muscle-specific motor-evoked potentials) during precision or whole-hand grasping tasks. In line with previous data, perturbation of aIPS (but not mIPS) activity disrupted PMv-M1 connectivity, which behaviorally implied loss of the digits muscle pattern specific for the object to grasp (Davare et al., 2010).

1.2.1. Sensorimotor transformations for memory-based grasping

In everyday life we often perform actions towards familiar objects that are not accessible to our perceptive filed at that moment, like when we look for our glasses or the light switch on the nightstand in the dark. In cases like this, we perform memory-based actions, which are required when a variable delay between object presentation and object-directed action is introduced; hence, sensorimotor transformations for grasping are based on sensory information on the target that are not available online anymore, but they are stored in our memory. Since everyday object-directed actions rely mostly on vision and haptics, actions driven from visual and haptic memory have been examined. A recent TMS study showed that PMv is crucially involved in movement preparation during memory-based grasping, but only when sensory information on object size has been visually and not haptically acquired (Maule et al., 2015). In fact, this result is in line with the proposal that PMv contains a "visuo-motor" working memory which holds visual information previously acquired on objects that may become relevant to guide incoming actions (Davare et al., 2009; Li et al., 2016; van Ede et al., 2019). On the contrary, when memory-based grasping is driven from tactile rather than visual information, sensory motor transformations seems to use a proprioceptive working memory for temporaneous detention of tactile information contained in the secondary somatosensory cortex (S2; Maule et al., 2015). S2 is located in the parietal operculum (OP) within the upper bank of the lateral sulcus; it contains complete tactile sensory representation of the body, as well as somatosensory information in a somatotopic organization (Eickhoff et al., 2007; Krubitzer et al., 1995; Mazzola et al., 2012; Ruben et al., 2001). In line with this, TMS over OP showed to affects thumb-index configuration during memory-based grasping driven from haptic information (Cattaneo et al., 2015). In conclusion, sensorimotor transformations necessary for memory-based actions seems to make use of different working memories basing on the sensory channel used for the first exploration of the target object.

1.3. How do we observe sensorimotor transformations?

Results of research of the last decades clearly state that the neuroscientific investigation on voluntary actions must consider the strict link between the neural basis of movement and the relative behavioral output. As we can see from the abovementioned studies, the visible output of the dorsal pathway functioning for actions is the motor behavior itself. For this reason, neuroscientific research often avails of behavioral parameters measurement of movement, such as accuracy or reaction and execution times. Nonetheless, the literature on reach-to-grasp actions taught us that the most direct expression of sensorimotor transformations remains the grip component of such actions. In fact, most of the abovementioned investigations on the grasping networks tried to establish the relationship between the cortical sites and the motor behavior by means of hand kinematics recording techniques that allowed to observe and quantify grip configuration changes for each experimental manipulation.

As mentioned, precision grip of small objects requires a more accurate hand configuration compared to power grip or whole-hand grip of large objects, as well as more online control of the action. This is reflected in longer reaction times (the time interval from the go signal and the actual movement onset) and movement execution times (the time interval from the movement onset to the hand-objects contact; Grol et al. 2007). As described, precision grip seems to be coded by the aIPS-PMv dorsolateral pathway, as shown in both human (Davare et al., 2010; Grol et al., 2007; Rice et al., 2006; Tunik et al., 2005) and non-human (Fogassi et al., 2001; Matsumura et al., 1991) primates. Anyway, kinematic measures allowed to highlight the tight relationship between object shape and fingers configuration during reaching (Binkofski et al., 1998; Binkofski & Buxbaum, 2013; Davare et al., 2006, 2007; Grol et al., 2007) and hand adjustment during online correction of the movement (Glover et al., 2005; Rice et al., 2006; Tunik et al., 2005). Indeed, a wide number of investigations pointed out the gradual

scaling of grip aperture, that is the flexion of fingers involved in the movement, directly related to the object size and shape in reach-to-grasp actions. As a matter of fact, when sensorimotor transformations are correctly implemented, hand shaping is fully influenced by – as well as informative of – the target size (Aleotti & Caselli, 2006; Ansuini et al., 2015; Berthier et al., 1996; Karl & Whishaw, 2013; Santello & Soechting, 1997, 1998; Schettino et al., 2003; Winges et al., 2003). This influence becomes evident also during the observation of actions, namely were are able to predict the size of the target object of a grasping action performed by others just by looking at their hand shaping (Ansuini et al., 2016; Avenanti et al., 2017). Furthermore, neuropsychological and virtual lesion studies demonstrated that lesions on areas responsible for sensorimotor transformations impair the grip component, leading to an erroneous hand shaping for the object (Binkofski et al., 1998; Davare et al., 2006, 2007; Glover et al., 2005; Rice et al., 2006; Tunik et al., 2005). Notably, the same correlation between grip aperture and object size was recognized during grasping actions towards haptically-memorized objects (Cattaneo et al., 2015; Maule et al., 2015).

1.4. Conclusions and aim of the work

To better investigate and understand the genesis of movement, neuroscientific research mostly focused on simple as well as essential movements in everyday behavior: object-directed reach-to-grasp actions. As a matter of fact, despite its directness, the study of reach-to-grasp act allowed to shed light on many aspects of the movement: firstly, the knowledge of the hierarchy of the cortical motor system, followed by sensorimotor associations, space coding, object representation across several frames of reference, and so on. From a behavioral point of view, it is well known that the reach-to-grasp movement requires processing of both extrinsic (i.e., spatial location) and intrinsic features (i.e., shape, size, orientation) of the target object. It has

been proposed that the reaching component of the reach-to-grasp action uses the spatial coding to direct the limb toward the target, while the grasping component uses target's intrinsic properties to adjust the hand for the object. In this view, the accurate fingers' configuration is given by sensorimotor transformations, which convert sensory information about object intrinsic properties onto accurate motor commands to properly pre-shape the hand to grasp the target. Compelling evidence from both human and non-human primates suggest that reach-to-grasp movements rely on complex and reciprocal parieto-frontal connections and, specifically, a dorsomedial (SPOC-mIPS-PMd) and a dorsolateral pathway (aIPS-PMv) subserving reaching and grasping component respectively. Data from neuroimaging and causal investigations state that the neural underpinning of sensorimotor transformations could actually rely on the dorsolateral grasping network. Since activity of the aIPS-PMv network, namely the sensorimotor transformations themselves, seems to be directly responsible for the grasping component, neuroscience combined neuroimaging investigation and techniques of hand kinematics recording during reach-to-grasp movements to get a full picture of processes underlying the movement.

The present work aims to deepen some facets of sensorimotor transformations for hand-object interaction in reach-to-grasp actions. Specifically, two studies dealing with different aspects will be discussed: the first one availed of a hypothesis-independent dense TMS mapping approach in order to establish the role of each premotor sector in sensorimotor transformations during visually-based grasping. On the other hand, the second study investigated how hand-object interaction is modulated by the interplay between visual frames of references and the representation of a haptically-explored object, hence in absence of visual information. Evidence from both studies were determined by the behavioral output given by hand's kinematics measurement provided by a sensor-based glove able to detect fingers' flexion during grasping. In conclusion, the present work is articulated in three parts: the first one describes in detail the

glove and how it was assembled and evaluated. The second part includes our TMS study designed to draw a functional map of human PMC for visually-guided grasping. Finally, the last chapter describes the investigation on how the gaze direction modulated hand shaping during haptically-based grasping.

Chapter 2

How to measure hand-movements: evaluation of a sensor-glove to detect fingers' flexion for hand-object interactions

Abstract

Sensorimotor transformations ensure the elaboration of the accurate motor plan to reach and grasp surrounding objects, namely the adequate hand shaping for object geometrical properties (e.g., shape, size, orientation). Hence, the measure of kinematic parameters during movements is a crucial element in the study of the motor behavior. In the last decades, sensor gloves have been very successful for objective measurement of fingers' movement in research and clinical scope thank to their reliability, their compatibility with other devices or techniques of investigation, as well as their low cost. Here a novel sensor glove equipped with five resistive bend sensors is described and evaluated. We asked twenty participants to perform whole-hand reach-to-grasp actions toward three differentially sized cylinders while wearing the glove, and analyzed the output of each sensor. Since the grip aperture during reaching is strictly related to the target size, we checked that the output from sensors was no less informative of cylinders diameter. Results indicate that four out of five sensors accurately discriminated object size, as

they recorded growing maximum finger extension (MFE) for small, medium and large object. Therefore, our custom-built glove provided reliable information on finger joints motions during reaching. We concluded that this data-glove can be adopted for further investigations on the kinematics of reach-to-grasp movements, as long as the four resistive sensors that accurately discriminated object size are considered.

2.1. Introduction

Neuroscientific research of the last decades has made great progresses in the knowledge of the neural and behavioral component of movement through many kinds of investigation. As described in chapter 1, research availed of a wide range of investigation techniques on both human and non-human primates to shed light not only on the neural underpinning of the genesis of the movement, but also on how the cerebral regions involved in motion interact with each other. Nonetheless, research of the last decades clearly concluded that the mere analysis of areas involved in motor behavior gives helpful but still incomplete information. Consequently, to better understand the effects of sensorimotor transformations for actions, we need to quantify the observable component of the movement, such as reaction and execution times or accuracy. Still, the most effective way to study the motor behavior remains the adoption of tools that directly measure the movement per se. For example, the kinematics studies on hand's actions investigate fingers movement by means of infrared emitting diodes placed on fingers themselves. The diodes are then red by one or more cameras, so that each motion is recorded and recreated in a three-dimensional space. In this way, it's possible to determine several components of the recorded movements, such as velocity, variability, rotation or even the

distance between different parts of the moving limb (Ansuini et al., 2015; Camponogara & Volcic, 2019; Karl et al., 2012; Sartori et al., 2013).

However, in the study of reach-to-grasp movements of the last decades, many authors availed of a simpler device which records the movements restricted to hand's fingers, namely a glove able to measure fingers' flexion and, hence, estimate hand's posture during the ongoing movement by means of resistive sensors embedded in correspondence of fingers' joints. There are many distinctive features that made this sensor glove a promising and desirable tool to adopt for the measurement of hand configuration during motor tasks. First, the sensors embedded in the device give an accurate and steady signal that results in a linear pattern properly describing each phase of the movement (Santello et al., 2016). Second, the glove has obtained success thanks to its easy application that make it ideal in the experimental context, since it is compatible with other neuroscience methods such as EMG recording, TMS, (Castellini & Van Der Smagt, 2013; Fricke et al., 2017, 2019; Gentner & Classen, 2006) or virtual reality (Aleotti & Caselli, 2006). Moreover, the glove found many applications also in clinical environment for neuropsychological assessments or rehabilitation treatments (Lang & Schieber, 2003, 2004b) and in the field of human-robot interaction (Bianchi et al., 2013a, 2013b) . Third, compared to other methods for motion recording (i.e., the kinematics), the glove is a low-cost device (Gentner & Classen, 2009). As a consequence, similar version of sensor gloves has been developed (Fricke et al., 2017, 2019; Gentner & Classen, 2009; Simone et al., 2007), commercialized (e.g., CyberGlove Systems, HumanGlove, or DataGlove family) or evaluated (Dipietro et al., 2003). During the past years, many authors used several versions of the sensor glove to study the hand kinematics during object-directed actions (Ansuini et al., 2006, 2008; Donnarumma et al., 2017; Santello & Soechting, 1998; Schettino et al., 2003; Winges et al., 2003) or to analyze the hand synergies during both transitive (Castellini & Van Der Smagt, 2013; Fricke et al., 2017; Häger-Ross & Schieber, 2000; Jarque-Bou et al., 2019) and

intransitive movements (Bianchi et al., 2013a; Fricke et al., 2019; Gentner & Classen, 2006; Jerde et al., 2003; Santello, 1998).

On this basis, we developed our own glove to measure hand shaping during our experiments. Before using the device for the studies that will be introduced later, we conducted a study to evaluate our glove and ensure that each flexible sensor installed was functional and suitable for the aim of our experiments. As previously mentioned, one of the direct consequence of sensorimotor transformations during visually-guided grasping is the tight correlation between the target size and the hand shaping, so that the grip aperture is already fully influenced by – and therefore informative of – the object size (Berthier et al., 1996; Karl & Whishaw, 2013). In line with this, several studies that took advantage from sensor gloves similar to ours found the same correlation between the hand shaping and the target size (Aleotti & Caselli, 2006; Santello & Soechting, 1997, 1998; Schettino et al., 2003; Winges et al., 2003). From these findings, it appears clear that the grip aperture is a trustworthy index of hand shaping and, therefore, successful sensorimotor transformations, as well as an ideal output to study the motor behavior during reach-to-grasp actions.

With these key assumptions, we tested our custom-built glove asking our participants to perform visually-guided grasping towards three differently sized cylinders. In particular, we aimed to verify that our resistive sensors were able to accurately discriminate fingers' flexion for each object. In this way, we wanted to ensure that our sensor glove was actually a reliable device to measure finger joints movements and, therefore, provide a correct index of hand shaping during reach-to-grasp actions. In other words, we hypothesized that, once we assembled the glove, its good functioning would have been reflected in a match between the extension of its sensors and the diameter of the target objects. If so, the glove would constitute the ideal tool to measure hand shaping during our following investigations on both visually- and haptically-guided grasping.

2.2. Materials and methods

2.2.1. Participants

Twenty participants (9 females) with age ranging from 20 to 32 (mean age ± SD: 22.6 ± 4.5) took part in this experiment. All subjects were right-handed, and suffered from no neurological, psychiatric or medical condition. All volunteers gave their written informed consent before the experimental session. The experimental protocol was approved by the ethic committee of University of Verona and was carried out in accordance with the ethical standards of the Declaration of Helsinki.

2.2.2. Apparatus

Participants sat in a comfortable chair in front of a table where the experimenter placed in between trials different objects. We used 7-cm-high metallic cylindrical objects of three possible diameters (1, 3 or 5 cm, Figure 3A) that were glued to a 15x15-cm plywood to facilitate their placement during the trials. We fixed a squared polystyrene base (mean distance ± SD: 52.8 ± 6.9 cm) aligned with subject's body midline that perfectly fitted with objects' plywood base. In this way, we ensured that the objects were placed always in the same position during each experimental session. A button was set on the table between the participant (mean distance ± SD: 38.3 ± 5.1 cm) and the object (mean distance ± SD: 27.4 ± 7.7 cm) to define the space of the baseline position, in which participants were asked to rest their right hand on the button with all fingers closed and pointing down on it (Figure 3B). The distances between the elements of the experimental setting (the participant, the objects' support base and the button) were set depending on the space for movement that each subject reported to find comfortable. During the experiment, participants wore the glove to measure fingers' flexion during the movements. None of the participants referred to have discomfort due to the glove or its wires. Finally, the

experimenter sat on the opposite side of the table to change the objects before each trial. A screen pointed toward the experimenter informed him on which of the three objects had to be placed on the support.
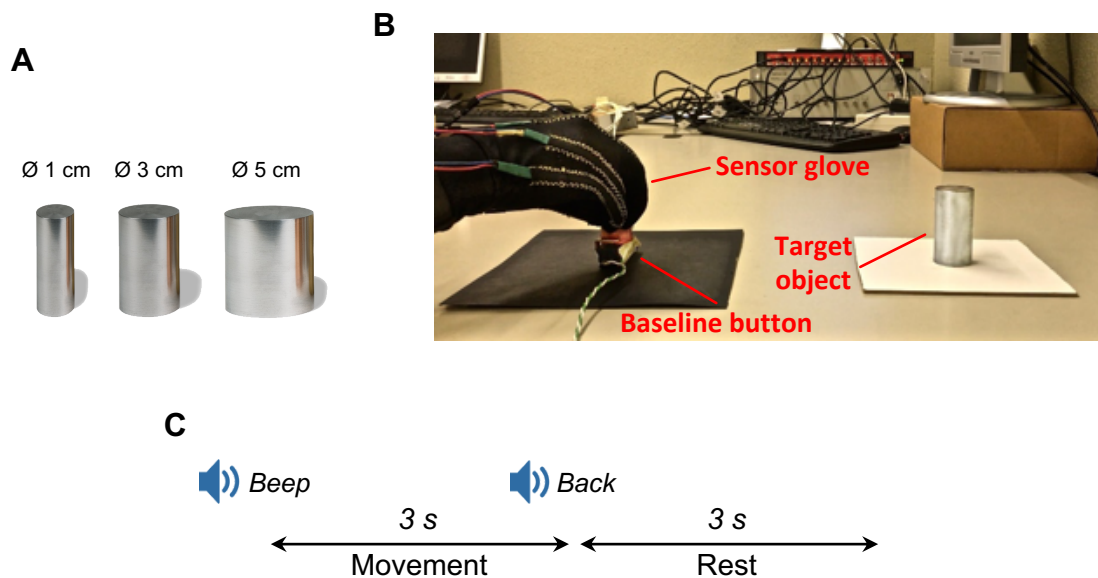
Figure 3. Experimental setup and paradigm
(A) Objects used in the main experiment. The three cylindrical objects had a height of 7 cm and diameter of 1, 3 and 5 cm. (B) Experimental setup. Participants sat in front of a button that served as the baseline position and pressed it with the fingers closed before and after each trial. The object was placed in front of the button and was changed by the experimenter before the beginning of each trial. (C) Timing of trials. After assuming the baseline position, a "beep" sound instructed participants to leave the button, grasp – without lifting – the object using all their fingers, and maintain the grip for few seconds. The "back" sound instructed participant to return to the baseline position and rest for 3 s (time needed for the experimenter to change the object before the following trial).

2.2.3. Procedure and experimental design

Participants assumed the baseline position on the button. A "beep" sound instructed participants to leave the button and perform the grasping movement toward the cylindrical object aligned with their body midline. Subjects were specifically asked to grasp the object – without lifting it – from the top using all their fingers and maintaining the grip until the "back" cue occurred after 3 s, inducing them to return to the baseline position on the button. A 3 s

window was in between a trial and the other to allow experimenter to change the object for the

following trial (Figure 3C).

Each of the three objects was presented 20 times, for a total of 60 trials presented in a

unique block in random order. This led to an experimental design with the SIZE factor of 3

levels (small, medium, large).
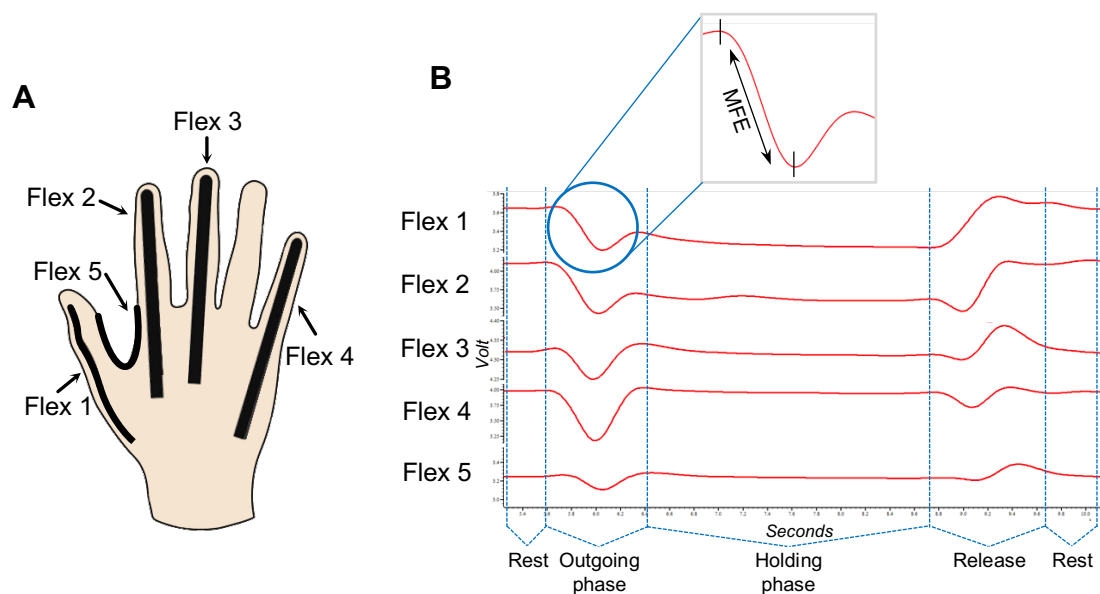
Figure 4. Glove used for acquisition of hand configuration and relative data
(A) Schema of the position of flexible sensors of the hand. Participants wore a glove equipped
with five resistive bend sensors that allowed us to measure MFE. Each sensor consisted of a
resistance variable to its own flexion. The sensors were connected to an analogical-digital
converter so that we could quantify the voltage variations of each resistor for each finger flexion.
Sensors were placed as follows: one on the thumb (flex 1), one on the index finger (flex 2), one
on the middle finger (flex 3), one on the little finger (flex 4) and last one on the arch between the
thumb and the index finger (flex 5). (B) Example of signal generated by the voltage variations of
each sensor for a whole trial recorded with Signal software from one of the participants. For each
trial, the pattern was clear and consistent enough to allow us to recognize the phases of the ongoing
trial (rest – grasping – rest) and, more specifically, the reaching action: outgoing phase, contact
with the object (hold), return phase (release). In the outgoing phase, MFE was calculated as the
absolute value of the difference between the voltage recorded in the baseline position and the peak
during the outgoing phase of the grasping movement, immediately before participants' fingers
held the cylinder.

2.2.4. Grip aperture measurement

We assembled the sensor glove to measure the maximum grip aperture of participants' right hand and, hence, get an index of the hand shaping during precision whole-hand grasping. To this end, we strategically placed five 10 KΩ flexible resistive bend sensors (flexsensors 4.5'' – Sprectrasymbol, USA) in a glove made by stretchable fabric of Lycra. Each sensor was 114-mm-long and was inserted in little tailored pockets over the metacarpophalangeal and proximal interphalangeal joints of the thumb, index, middle and little fingers (four out of five sensor) and in the thumb-index arch (Figure 4A). Note that we did not place any sensor on the ring finger because literature on whole-hand grasping tells us that its movements are strongly correlated with those of the little finger, regardless of the goal of the action (Ansuini et al., 2006, 2008; Häger-Ross & Schieber, 2000; Lang & Schieber, 2004a). Given the redundance of ring finger's movement compared to little finger's onces, we did not measure ring finger's flexion. Furthermore, to make the glove comfortable for each participant, we had it in three different sizes (S, M, L) and used the most appropriate depending on participant's hand size, as long as the glove remained close-fitting on the hand. Fifteen of our participants used the M size, three used the L size, and the remaining two the S size.

Each sensor was connected to a different channel of a Power1401 analog-digital converter (Cambridge Electronic Design, CED, UK) through a BNC cable. The analog-digital converter was in turn connected to a computer in which the Signal software (Cambridge Electronic Design, Cambridge, UK) allowed us to acquire data from glove's sensors and, thus, to observe the variation of the resistance from each flexible sensor connected to the analog-digital converter. Flexion of glove sensors produced a signal that fell within a 0-5-V range. The output of the sensors was sampled at 100 Hz rate intervals. Remarkably, each sensor generated a clear and linear pattern that can be described as a steady pattern that easily allows to recognize each phase of the trial (rest – grasping – rest) and, more importantly, the ongoing grasping

movement: the outgoing phase (i.e., the hand leaves the baseline position to head toward the object), the holding phase (contact with the object) and the release phase (i.e., the hand leaves the object to return to the starting position; Figure 4B).

To obtain an index of hand shaping during the reaching movements, we calculated the *maximum finger extension* (MFE) from each bend sensor installed in the glove. Specifically, MFE was calculated as the absolute value of the difference between the voltage recorded during the baseline position and the peak during the outgoing phase of the grasping movement, immediately before the participant's fingers held the cylinder (Figure 4B).

The software OpenSesame (Mathôt et al., 2012) was used for auditory stimuli presentation, to determine the sequence of the objects to be displayed by the experimenter, and to trigger the analog-digital converter for the recording of sensors' flexion with the software Signal software, that registered a frame for each trial.

2.3. Data analysis

We normalized MFE's data calculating z-scores within each sensor and each participant in order to make the data from each finger comparable. For each object size, we removed trials whose MFE deviated more than 2 standard deviations from the mean of each flexible sensor (4.4% of trials). All frames recorded by the Signal software showed a kinematics that clearly allowed the MFE calculation; so, no deletion of any trial was needed.

We assumed that if our custom-built glove was an adequate tool to measure finger's movement during precision whole-hand grasping and, hence, give an accurate index of hand shaping, each sensor would have been able to accurately discriminate each of the three object sizes. In particular, we expected to observe a gradient of extension of sensors associated with

cylinders' diameter. To test our hypothesis, we performed a repeated measures ANOVA with 2 within-subjects factors: FLEX (5 levels: flex 1, flex 2, flex 3, flex 4, flex 5) × SIZE (3 levels: small, medium, large). Post-hoc analysis for significant interactions were performed with Tukey's Honestly Significant Difference (HSD) test. Effect sizes of significant results were reported as partial eta-squared (p-eta^2) coefficients. All the analyses were conducted using SPSS (IBM Corp. Released 2012. IBM SPSS Statistics for Macintosh, Version 21.0. Armonk, NY: IBM Corp.), with the significant threshold set al 0.05.

Sensor:	Flex 1 (thumb)	Flex 2 (index)	Flex 3 (middle)	Flex 4 (little)	Flex 5 (thumb-index)
Small cylinder	-0.43 (0.09)	-0.42 (0.07)	-0.64 (0.06)	-0.69 (0.05)	0.04 (0.04)
Medium cylinder	-0.08 (0.05)	-0.02 (0.05)	0.07 (0.03)	0.01 (0.04)	-0.04 (0.03)
Large cylinder	0.5 (0.08)	0.43 (0.07)	0.57 (0.07)	0.7 (0.06)	0 (0.03)

Table 1
Z-score transformed Maximal Finger Extension (MFE) for each experimental condition. Mean values (Standard Error) are given.

2.4. Results

The ANOVA with 2 factors FLEX × SIZE conducted on the average of MFE revealed a main effect of SIZE ($F_{2,38} = 111.01$; $p < 0.0000001$; p-eta$^2 = 0.85$) and, more importantly, a significant interaction FLEX × SIZE ($F_{8,152} = 19.31$; $p < 0.0000001$; p-eta$^2 = 0.5$) illustrated in Figure 5. No main effect of FLEX was observed ($p > 0.1$). Mean values of all the experimental conditions are reported in Table 1. The FLEX × SIZE interaction was further investigated by means of distinct 1-way ANOVAs for each of the five sensors. The main effect of SIZE was confirmed in 1-way ANOVAs conducted on Flex 1 on the thumb ($F_{2,38} = 2.73$; $p < 0.0000001$; p-eta$^2 = 0.59$), Flex 2 on the index finger ($F_{2,38} = 1.37$; $p < 0.0000001$; p-eta$^2 = 0.62$), Flex 3 on the middle finger ($F_{2,38} = 0.07$; $p < 0.0000001$; p-eta$^2 = 0.8$) and on the Flex 4 ($F_{2,38} = 1.68$; $p <$

0.0000001; p-eta^2 = 0.88) in the little finger. Post-hoc comparisons performed with Tukey HSD test for each of these ANOVAs revealed a growing MFE for small, medium and large object for all the four sensors (all *p* < 0.02; for all the statistical values of the post-hoc comparisons see table 1). On the contrary, ANOVA performed on Flex 5 values was the only one with no significative effect ($F_{2,38}$ = 0.53; *p* = 0.5; p-eta^2 = 0.03). Results of all post-hoc comparisons are shown in Table 2.
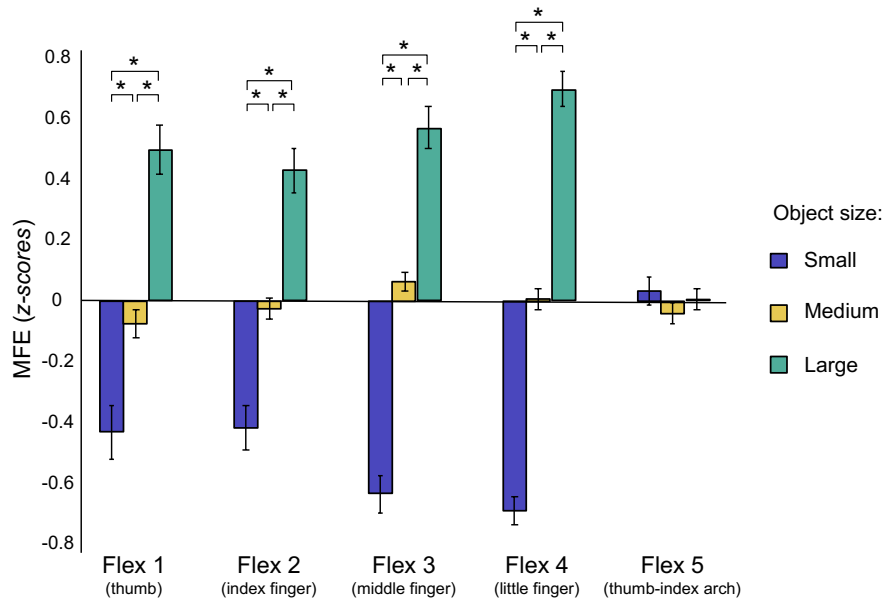
Figure 5. Flex × Size interaction
Bars represent the average MFE for each of the three object sizes for each resistive sensor. A 1-way ANOVA was carried out for each sensor to check the influence of the object size on sensor's flexion. Overall, there was accurate discrimination of object size for each sensor, as MFE was scaled according to each of the three object sizes, with the only exception of Flex 5 (namely, the sensor on the thumb-index arch), in which no variation of flexion was observed. Asterisks indicate significant statistical differences for post-hoc comparisons (*p* < 0.02, corrected). Error bars denote ± 1 standard error of the mean (SEM).

To summarize, the FLEX × SIZE interaction entails that not all sensors discriminated accurately the object size. In fact, we observed a consistent gradient of extension in all the

flexible sensors except for the one installed in the thumb-index arch, which showed a constant flexion independently of the cylinders' diameter. Hence, the accurate size discrimination that we expected did not concern all the flexible sensors: it occurred in sensors that we installed in hand's fingers, but not in the only one that we placed in thumb-index junction. Overall, we can conclude that our sensors are able to accurately detect fingers' movements during a whole-hand precision grasping.

Sensors:	Small *vs* Medium	Small *vs* Large	Medium *vs* Large
Flex 1 (thumb)	0.006	0.00003	0.00003
Flex 2 (index)	0.001	0.00003	0.00006
Flex 3 (middle)	0.00003	0.00003	0.00003
Flex 4 (little)	0.00003	0.00003	0.00003
Flex 5 (thumb-index)	0.99	1	1

Table 2
Statistical values for post-hoc t-tests performed on the 1-way ANOVAs conducted for each sensor embedded in the glove. T-tests are corrected with Tukey's Honestly Significant Difference (HSD) test.

2.5. Discussion

2.5.1. Hand finger aperture is informative of object size

We assembled a sensor glove equipped with flexible resistive sensors to detect fingers' aperture during visually-based reach-to-grasp actions performed with all fingers, with the purpose of using it for our next studies on motor behavior. To this end, we placed five resistive sensors corresponding with the thumb, the index finger, the middle finger, the little finger and the thumb-index arch. Before using the glove for our experiments, we wanted to ensure that the signal recorded from each sensor was a reliable index of fingers' movements and, therefore, that the glove itself was an ideal device to measure grip aperture during reach-to-grasp actions. For this reason, we asked our participants to reach and grasp three differently sized cylinders

while wearing the glove, in order to check whether the signal recorded from each flexing sensor correctly matched with object size.

Our results proved that the object size is accurately recognized by almost all sensors. Specifically, the four sensors placed over the metacarpophalangeal and proximal interphalangeal joints of the thumb, index finger, middle finger the little finger remarkably showed a gradual variation of resistance related to object diameter. In other words, we clearly observed a finger aperture proportional for the three cylinders, considering only those sensors installed on fingers' joints (flexs 1 to 4) and not the only one placed in the thumb-index arch.

The vast majority of studies that adopted other tools to record hand's kinematics related to the object size focused only on precision grip performed with thumb-index pair (N. R. Cohen et al., 2009; Cuijpers et al., 2004; Leoné et al., 2015; Rand et al., 2007; Schlicht & Schrater, 2007). However, the existing kinematics studies focused on whole-hand actions demonstrated that, during the reaching, grip aperture is related to the target size (Berthier et al., 1996). In fact, it has been showed that such gradual scaling for the object shape occurs since the developmental age (Zoia et al., 2006). Crucially, our results are in line with other previous investigations that adopted a dataglove similar to ours to detect fingers' flexion during a reaching movement. For instance, an analogue gradient of fingers' flexion related to object size was found by Santello & Soechting (1997), that asked their participants first to assume a hand posture that was supposed to fit a visually-perceived object, and then grasp it. Here, participants showed high accuracy in matching their grip aperture with the target object. In another study (Santello & Soechting, 1998), the same authors presented objects with similar sizes, but turned in their concave, convex or flat surface. Even in this case, hand aperture was influenced by object shape. Winges and collogues (2003) used the sensor glove to demonstrate that, during the reaching of an object whose vision was occluded with different intervals, the fingers configuration adapts to object shape independently of the visual delay. Another study that observed a correlation

between the grip aperture and the object size was conducted by Schettino and collogues (2003), that asked their participant to perform reaching movements toward several objects with different possible visual feedback (full vision, no vision, vision of object only). Here, authors observed different timings of hand pre-shaping's components depending on the visual feedback available; nevertheless, fingers' movements (i.e., flexion/extension and abduction/adduction) was influenced by object shape independently from the visual condition. Finally, Aleotti & Caselli (2006) found the analogue correlation between grip aperture and target size measuring hand posture by means of a sensor glove during the reaching of virtually-perceived everyday object.

2.5.2. Target size is not reflected on thumb-index junction aperture

The mobility gradient that we observed regards all those sensors installed on fingers' joints, but not the only one placed in the thumb-index arch (flex 5), in which we found no modulation of the resistance for the three objects. In other words, the posture of the thumb-index arch remained constant independently of the diameter of the cylinder to grasp. Since our glove is the first to embed a sensor in this part of the hand, this data it's hard to relate to the previous literature. Effectively, the other gloves commercialized (e.g. CyberGlove Systems, HumanGlove, or DataGlove family) or assembled by authors themselves (Fricke et al., 2017, 2019; Gentner & Classen, 2009; Simone et al., 2007) were equipped with a greater number of sensors, as more sensors were placed on the same finger in order to provide different recordings for the proximal and distal parts. Nevertheless, no one of those studies measured the flexion from the thumb-index junction. Despite this, as previously described, overall results of these studies that analyzed the link between fingers aperture and target size during grasping are compatible with ours. We know for sure that during reaching there is a distancing between the thumb and the index finger when the hand reaches its maximum grip aperture, and then the two

fingers come closer to grasp the target object. Clearly, the thumb-index distance and its variation always depend on the object size (Cuijpers et al., 2004). However, it is possible that such a distance depends merely on the movement of the two fingers, namely from the flexion of the most distal phalanges. If so, the thumb-index distance could change, but without significative changings of the aperture of the thumb-index arch. This hypothesis could explain why we did not detect any variation of flexion from flex 5. Besides, we can't find any other possible explanations from kinematics studies, because infrared emitting diodes are typically placed on fingers rather than on their junctions.

2.6. Conclusions

In conclusion, we wanted to assess the reliability of our custom-built glove measuring its sensors' flexion during the reaching of three differently sized cylinders, assuming that each sensor would have provided an index of finger flexion related to the object size. In accordance with previous studies adopting similar datagloves, we saw that the three sizes are accurately discriminated by the sensors placed on fingers' joints; in contrast, no size discrimination was observed in the sensor installed in the thumb-index arch. In the light of this data, we concluded that our glove is a valid device for fingers flexion measurement, as long as we consider the 4 sensors whose signal was informative of the cylinder diameter. Thus, we took advantage of our custom-made glove for the next investigations on both visually- and haptically-guided grasping that we carried out, excluding the sensor that did not provide any significative information on hand shaping. So, in the two studies afterwards introduced the glove will be used for hand shaping measurement placing the sensor only on the thumb, the index finger, the middle finger

and the little finger. We are aware of the limitations of this device compared to kinematic tracking, which would provide more parameters like velocity of execution, hand inclination and orientation on a three-dimensional plane etc.. Nonetheless our data-glove allows to record and analyze finger joints motions, which is indeed our main interest.

Chapter 3

The topography of visually-guided grasping in the premotor cortex: a dense-transcranial magnetic stimulation (TMS) mapping study[1]

Abstract

During visually-guided grasping, sensorimotor transformations at the cortical level occur along the parieto-frontal grasping network where visual information re-coded and translated in the motor command to appropriately pre-shape the hand. Grasping-related activity is represented in a diffuse, ventral and dorsal system in the posterior parietal regions, but no systematic causal description of a premotor counterpart of a similar diffuse grasping representation is available. To fill this gap, we measured the kinematics of right finger movements in 17 healthy participants during grasping of three differently sized objects. Single-pulse transcranial magnetic stimulation (spTMS) was applied 100 ms after visual presentation of the object over a regular grid of 8 spots covering the left premotor cortex (PMC) and 2 Sham stimulations. Maximum finger aperture during reach was used as the feature to classify object size in different types of classifiers. Classification accuracy was taken as a measure of the

---

efficiency of visuo-motor transformations for grasping. Results showed that TMS reduced classification accuracy compared to Sham stimulation when it was applied over two spots in the ventral PMC and 1 spot in the medial PMC, corresponding approximately to the ventral premotor cortex and the dorsal portion of the supplementary motor area respectively. Our results indicate a multifocal representation of object geometry for grasping in PMC that matches the known multifocal parietal maps of grasping representations. Additionally, we confirm that by applying a uniform spatial sampling procedure TMS can produce cortical functional maps independent of a priori spatial assumptions.

3.1. Introduction

3.1.1. Visually-guided grasping is modularly represented in the cerebral cortex

Reach-to-grasp action towards visually-perceived objects is one of the most used action to interact with our surroundings in everyday life, as well as the most studied movement in neuroscientific research. Although this behavior may seem simple and immediate, research of the last decades proved its complexity, as well as its modularity in the brain. Talking about the neural underpinning of the visually-guided grasping, the first example of such modularity is the different contributions of the ventral and the dorsal visual streams (Goodale & Milner, 1992). The ventral pathway, projecting from the striate cortex to the infero-temporal cortex, is known to be involved in the object recognition, so that information about the target is long-term stored depending on its category of belonging. On the other hand, the dorsal pathway projecting from striate cortices to PPC, is crucial for the spatial coding of the target object; more importantly, it mediates sensorimotor transformations during object-directed visually-guided actions (N. R. Cohen et al., 2009; Mahon et al., 2007; Milner & Goodale, 2008; Pietrini et al., 2004). As

illustrated in chapter 1, the dorsal visual pathway is further subdivided in a dorsomedial pathway connecting SPOC, mIPS and PMd, and a dorsolateral pathway including aIPS and PMv (see Figure 2 in chapter 1). Evidence from both human and non-human primates showed that these two dorsal systems subserve the reaching (hand's transportation toward the target) and the grasping component (the hand shaping according to the target), respectively. Therefore, it's assumed that the combined activity of these two pathways during visually-based reach-to-grasp movements ensures that the upper limb goes to the correct direction and with the correct hand configuration (for reviews see Binkofski & Buxbaum, 2013; Culham et al., 2006; Culham & Valyear, 2006; Davare et al., 2011; Filimon, 2010; Galletti & Fattori 2018; Grafton, 2010; Karl & Whishaw, 2013; Olivier et al., 2007; Turella & Lingnau 2014).

The study here introduced is focused on which of the premotor sectors are actually recruited to guide hand shaping driven from visual information on object geometrical properties while reaching for the object itself.

3.1.2. Conflicting evidence on functional specialization of PMC for visually-guided grasping

The division of the dorsal stream in a dorsomedial and dorsolateral pathway hypothetically coding for the reaching and the grasping components has been largely confirmed; nevertheless, it does not provide clear and definitive information on cortical specialization for visually-guided grasping for two main reasons.

First, increasing evidence are not entirely in line with such dichotomy between dorsomedial and dorsolateral streams. As a matter of fact, recent findings in humans (Fabbri et al., 2014; Gallivan et al., 2013; Gallivan et al., 2011; Monaco et al., 2015; Turella et al., 2016; Verhagen et al., 2012) suggested that both the dorsolateral and the dorsomedial pathways could code for grasping information. Such observations of object- and grasping-related activity in the

dorsomedial pathway is actually inspired and corroborated by findings in non-human primates, which demonstrated grasping-relevant information both in the medial occipito-parietal cortex (Fattori et al., 2010; Fattori et al., 2012) and medial PMC (Bonini, 2016; Gerbella et al., 2017; Lanzilotto et al., 2016; Livi et al., 2019). Growing body of evidence in human show parietal activity within the dorsomedial pathway encoding grasp-related parameters. Gallivan and colleagues (Gallivan et al., 2011, 2013) demonstrated that preparatory activity along the dorsomedial circuit, in particular SPOC, decodes reach-to-touch versus reach-to-grasp movements. A recent TMS study (Vesia et al., 2017), directly demonstrated a crucial role of SPOC in encoding hand shaping during action preparation. Moreover, some studies directly showed that the dorsomedial and the dorsolateral pathways are not completely anatomically segregated (Gharbawie et al., 2011; Janssen et al., 2018; Livi et al., 2019; Orban, 2016); hence, there could be an interplay between these two pathways for the movement instructions.

Second and consequent to the first point, while it is well known that grasping representations in the PPC are distributed between the dorsolateral and the dorsomedial systems (Orban, 2016), the understanding of how grasping is represented in human PMC still presents considerable gaps. As previously described, a functional division between PMv and PMd reflecting the subdivision between the dorsomedial and the dorsolateral system has been identified in monkeys. Therefore, in this view, PMd encodes the target position (Hoshi & Tanji, 2007; Mirabella et al., 2011; Pesaran et al., 2006), while PMv matches visual information on object intrinsic properties and motor instructions required for the action (Borra et al., 2017; Hoshi & Tanji, 2007; Giacomo Rizzolatti & Matelli, 2003). However, such a distinctive functional attribution has not been identified in human brain, and it would be erroneous to rely on the functional map defined for monkeys (Sereno & Tootell, 2005). In addition, an important, yet unresolved question is whether grasping information represented in the medial parietal regions (Gallivan et al., 2011; Vesia et al., 2017) has a counterpart in the medial premotor

regions. Neuroimaging studies demonstrated that both visually-guided (Gallivan et al., 2011, 2013) and non-visually-guided (Fabbri et al., 2014) reach-to-grasp actions activated not only the PMv, but also a more medial-dorsal part of PMC (Turella & Lingnau, 2014). However, functional neuroimaging lacks the temporal resolution to investigate the neural correlates of on-going movements and most fMRI studies focus on the preparatory phase prior to the actual voluntary movement (Beurze et al., 2007; Beurze et al., 2009). Therefore, from a functional perspective, the specificity of premotor activity can be difficult to interpret because these approaches cannot determine whether this neural activation reflects neural processing that is actually critical for grasping movements. Hence, techniques with a better temporal resolution (but still without loss in the spatial resolution) are needed to address this question. For example, the approach of the single cell recording adopted for monkey allowed to highlight a crucial involvement of some populations of neurons of the pre-supplementary motor area (area F6), that is far more dorsal than the PMC typically attributed to visually-guided hand-object interactions (Lanzilotto et al., 2016). Clearly, the single cell recording is too invasive for humans; hence, techniques of non-invasive brain stimulation are preferred due to its excellent spatial and temporal resolution. In particular, Transcranial Magnetic Stimulation (TMS) can provide more accurate information about where and when grasping movements are coded. However, most of TMS studies on voluntary actions explored single foci that were chosen a priori within PMC, therefore they yielded limited spatial information on the overall functional organization of the premotor region.

3.1.3. Aim of the study

To summarize, visually-based reach-to-grasp actions rely on sensorimotor transformations that occur along a parieto-frontal network consisting of two sub-networks connecting the ventral portions of PPC to the PMv (dorsolateral pathway) and the dorsal

portions of PPC to PMd (dorsomedial pathway; Rizzolatti & Matelli, 2003; Turella & Lingnau, 2014). A modular model of reach-to-grasp actions has been proposed, associating activity of the dorsolateral parieto-frontal pathway with the grasping component (namely, the pre-shaping of hand grip according to the shape, size and orientation of the object) and activity of the dorsomedial pathway with the reaching component (the hand's transportation towards the object; Galletti & Fattori, 2018; Karl & Whishaw, 2013). However, several neuroimage studies conducted on humans (Fabbri et al., 2014; Gallivan et al., 2011, 2013; Monaco et al., 2015; Turella et al., 2016; Verhagen et al., 2012) did not support such modularity, showing both object- and grasping-related activity in the dorsomedial pathway (Culham et al., 2003; Gallivan & Culham, 2015; Grafton et al., 1996; Grol et al., 2007; Vesia et al., 2018). Thus, data on the specific contribution of human PMd and PMv to visually-based grasping are still conflicting. Besides, compelling evidences from monkeys (Gerbella et al., 2017; Lanzilotto et al., 2016; Livi et al., 2019) suggest that it is plausible that visually-guided hand-object interactions require not only the canonical premotor areas (e.g., PMd and PMv), but also areas located in more dorso-medial portions of PMC. Taken together, these data lead to the necessity of shed light on the involvement of premotor sectors in visual grasping by defining a functional map of the whole premotor region.

To fil this gap, in this study we explored the topographic distribution of goal-directed sensorimotor functions by asking our participants to perform grasping movements towards three differently sized cylindrical objects during online TMS on PMC. Event-related TMS was applied to single spots of a dense grid of 8 points on participants' left hemi-scalp, putatively covering the whole of premotor region. Single-pulse TMS (spTMS) was applied at 100 msec after the "go" signal, a time window which has been previously demonstrated critical for hand movement preparation and visuo-motor transformations (Davare et al., 2006). Crucially, we measured finger flexion during reaching to check any possible effect of TMS over a given

premotor sector. Thus, this study aims to define a functional map of the whole premotor region to clarify the involvement of each premotor sector in visually-guided object-directed reaching.

3.1.4. TMS statistical mapping

We availed of a dense TMS (d-TMS) spatial mapping, a cutting-edge methodological approach consisting of stimulating a cortical region across a uniform array of adjacent target-foci, thus allowing to draw a detailed cartography of circumscribed cortical regions. One of the strengths of this approach is that it fulfills the potentiality of TMS as a functional brain mapping tool, as it provides reliable spatial information of small functional brain maps (Cattaneo, 2018). As evidence of its reliability, d-TMS mapping found large application in the field of non-invasive pre-surgical assessment of brain functions, in which the accurate spatial mapping is essential. In particular, it has been increasingly adopted for preoperative mapping of the primary motor cortex (Byrnes et al., 2001; Forster et al., 2011; Krieg et al., 2012; Picht et al., 2009, 2011; Thickbroom et al., 2004) and Broca's area (Könönen et al., 2015; Picht et al., 2013; Tarapore et al., 2016a, 2016b). In the case of neurosurgical patients, the alternative of d-TMS mapping would be the direct cortical stimulation (DCS), namely an intraoperative stimulation through a dense grid array of electrodes placed directly on the cerebral cortex during awake craniotomy (Silverstein, 2012). Crucially, a good correlation between preoperative d-TMS mapping and intraoperative DCS functional maps has been repeatedly reported (Forster et al., 2011; Krieg et al., 2012; Picht et al., 2009, 2011, 2013), thus confirming the accuracy of data arising from this technique. Consequently, this approach obtained compelling results also beyond the neurosurgical field, demonstrating to be successful in mapping different cognitive functions (Busan et al., 2009; Cattaneo & Barchiesi, 2011; Cattaneo & Parmigiani, 2021; Ellison et al., 2004; Finocchiaro et al., 2015; Lega et al., 2019; Maule et al., 2015; Oliver et al., 2009; Parmigiani et al., 2015; Salatino et al., 2014; Schaeffner & Welchman, 2017; Stoeckel et

al., 2009). For this reason, we used d-TMS mapping to draw a functional map of the whole PMC for visually-guided grasping movement, rather than adopting the a priori localization of the coil. Note that the accuracy of functional mapping depends on the neuronavigation method, which could include the reconstruction of participant's scalp from his individual MRI scan, or from an estimated MRI scan resulting from the digitization of some skull landmarks. Since the first method is the most accurate (Sack et al., 2008), we defined the array of target-foci from participants' MRI scans.

To better support our data, a hypothesis-independent approach was used for data analysis; namely, data-driven classification algorithms were programmed in collaboration with the Department of bioinformatics of the University of Verona. Besides, to increase the significance of the results, we used different classifiers (Duda et al., 2001; Bishop, 2006). Specifically, we analyzed participants' grip aperture during reaching of the three differently sized object and measured the accuracy of each classifier in predict which of the three objects was the target of the action. If classifiers fail to discriminate the three object sizes during the stimulation on a given TMS spot compared to sham stimulation, then we can infer that the stimulated site is critically involved in visually-based reaching movements.

3.2. Materials and Methods

3.2.1. Participants

Seventeen participants (10 females) with age ranging from 20 to 34 took part in the experiment (mean age ± SD: 25.71 ± 4.15). All subjects were right-handed, had normal or corrected-to-normal visual acuity in both eyes, and were naïve to the purposes of the experiment. Before the experimental session, each participant give his informed consent and filled-in a questionnaire to declare to suffer from no neurological, psychiatric or medical

condition that could be a contraindication for TMS use (Rossi et al., 2009; Rossini et al., 2015). Written informed consent was obtained from all participants prior to the beginning of the experiment. The study protocol was approved by the local ethical committee and the experiment was conducted in accordance with the Declaration of Helsinki.
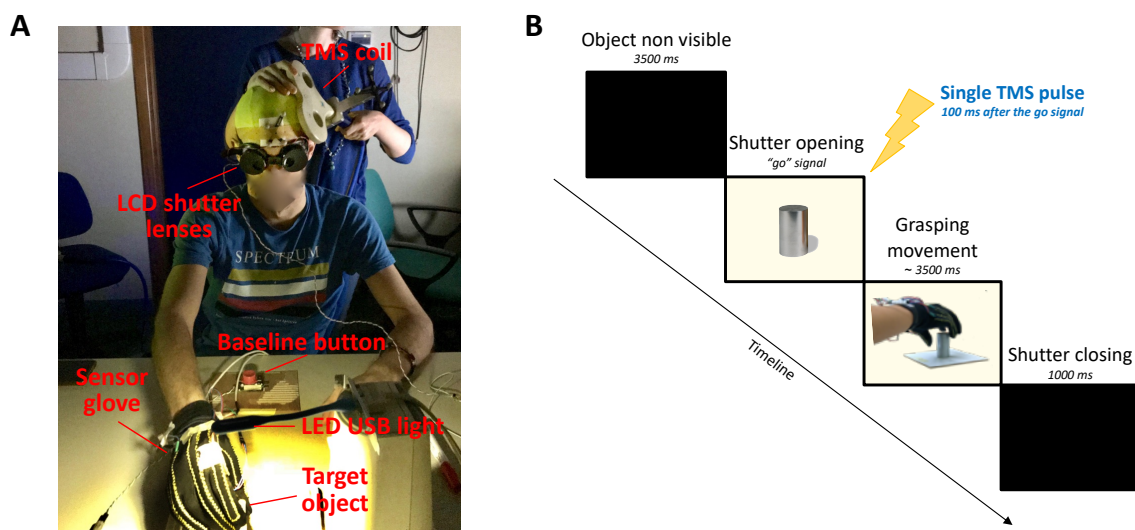
Figure 6. Experimental setting and timeline of each trial
(A) Experimental setup. Participants wore the sensor glove for fingers' extension measurement and glasses equipped with LCD shutter lenses preventing the view of the target object aligned with participant's body midline. The baseline button was placed between participants and the cylinder. A mini LED USB above the cylinder enlighten it during the grasping phase. (B) Schematic representation of the trial sequence: The object remains invisible for 3500 msec. Each movement started with the shutter opening, indicating the go signal. Participant were instructed to grasp the object and to keep the hand on the object until shutter closing (3500 msec). The following trial started after 4500 msec.

3.2.2. Apparatus

Experimental setup is represented in Figure 6A. The whole experiment was conducted in semi-dark condition and the experimental setup was alike the one adopted in the study previously introduced in this work. Participants sat comfortably in front of a table where one of the three differently sized metallic cylindric objects (height of 7 cm and diameter of 1, 3 or 5

cm, as Figure 3A) was placed by the experimenter in between trials (mean distance ± SD from nasion: 59.3 ± 3.5 cm) aligned with participants' body midline. Here too, the objects were glued to a 15x15-cm plywood that perfectly fitted the polystyrene base fixed on the table, in order to make cylinders' position stable. We placed the baseline button on the table between the participant (mean distance ± SD: 40.2 ± 2.6 cm) and the object (mean distance ± SD: 26.2 ± 2.2 cm) and instructed subjects to maintain the baseline position (i.e., all right hand's fingers pointing down on the button) during the rest phases of the trials. Notably, in this experiment the baseline button was connected to one of the computers to provide the measure of the reaction times (RTs), so that RTs were recorded as soon as participants leave the baseline button. The distances between the elements of the experimental setting (the participant, the object's support base and the button) were set according to what each subject referred to find comfortable to perform the required movements. In addition, participants wore custom-built glasses with LCD shutter lenses, controlled by a specific voltage (5 V) administered by a Power1401 analog-digital converter (Cambridge Electronic Design, CED, UK), that makes them opaque or transparent, so that subjects could see the object to grasp only from the "go" signal just before the beginning of the grasping movement. Moreover, since experiments were conducted in the dark, a flexible mini-LED USB light was placed over the object to be grasped, and connected to the analog-digital converter that administered the output by which the light was turned on. The experimenter sat on the opposite side of the table to change the objects before each trial. A screen pointed toward the experimenter informed him on which of the three objects had to be placed on the support.

3.2.3. Procedure and experimental design

Timing of each experimental trial is represented in Figure 6B. Participants maintained the baseline position in the dark, since the LED USB light was off and the LCD shutter lenses

were closed. When the "go" signal occurred, they were instructed to leave the baseline position to reach and grasp – without lift – the cylinder from the top using all their fingers. The "go" signal was represented by 3 different events that happened simultaneously: first, a "beep" sound; second, the opening of the LCD shutter lenses, so that they became transparent and allowed the view of the object; third, the mini LED USB light turned on to facilitate the view of the object. Thus, participants were asked to maintain the grip on the object until the light turned off and the lenses became opaque (3500 ms after the "go" signal). When the object was occluded from the view, participants returned to the baseline position and waited for the subsequent "go" signal (after ~4500 ms).

Single-pulse transcranial magnetic stimulation (spTMS) was delivered 100 ms after the "go" signal over 8 different spots of the left premotor area and 2 sham sites, for a total of 10 sites of stimulation. Therefore, we had a 3 × 10 factorial design, consisting of factors SIZE (3 levels: small, medium, large) and TMS (10 levels, one for each stimulated spot) which led to 30 trial types. Each trial type was presented 18 times, for a total of 540 trials that were divided in 20 blocks. In each block participants performed 27 reach-to-grasp actions (9 for each object size) while we stimulated one of the 10 TMS sites (8 active, 2 sham); therefore, there were 180 trials in total, separated into 10 blocks. This led to a total of 54 grasping movement (18 for each object size) for each stimulated site. The order of the first 10 blocks (one for each stimulation site) was pseudo-randomized so that the TMS conditions were equally distributed across participants. After performing the first 10 blocks the order of the remaining 10 blocks was reversed relative to the first part. In doing so, we ensured to minimize any carry over effects related to stimulation site. Each experimental session lasted approximately 3 hours.

3.2.4. Grip aperture measurement

Similarly to previous investigations of fingers dynamics (Dipietro et al., 2003; Fricke et al., 2017, 2019; Gentner & Classen, 2009; Kumar et al., 2012) and the evaluation study introduced in chapter 2, kinematics information on finger movements was acquired by means of our custom-made glove in which four 114 mm long flexion sensors (flexsensors 4.5'' – Spectrasymbol, USA) were embedded over the metacarpophalangeal and proximal interphalangeal joints of the thumb, index, middle and little fingers. Note that, in the light of results of the evaluation experiment, we made use only of those sensors whose signal was informative of effective fingers' flexion relative to the grasping of the same three differently sized cylinders adopted in the present experiment too (see chapter 2). As in the previous study, the analog-digital converter was used to connect the glove to the computer and in which the Signal software acquired the signal from each sensor and showed a clear and steady pattern related to the trial phase (see Figure 8 for an example). For more specific technical details on glove's assembly and setting, see the section "Grip aperture measurement" of the chapter 2. We used software OpenSesame (Mathôt et al., 2012) was used for auditory stimuli presentation and to trigger the analog-digital converter that, in turn, triggered the LCD shutter lenses, the mini LED USB light, the TMS and the Signal software to record a frame of fingers' movement for each trial.
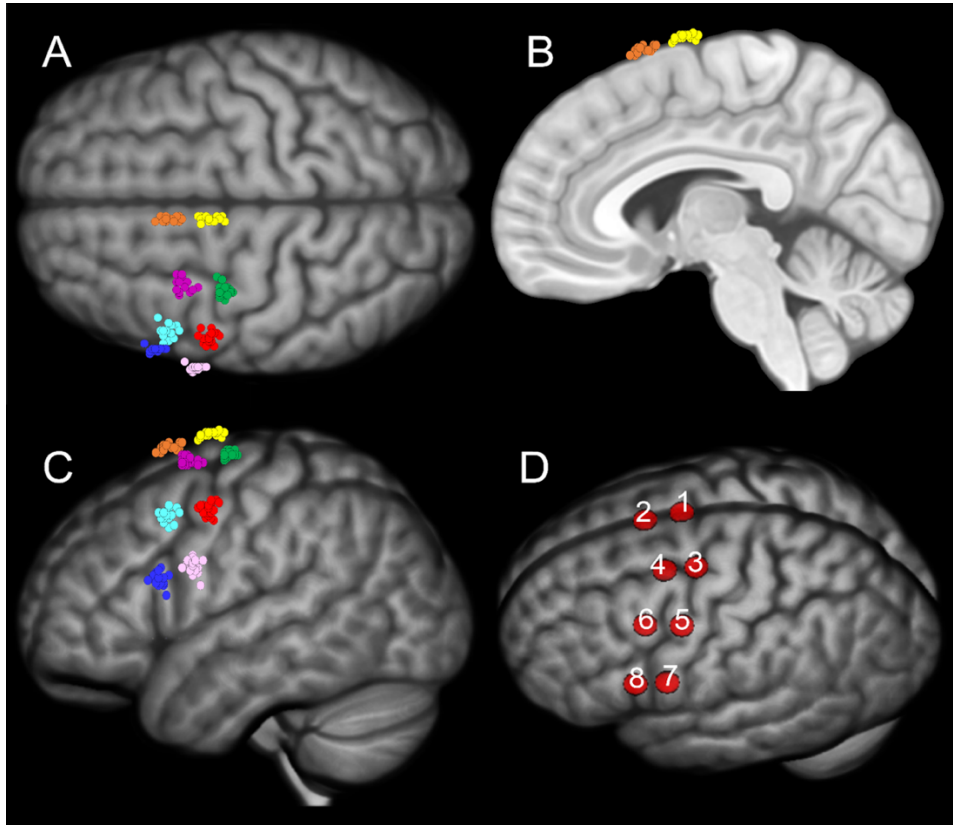
Figure 7. The 8-spot grid of target-foci

The grid was designed to cover the whole premotor region along its medio-lateral dimension, form the midline to the ventral region. Each spot for each participant is visualized in MNI space in the superior (A), medial (B) and lateral (C) view. A schematic illustration of nemrated 8 stimulation sites is represented is figure 7D.

Spots	x	y	z
1	-8 (0.9)	-1 (3.1)	80 (1.1)
2	-8 (0.8)	14 (3)	75 (1.3)
3	-36 (2.7)	-8 (4.5)	72 (1.3)
4	-35 (2.2)	6 (2.5)	70 (1.4)
5	-54 (2.1)	-1 (2.1)	50 (2.5)
6	-51 (2.6)	14 (2.1)	48 (2.4)
7	-68 (0.8)	5 (2)	28 (2.9)
8	-64 (0.8)	18 (2.1)	22 (2.6)

Table 3

MNI coordinates of the 8 target-foci numerated as in Figure 7D. Mean (SD) values of coordinates for all the seventeen participants are given.

3.2.5. Neuronavigation

All participants underwent high-resolution MP-RAGE anatomical MRI scans. Individual anatomical scans were converted to the nifti format and loaded on a neuronavigation software (SofTaxic, E.M.S., Bologna, Italy). Surface renderings of the brain surfaces were used to mark an 8-spot grid covering the whole premotor region. As shown in Figure 7, the grid had a 2x4 structure, with the long side extending along the medio-lateral dimension, form the midline to the ventral premotor region and the short side extending along the caudal-cranial direction. The spots were localized according to individual anatomical landmarks. First, we localized the 4 spots of the posterior row (spots 1, 3, 5 and 7) in the following way: spot 1 was localized 5 mm lateral to the midline, 5 mm anterior to the end of the paracentral lobule. Spot 4 was localized in the apex of the crown of the precentral gyrus, 10 mm inferior to the junction between the precentral sulcus and the inferior frontal sulcus. Spots 2 and 3 were localized along an imaginary line connecting spots 1 and 4, at equal spacings. The anterior row was set by simply moving 2 cm cranial from the 4 spots of the posterior row. While images in native space were used for actual neuronavigation, all individual brains and grids were also normalized to MNI space to allow for inter-individual comparisons and group analysis. Mean MNI coordinates of the 8 stimulated points are reported in Table 3. Furthermore, two spots (sham 1 and sham 2) where sham stimulation was to be applied, were localized in the dorsal and ventral part of PMC as control condition. A 3D optical digitizer (Polaris Vicra, NDI, Waterloo, Canada) was used in combination with the SoftTAxic neuronavigation software to co-register in the same virtual space the participant's head, the digitizer pen and the TMS coil throughout the whole experiment to monitor coil position on every spot of the grid.

3.2.6. Transcranial Magnetic Stimulation (TMS)

SpTMS were delivered 100 ms after the "go" signal using a Magstim Super Rapid2 system (Magstim Company, Whitland, UK) with a 70-mm figure-of-eight stimulation coil placed over the stimulation sites tangentially to the skull, with the handle pointing backward at a 45° angle from the midsagittal line. During the sham stimulation the coil was held at a 90° position to ensure that the magnetic field did not stimulate any area. Indeed, this sham condition has been proven to be ineffective in producing an electric field capable of changing neuronal excitability (Lisanby et al., 2001). In a preliminary phase, we measured the resting motor threshold (rMT) of each participant, so that the intensity of sp-TMS was set 120% of the individual rMT and was kept constant between sessions. rMT was estimated using the software Motor Threshold Assessment Tool, version 2.0 (http://www.clinicalresearcher.org/software.htm) that uses an adaptive threshold tracking algorithm (Awiszus, 2003) instead of the canonical 'relative frequency' method. A MEP ≥ 50 μV peak-to-peak amplitude was fed back to the software as valid response (Rossi et al., 2009). Electromyographic recordings were made with 10-mm Ag/AgCl surface cup electrodes. The active electrode was placed over the FDI muscle of the right hand and the reference electrode over the metacarpo-phalangeal joint of the index finger. The electromyographic signal was sampled and amplified 1000x by using a Digitimer D360 amplifier (Digitimer Ltd, Welwyn Garden City, UK) and digitized by the abovementioned Power CED analog-digital converter at 5kHz sampling rate, band-pass filtered 10Hz-2KHz and then stored using the Signal software. The rMT of our participants varied between a range of 42% and 63% of the maximum stimulator output (mean rMT ± SD: 53% ± 5.9%); hence, the stimulation intensity was in a range between 50% and 76% of the maximum stimulator output (mean rMT ± SD: 63% ± 7.1%). For each participant we carefully checked firstly whether TMS pulses caused discomfort

and secondly whether stimulation over the 8 premotor spots evoked any MEPs and re-assessed the grid spots if this was the case.
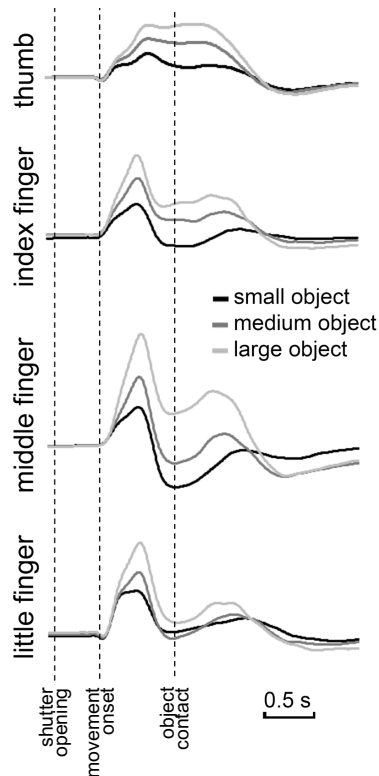
Figure 8. Example of recording of the first participant
Example of the flexion of the four sensors (thumb, index finger, middle finger and little finger) as a function of object size (small, medium, large cylinder). Each stage of the movement (baseline during the shutter opening, movement onset and contact with the object) is clearly detectable from sensors' pattern.

3.3. Data analysis

Data-driven classification algorithms to process our data was programmed. The output of each trial was the raw recordings from each of the 4 flexion sensors, starting in the resting position (baseline level), opening during reaching and closing upon the object (see Figure 8 for an example of recording). From the raw signal the following data were extracted: 1) The flex-sensor values corresponding to the peak finger aperture, defined as the difference between

initial baseline flex-sensor values and maximum peak value during reaching. This value is indicative of the maximum angle that the phalanxes form with respect to each other. We will refer to these as "peak aperture" 2) The peak velocity of flex-sensor signal while reaching peak aperture; we will refer to this value as "peak angular velocity". 3) the time of movement onset, corresponding to the time between the opening of the shutter lenses and the release from the response button (RTs). Peak aperture and peak angular velocity were analyzed by means of a classification procedure, which is aimed at building a model able to predict the category of an unknown object (among a set of pre-specified categories; Duda et al., 2001; Bishop et al., 2006; Rajkomar et al., 2019). In particular, in our study, for a given subject (and a given stimulation), the capability of a classifier in discriminating between the three different cylinders (small *vs.* medium *vs.* large), based on finger openings, was measured. The idea is that we can assess the impact of the stimulation on the subject by measuring the decrease in classification accuracy (i.e., if the task becomes more difficult for the classifier when the subject is stimulated). More in detail the following strategy was adopted:

- **Step 1.** For a given subject Sub_i and a given state $Stat_j$ (i.e., stimulation site) we define a classification problem in which every object is a single repetition of the given task (grasping the cylinder) done by the subject Sub_i who has been stimulated in the state $Stat_j$. Every experiment is described with the four opening values, and has associated the label 1, 2, or 3 according to the grasped cylinder, as shown in Table 4.

Repetition	Opening	Labels
1	$\mathbf{x}_1 = [x_{11}, x_{12}, x_{13}, x_{14}]$	$c_1\ (1, 2,\ or\ 3)$
2	$\mathbf{x}_2 = [x_{21}, x_{22}, x_{23}, x_{24}]$	$c_2\ (1, 2,\ or\ 3)$
…	…	…
N	$\mathbf{x}_N = [x_{N1}, x_{N2}, x_{N3}, x_{N4}]$	$c_N\ (1, 2,\ or\ 3)$

Table 4
Structure of experimental variables for the classification procedures.

- **Step 2.** For every classification problem (namely, for every subject-state), a classifier was chosen to calculate its classification accuracy with a cross-validation strategy, i.e. a mechanism which permits to test the classifier using objects not present in the training set (the set of objects used to learn the classifier). This ensures to estimate the generalization capability of the given classifier, that is its capability in classifying also objects not present in the training set (Duda et al., 2001). We used the variant called Leave-One-Out (LOO; Bramer, 2016), that should be preferred when the number of instances in a dataset is small (Wong, 2015). The procedure is as follows: in the first step, the classifier is trained with all the objects except the first, which is then used for testing; if the label predicted by the classifier is different that the true label of the testing object, then an error occurred. The scheme is then repeated by leaving out the second object and so on, until all objects have been tested. The final classification accuracy is measured as the number of the objects which have been correctly predicted by the classifier, divided by the total number of objects. Using this scheme, the testing set is always separated from the training set (this permits to measure generalization capabilities), whereas the size of the training set is maximized (this permits to have good estimates of the classifiers). An additional advantage of the Leave One Out is that it does not involve a randomness mechanism and, therefore, research reproducibility is allowed. In order to increase the significance of the results, different classifiers were used (Duda et al., 2001; Bishop, 2006), which ranged from the simple nearest neighbor up to more complex classifiers like Support Vector Machines or Random Forests. More in details, the following classifiers were used:

1) (1nn): The classic Nearest Neighbor rule, in which the testing object is assigned to the class of its most similar training object (i.e., the nearest object of the training set). Here we used the Euclidean Distance as proximity measure, employing the matlab prtools library (http://prtools.tudelft.nl/, Duin et al., 2000a) implementation `knnc`.

2) (knn(opt K)): The K-Nearest Neighbor rule, which generalizes the nearest neighbor by assigning an unknown object to the class most frequent inside its K most similar points of the training set (the K nearest neighbors of the testing object). Also in this case, we used the Euclidean Distance, and we found the optimal K using another Leave One Out strategy on the training set (as provided in the `knnc` routine of the prtools library).

3) (ldc): The Linear Discriminant Classifier, a probabilistic classifier which implements the Bayes Decision Rule: in this case every class is modelled with a different Gaussian distribution, and the covariance matrix is shared among the different classes. In particular, the joint covariance matrix is the average of the class specific covariance matrices, each one weighted by the a priori probability (function `ldc` of prtools).

4) (qdc): The Quadratic Discriminant Classifier, which is similar to `ldc` but the covariance matrix is different for every class (function `qdc` of prtools).

5) (svm): The Support Vector Machine (Cristianini & Shawe-Taylor, 2000), a classifier based on the Statistical Learning Theory. Here the rbf kernel was used with the scale parameter automatically estimated on the training set (as provided in the Matlab Statistics and Machine Learning toolbox routine fitcsvm).

6) (RF-100): The Random Forest classifier, an effective classifier (Breiman, 2001), based on an ensemble of decision trees. Here the routine TreeBagger from the Statistics and Machine Learning toolbox was used using 100 trees.

    - **Step 3.** At the end of the previous step 17 accuracies (corresponding to the 17 subjects involved in the study) have been computed for every state stimulation and for every classifier. In order to see the impact of the stimulation in a given state $Stat_j$ we can compare the accuracy obtained in such state with the accuracy obtained in the Sham state. In order to have a more robust estimation of the Sham (i.e., the baseline accuracy), the accuracies obtained in the Sham1 and Sham2 were averaged.

- Step 4. Moreover, in order to have a statistical significance, we performed a pair t-test to compare the 17 accuracies obtained by a given classifier in a given state with the accuracies obtained by the same classifier in the sham state, with the hypothesis that the two matched samples come from distributions with equal means (i.e., the difference between them is assumed to come from a normal distribution with unknown variance). Significance level was set at 0.05, and multiple tests were corrected by the Bonferroni rule. The effect of TMS on RTs was tested using a linear mixed model using R (R Development Core Team, 2016) and the lme4 package (version 1.1-12; Bates et al., 2015). Statistical significance was tested with the F-test with Satterthwaite approximation of degrees of freedom. The experimental factor TMS (the 8 active spots and the collapsed sham spots), SIZE (small *vs.* medium *vs.* large) and their interaction were entered as fixed-effect factors in a linear mixed model that predict reaction times (the sham condition was the reference level for all comparisons). Random 320 coefficients across participants were estimated for intercept and for the factor TMS.

- Data visualization. Data of one of the subjects are visualized in Figure 9 for illustration purposes. The plots represent the first two principal components of each set of experiments. More in details, each flexor sensor (represented with 4 values) was projected in a bi-dimensional space, using a classic and well-known linear transformation, the Principal Component Analysis (Jolliffe, 2002) (in particular we used the matlab prtools library [prtools] (Duin et al., 2000b) implementation pcam).
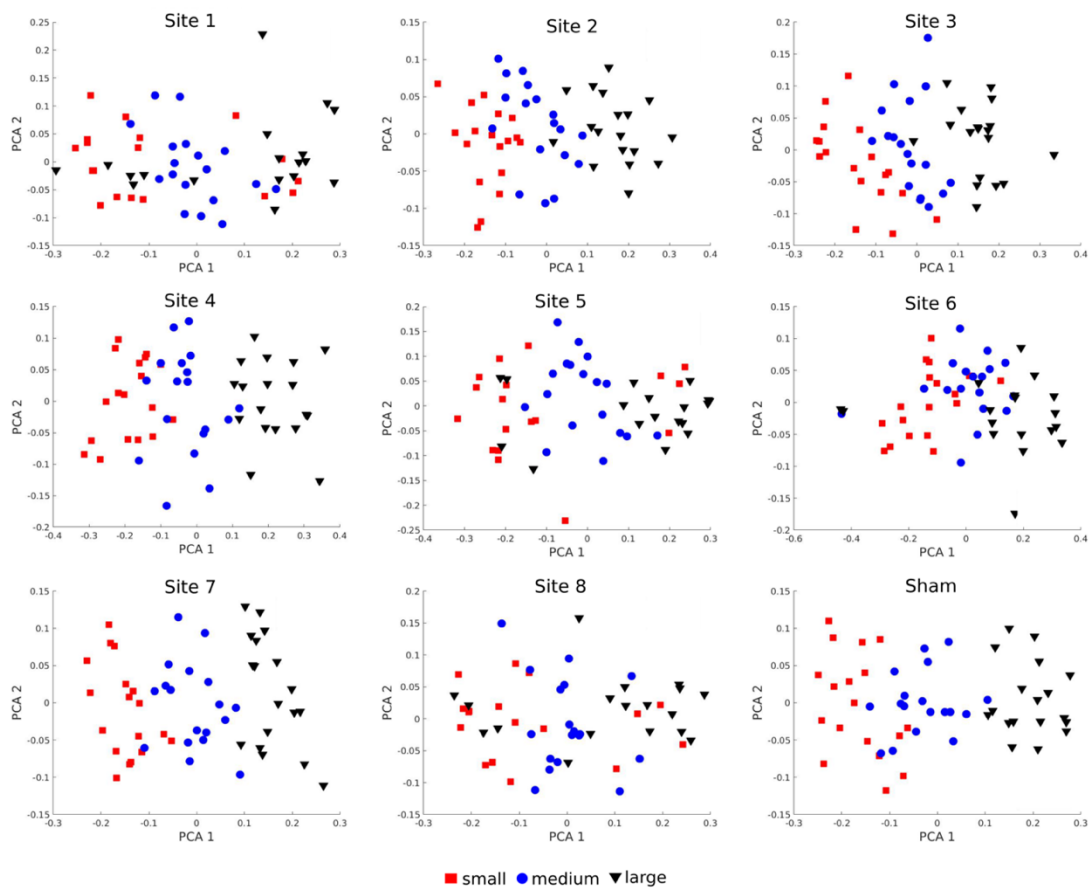
Figure 9. Principal components

Example of the first two principal components (PCA) for each stimulation site extracted from the four flexion sensors data of one the participants.

3.4. Results

3.4.1. Peak aperture

Mean accuracy and statistics for the six different classifiers as a function of the 8 premotor stimulation sites are indicated in Table 5. Results indicated that, overall, the accuracy of the six classifiers in discriminating the grip aperture associated with the three cylinders during the sham stimulation, as well as the accuracy with which the active TMS will be compared, is 63%, which is significantly higher compared to a random classifier (random classifier accuracy = 33%, $p < 0.01$). Overall, results consistently indicated that the accuracy of

the classifiers under active TMS is significantly reduced compared to sham condition during the stimulation of the site 1 in the medial part of PMC (mean accuracy = 46%), site 5 in PMv (mean accuracy = 52%) and site 8 in PMv (mean accuracy = 52%).
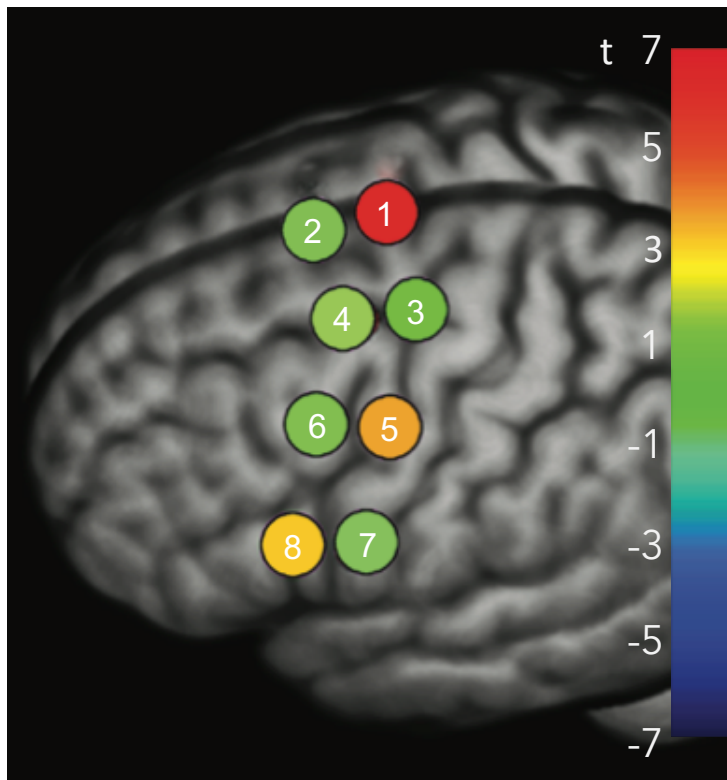
Figure 10. Statistical map projected on the brain of the average t-values per site across the six classifiers

Negative t-values indicate a better ability of the classifiers to discriminate the three object sizes compared to the sham control condition. Positive t-values indicate a worse ability of the classifiers to discriminate the three objects compared to the sham control condition. Significative decrease of classifiers' accuracy was observed after the stimulation of sites 1 (mean accuracy = 46%), 5 (mean accuracy = 52%), and 8 (mean accuracy = 52%).
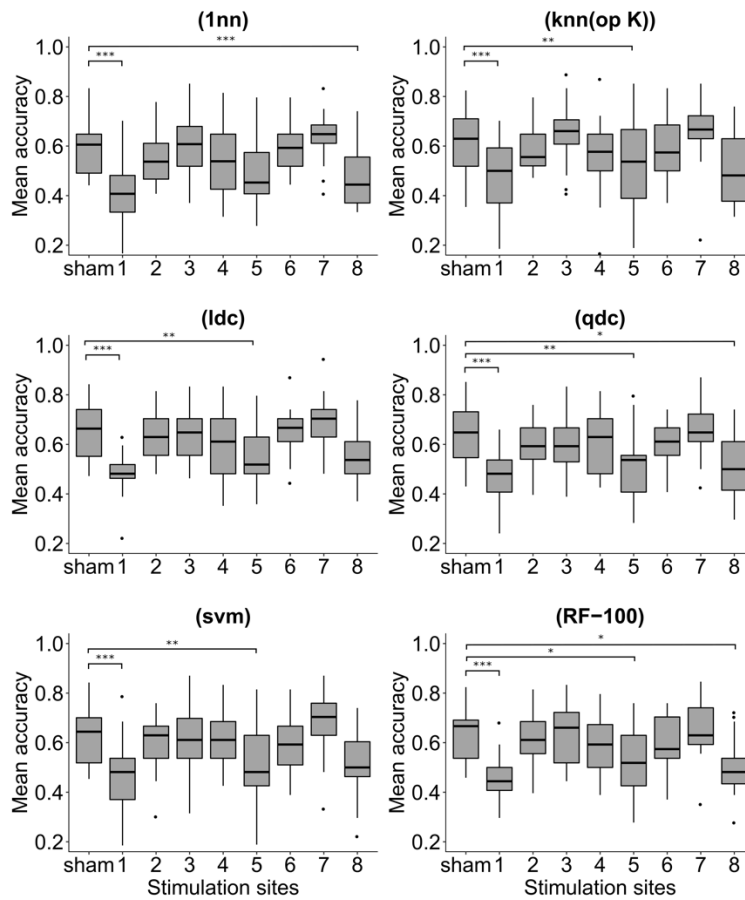
Figure 11. Mean classification accuracy for the six classifiers as a function of the 9 stimulations (8 active + sham)

Analysis revealed a decreasing of classifiers' accuracy in discriminating the three objects during the stimulation of sites 1 (all six classifiers), 5 (five out of six classifiers) and 8 (three out of six classifiers) compared to sham stimulation. No significant decrease of classifiers' accuracy emerged after the stimulation of sites 2, 3, 4, 6 and 7 compared to sham. Asterisks indicated the significant contrasts between sham and the active spots (*** < 0.001; ** < 0.01; * < 0.05; corrected).

More specifically, analysis indicated that after the stimulation of the site 1 the accuracy is significantly reduced for all the six classifiers ((1nn): $t(16) = 6.39$, $p < 0.001$; (knn (opt K)): $t(16) = 5.41$, $p < 0.001$; (ldc): $t(16) = 6.38$, $p < 0.001$; (qdc): $t(16) = 6.53$, $p < 0.001$; (svm): $t(16) = 6.39$, $p < 0.001$; (RF-100): $t(16) = 6.72$, $p < 0.001$; see Figure 10). Analogously, stimulation of site 5 significantly impaired the accuracy of five out of six classifiers compared to the sham stimulation ((knn (opt K)): $t(16) = 3.91$, $p = 0.009$; (ldc): $t(16) = 4.22$, $p = 0.005$; (qdc): $t(16) = 4.43$, $p = 0.003$; (svm): $t(16) = 3.68$, $p = 0.01$; (RF-100): $t(16) = 3.35$, $p = 0.003$).

Classifiers

TMS site	Overall mean accuracy (%)	(1nn) Mean accuracy (%)	t	p	(Knn (opt K)) Mean accuracy (%)	t	p	(ldc) Mean accuracy (%)	t	p	(qdc) Mean accuracy (%)	t	p	(svm) Mean accuracy (%)	t	p	(RF-100) Mean accuracy (%)	t	p
1	**46%**	**41.9%**	**6.39**	**< 0.001**	**47.5%**	**5.41**	**< 0.001**	**47.5%**	**6.38**	**< 0.001**	**47.2%**	**6.53**	**< 0.001**	**46.2%**	**6.39**	**< 0.001**	**46.6%**	**6.72**	**< 0.001**
2	60%	56.1%	1.61	1.0	59.5%	0.57	1.0	63.5%	0.87	1.0	60.2%	1.42	1.0	58.7%	1.56	1.0	61.7%	0.84	1.0
3	62%	61.0%	0.25	1.0	64.6%	1.19	1.0	63.2%	0.90	1.0	60.1%	1.36	1.0	61.7%	0.26	1.0	63.2%	0.17	1.0
4	60%	53.6%	1.98	0.51	55.1%	1.81	0.71	60.6%	1.98	0.51	60.5%	1.01	1.0	59.7%	1.17	1.0	58.1%	1.86	0.65
5	**52%**	49.2%	2.94	0.07	**50.5%**	**3.91**	**0.009**	**55.4%**	**4.22**	**0.005**	**51.1%**	**4.43**	**0.003**	**51.2%**	**3.68**	**0.01**	**52.7%**	**3.35**	**0.03**
6	60%	59.3%	0.28	1.0	58.5%	1.17	1.0	64.6%	0.52	1.0	60.0%	1.37	1.0	59.1%	1.49	1.0	60.0%	1.48	1.0
7	66%	63.3%	1.44	1.0	64.6%	1.60	1.0	69.3%	1.67	0.90	65.5%	0.69	1.0	66.3%	1.58	1.0	65.2%	0.51	1.0
8	**52%**	**47.3%**	**3.78**	**0.01**	52.2%	2.63	0.14	55.9%	2.81	0.10	**52.0%**	**3.17**	**0.04**	52.2%	2.57	0.16	**50.7%**	**3.89**	**0.01**
Sham	63%	60.1%			61.0%			65.7%			63.8%			62.6%			63.9%		

Note: Degree of freedom for all tests are 16

Table 5
Mean accuracy and statistics (t-values and p-values, Bonferroni correction) for the six different classifiers, as a function of the 8 premotor stimulation sites.

56

Finally, three out of six classifiers failed in discriminating the movements toward the three different objects after the stimulation of the site 8 ((1nn): $t(16) = 3.78$, $p = 0.01$; (qdc): $t(16) = 3.17$, $p = 0.04$; (RF-100): $t(16) = 3.89$, $p = 0.001$). Results indicated that the accuracy of all the six classifiers was comparable between the sham and the stimulation site number 2 (all $p = 1.0$), number 3 (all $p = 1.0$), number 4 (all $p > 0.51$), number 6 (all $p = 1.0$), and number 7 (all $p > 0.9$; see Figure 10 and Figure 11 and Table 5 for details). In order to further inspect what specifically drove the reduced classifiability of movement kinematics after TMS stimulation, we plotted the difference between the mean peak aperture in each active spot and the sham condition, as a function of sensors, object size and stimulation sites (see Figure 12). Positive values of such difference indicate a greater mean aperture compared to the sham condition and negative values smaller mean aperture compared to the sham in the same condition. Therefore, the visual inspection of the data consistently shows that under the stimulation of spots 1, 5 and 8 participants tended to overestimate the size of the smaller object and to underestimate the size of the larger object compared to the sham control condition, a pattern that is likely the reason of the reduced accuracy of the classifiers to correctly discriminate hand's kinematics relative to the three object sizes.
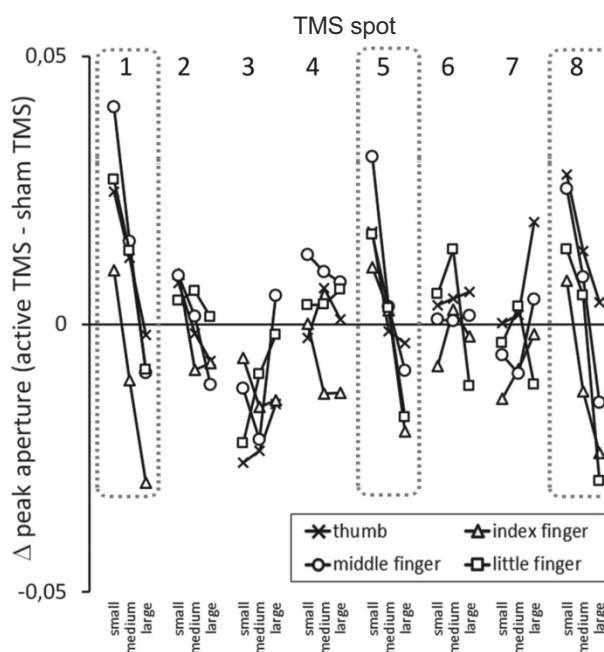
Figure 12. Peak aperture in each active spot as a function of sensors, object size and stimulation sites
The difference between peak aperture values in the active condition minus the peak aperture in the sham condition is shown, separately for each sensor (thumb, index, middle and little finger), for each object (small, medium and large) and for each stimulation site. Positive values indicate that active TMS is associated with a greater mean aperture compared to the sham condition. Vice-versa, negative values indicate that TMS is associated with smaller mean apertures compared to the sham condition. Dashed lines indicate spots 1, 5 and 8 in which TMS reduced classifiability of object in the main analysis.

3.4.2. Peak angular velocity

Following the same logic of the peak aperture analysis, for a given subject and a given stimulation, the capability of a classifier in discriminating the three cylinders was measured basing on maximum fingers opening velocity. Overall, the results corroborated and strengthened the results concerning the peak aperture. Indeed, analysis consistently indicated that the accuracy of the classifiers is significantly reduced after the stimulation of the site 1 (mean accuracy = 35%), 5 (mean accuracy = 36%) and 8 (mean accuracy = 36%) compared to sham stimulation (mean accuracy = 57%). Mean accuracy and statistics for the six different classifiers, as a function of the 8 active stimulations are indicated in Table 6.

Classifiers

TMS site	Overall Mean Accuracy (%)	(1nn)			(Knn (opt K))			(ldc)			(qdc)			(svm)			(RF-100)		
		Mean accuracy (%)	t	p	Mean accuracy (%)	t	p	Mean accuracy (%)	t	p	Mean accuracy (%)	t	p	Mean accuracy (%)	t	p	Mean accuracy (%)	t	p
1	35%	37.8 %	4.46	< 0.001	33.8%	5.42	< 0.001	36.6%	7.60	< 0.001	34.3%	7.57	< 0.001	34.2%	5.67	< 0.001	34.6%	6.71	< 0.001
2	54%	53.2%	0.28	1.0	53.8%	0.66	1.0	55.6%	1.65	0.93	53.6%	1.93	0.56	54.0%	0.96	1.0	54.0%	0.74	1.0
3	54%	53.2%	0.24	1.0	55.0%	1.19	1.0	56.5%	1.17	1.0	52.9%	2.58	0.15	52.7%	1.60	1.0	53.8%	0.91	1.0
4	54%	49.7%	1.12	1.0	54.5%	0.36	1.0	56.6%	0.91	1.0	54.2%	1.76	0.77	52.0%	1.94	0.55	56.6%	0.21	1.0
5	36%	36.0%	7.58	< 0.001	30.1%	6.04	< 0.001	40.2%	6.20	< 0.001	39.1%	7.57	< 0.001	33.4%	9.91	< 0.001	37.2%	8.46	< 0.001
6	57%	56.0%	1.50	1.0	55.2%	0.16	1.0	60.8%	0.73	1.0	57.5%	0.73	1.0	55.8%	0.58	1.0	55.3%	0.42	1.0
7	58%	56.3%	1.68	0.89	54.0%	0.40	1.0	60.0%	0.25	1.0	59.1%	0.22	1.0	57.1%	0.14	1.0	59.1%	1.14	1.0
8	36%	34.5%	5.23	< 0.001	36.0%	4.25	0.004	38.1%	7.20	< 0.001	35.1%	6.11	< 0.001	34.3%	6.20	< 0.001	35.1%	3.89	< 0.001
Sham	57%	52.5%			55.6%			59.4%			58.6%			56.9%			56.0%		

Note: Degree of freedom for all tests are 16

Table 6

Peak angular velocity: Mean accuracy and statistics (t-values and p-values, Bonferroni correction) for the six different classifiers, as a function of the 8 premotor stimulation sites.

More in details, analysis indicated that the accuracy is significantly reduced after the stimulation of the site 1 in the medial part of PMC, for all the six classifiers considered, ((1nn): $t(16) = 4.46$, $p < .001$; (knn (opt K)): $t(16) = 5.42$, $p < .001$; (ldc): $t(16) = 7.60$, $p < .001$; (qdc): $t(16) = 7.57$ $p < .001$; (svm): $t(16) = 5.67$, $p < .001$; (RF-100): $t(16) = 6.71$, $p < .001$). Furthermore, analysis also demonstrate that, overall, the six classifiers are less accurate in discriminating the three cylinders after stimulation of site 5 in PMv (mean accuracy = 36%), compared to the sham stimulation (mean accuracy = 57%). All the six classifiers showed significantly lower accuracy compared to the sham conditions ((1nn): $t(16) = 7.58$, $p < .001$; (knn (opt K)): $t(16) = 6.04$, $p < .001$; (ldc): $t(16) = 6.20$, $p < .001$; (qdc): $t(16) = 7.57$, $p < .001$; (svm): $t(16) = 9.91$, $p < .001$; (RF-100): $t(16) = 8.46$, $p < .001$). Finally, the overall accuracy was also reduced after stimulation of the lateral part of the ventral premotor cortex, site 8 (mean accuracy = 36%), compared to the sham control conditions. Also for site 8, all the six classifiers are significantly less able to discriminate the movements toward the three different objects, compared to the sham ((1nn): $t(16) = 5.23$, $p < .001$; (knn (opt K)): $t(16) = 4.25$, $p = .004$; (ldc): $t(16) = 7.20$, $p = p < .001$; (qdc): $t(16) = 6.11$, $p < .001$; (svm): $t(16) = 6.20$, $p < .001$; (RF-100): $t(16) = 6.43$, $p < .001$).
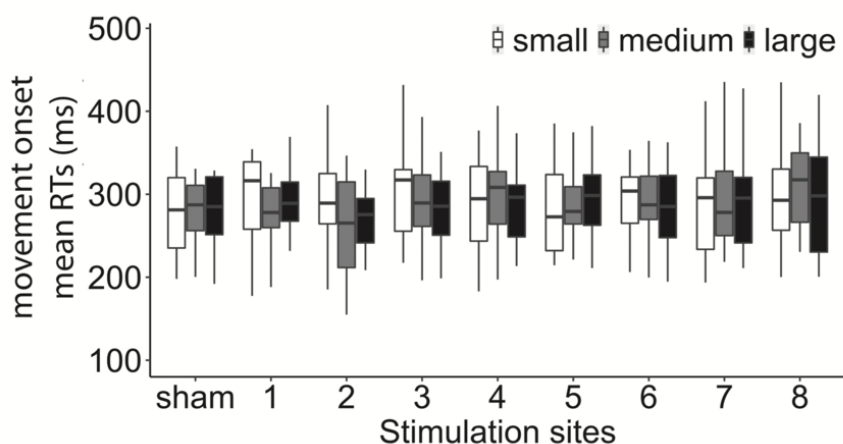
Figure 13. RTs as a function of TMS and size

Mean reaction times (ms) of movement onset as a function of the 9 stimulation sites (8 + 761 sham) and the three different objects (small, medium and large). No significative modulation of RTs was observed as a function of the TMS stimulation or the object size (all $p > 0.4$).

3.4.3. Reaction times

The recorded RTs (mean ± SD) were 299 ± 111 ms and median RTs was 281 ms. The analysis revealed a non-significant main effect of TMS ($F_{8,15.3} < 1$, $p = 0.9$), indicating that overall TMS did not significantly affect the start of the movement (all contrasts, $p > 0.4$), as well a non-significant main effect of size ($F_{2,5830.3} < 1$, $p = 0.6$). The interaction between TMS and size was also non-significant ($F_{16,5827.8} < 1$, $p = 0.5$, Figure 13).

3.5. Discussion

3.5.1. Main findings

We adopted a dense TMS approach and a hypothesis-free data analysis to draw a functional map on the whole premotor region to causally determine the role of each of its regions in visually-guided reach-to-grasp movements. We found that TMS altered fingers'

configuration during the reaching when applied over spots located in PMv and a single spot located near the midline, putatively corresponding to the supplementary motor area (SMA). In line with previous findings (Davare et al., 2006), TMS over these foci modulated kinematic parameters associated to the correct hand posture configuration, but not the time of movement onset. Therefore, our results indicate a critical role of those spots in direct visuomotor transformation. The present findings corroborate a robust body of evidence from both human and non-human primates showing hand-related information in the ventral portion of the PMC. More importantly, the present study is the first to directly indicate a causal involvement of the medial portion of PMC in mediating visuo-motor transformations during a visually-guided grasping movement.

3.5.2. Grasp information within PMv

We observed that TMS over two different spots within PMv disrupted the hand pre-shaping during reaching. This is because the classifiers consistently indicated a lower accuracy in object size discrimination while stimulating the spot located in the medial PMv and the one on the lateral-anterior PMv compared to the control sham stimulation. This result reinforces a considerable amount of evidence from both human (Cavina-Pratesi et al., 2010; Filimon, 2010; Grol et al., 2007; Turella & Lingnau, 2014; Vesia et al., 2017) and non-human primates (Brochier & Umiltà, 2007; Jeannerod et al., 1995; Tanné-Gariépy et al., 2002), attesting PMv as a crucial node in the visuo-motor transformation for grasp movements.

Monkeys' PMv consists of F5 and F4 areas. Several electrophysiological studies demonstrated that the activity of PMv neurons is strictly selective to code the grip configuration based on the intrinsic properties of the object to be grasped, thus confirming the role of PMv in shaping the hand posture appropriately for the target object (Murata et al., 1997; Raos et al., 2005; Rizzolatti & Luppino, 2001). Area F5 contains visuomotor ("canonical") neurons which

are active during both a grasping execution and the observation of grasping movements performed by others (Bonini et al., 2014b; Di Pellegrino et al., 1992; Rizzolatti et al., 2014). Furthermore, selective inactivation of monkeys' PMv leads to severe deficits in the grasping component of reach-to-grasp movements, keeping the reaching component unaffected (Fogassi et al., 2001). Analogously, TMS studies conducted in humans proved that stimulation of both the left and the right PMv (but not PMd) interfere with hand pre-shaping (Davare et al., 2006). Crucially, this effect was observed exclusively when the TMS was delivered 50 and 100 msec after the "go" signal but not later, thus suggesting an early involvement of PMv during hand movement preparation. For this reason, we chose to deliver TMS to our participants 100 ms after the "go" signal.

To conclude, we observed that, after early PMv stimulation, the classifiers were less able to associate the grip aperture to the small, medium or big cylinder. Such a decrease in the classification accuracy is a direct evidence that the PMv stimulation interferes with the hand configuration during the grasping movement.

3.5.3. Grasp information within SMA

To the best of our knowledge, our results provide the first causal evidence in human of the involvement of SMA in coding the grasping components of goal-directed hand behaviors. This novel finding is in line recent studies conducted in non-human primates that proved that neurons within the pre-supplementary motor area (area F6) are involved in the integration of visuomotor transformation for grasping (Gerbella et al., 2017; Lanzilotto et al., 2016; Livi et al., 2019). Activity of area F6, anatomically connected to the premotor and parietal areas of the grasping network (Gamberini et al., 2009; Gerbella et al., 2011; Luppino et al., 1993; Luppino et al., 2003; Rozzi et al., 2006), is typically associated with motor preparation of reach-to-grasp movements (Rizzolatti et al., 1990). Electrophysiological investigations showed that motor and

visuomotor neurons of area F6 shared common features with neurons in area F5 within PMv, thus suggesting a functional interplay between these F5 and F6 areas (Lanzilotto et al., 2016). In the light of these findings, a revision of the neural grasping network including F6 has been proposed (Bonini, 2016; Gerbella et al., 2017; Lanzilotto et al., 2016; Livi et al., 2019). Actually, the evidence about dorsal premotor areas is not surprising, if we consider that it is nicely related to the results already observed in the parietal cortex. Indeed, the grasping neurons of the medial occipito-parietal cortex (area V6A) of the macaque monkey have been consistently reported (Fattori et al., 2010, 2012). Thus, it is reasonable that grasping information represented in medial parietal regions has a counterpart in the medial premotor regions.

In human, SMA belongs to the network associated with the control of hand posture (Rizzolatti et al., 2014) and is classically associated with the planning and execution of goal-directed behaviors (Nachev et al., 2008; Rauch et al., 2013) and in motor sequence learning as well (Sakai et al., 1999). Nonetheless, its involvement in precision grip movements has been observed (for a review, see King et al., 2014). Furthermore, it is possible that such activation of SMA for reaching actions reflects a putative counterpart of the grasping information coded in medial parietal areas. Indeed, in line with evidences from monkeys, neuroimaging investigations demonstrated that preparatory activity in SPOC (the putative homolog of area V6A) accurately predicts forthcoming grasping movements (Gallivan et al., 2011, 2013). A following TMS experiment (Vesia et al., 2017) further confirmed these results, showing that the dorsomedial SPOC-M1 pathway codes for the handgrip formation during the reaching preparation.

The whole of the abovementioned data from both human and non-human primates are in line with a growing body of evidence proving that the hand-related information is coded within both the dorsolateral and the dorsomedial pathways, thus including PMv, but also a more medial-dorsal part of PMC (Fabbri et al., 2014; Gallivan et al., 2011, 2013; Monaco et al., 2015;

Turella et al., 2016; Verhagen et al., 2012). The study here introduced corroborates and significantly expand our understanding of the premotor involvement during grasping movement, demonstrating a causal involvement of the medial part of PMC in visuo-motor transformation necessary for an appropriate visually-guided behavior. Nevertheless, it would be interesting to clarify also the temporal dynamics with which the ventral and the dorsal premotor spots come into play in object-directed behavior by, for example, applying online TMS over the whole PMV with the dense spatial mapping approach at different time windows.

3.6. Conclusions

Using a dense TMS spatial mapping approach, the present study showed a detailed functional cartography of the entire premotor region, consistently indicating a multifocal representation of object geometry for reaching. Specifically, as largely demonstrated by previous findings, we confirmed that information about object's intrinsic properties that modulate hand's pre-shaping are coded in PMv. More importantly, our study provided the first evidence in human of a causal involvement of SMA in visuomotor transformation for grasping. Remarkably, our findings are enhanced by the double vantage of our approach: first, d-TMS mapping allowed to explore the whole premotor region to establish a functional premotor map for visually-guided reaching. Secondly, kinematic parameters were analyzed by means of classification algorithms in a relatively hypothesis-independent way, thus supporting our results. In accordance with monkey's literature (Gerbella et al., 2017; Lanzilotto et al., 2016), we suggested to extend the human cortical grasping network to include SMA as a crucial node.

Chapter 4

Gaze direction influences grasping actions towards unseen, haptically explored, objects[2]

Abstract

Haptic exploration produces mental object representations that can be memorized for subsequent object-directed behavior. Storage of haptically-acquired object images (HOIs), engages, besides canonical somatosensory areas, the early visual cortex (EVC); nevertheless, clear evidence for a causal contribution of EVC to HOIs representation is still lacking. The use of visual information by the grasping system undergoes necessarily a frame of reference shift by integrating eye-position. We hypothesized that if the motor system uses HOIs stored in a retinotopic coding in the visual cortex, then its use is likely to depend at least in part on eye position. We measured the kinematics the right hand of 15 healthy participants during whole-hand grasping of different objects occulted from vision, that had been previously explored haptically. During the task, the objects' position was fixed, in front of the participant, while subject's gaze varied between 3 possible positions: towards the unseen object or away from it, on either side. Results showed that the middle and little fingers' kinematics during reaching for the unseen object changed significantly according to gaze position. In a control experiment we

showed that intransitive hand movements were not modulated by gaze direction. We concluded that manipulating eye-position produces small but significant configuration errors (behavioral errors due to shifts in frame of reference) possibly related to an eye-centered frame of reference, despite the absence of visual information, indicating sharing of resources between the haptic and the visual/oculomotor system to delayed haptic grasping.

4.1. Introduction

4.1.1. Representation of haptically-acquired object shapes in the cerebral cortex

As most primates, our daily object-directed actions rely mainly on vision. However, when vision is not available, we need to use information from other senses in order to interact with our surroundings. When it comes to hand-object interactions, the sense that allows us to accurately extract information about the characteristics of objects, such as their size, shape and location, is touch. In fact, touch delivers many crucial information about the environment already from the early stages of life; consider, for example, an infant exploring his peripersonal space through touch. Despite humans interact with their surroundings with touch as much as they do with vision, research mainly focused on visual and visuomotor processing of objects, letting many open questions on tactile processing (Avanzini et al., 2016; Lee Masson et al., 2018; Styrkowiec et al., 2019).

The canonical model of haptic information processing for object manipulation depicts a circuit involving the ventral caudal nucleus of the thalamus, the anterior parietal cortex and two parallel streams through the secondary somatosensory cortex and the insula on one side and through the superior parietal lobule on the other (Goodman & Bensmaia, 2018; Hsiao & Yau, 2008; James et al., 2007; Yau et al., 2016). Such robust model has been repeatedly confirmed

in non-human and human primates on the basis of physiological, imaging and neuropsychological data (Caselli, 1991; Cattaneo et al., 2015; Lee Masson et al., 2016; Maule et al., 2015; Peltier et al., 2007; Sathian, 2016). In the recent years, however, a growing body of evidence points to a role of the early visual cortex (EVC) in processing haptic information. Activation of striate and extrastriate visual regions during tactile identification of objects has been observed in sighted individuals, even when visual information about the object was not available, and regardless of whether the haptically-explored shapes were familiar or not (S. I. Cunningham et al., 2015; Gallivan et al., 2014; James et al., 2002; Lee Masson et al., 2016; Merabet et al., 2007; Sathian, 2016; Snow et al., 2014). Moreover, the EVC also shows reactivation during grasping actions in the dark towards an object that has been haptically explored seconds earlier (Monaco et al., 2017). In addition, evidence for the potential existence of an access pathway of tactile information to the EVC is provided by studies in blind individuals. In the congenitally blind, the EVC is activated during Braille reading or tactile perception (Burton et al., 2006; Cheung et al., 2009; Ptito et al., 2008; Sadato et al., 1996; Sadato et al., 2002) thanks to neuroplasticity driven by sensory deprivation. Overall, these results show evidence that not only the EVC is involved in haptic exploration of objects, but it is also reactivated during subsequent grasping actions in the dark, suggesting that grasp-relevant properties about the object might be recruited from the EVC at the time of action even in absence of online visual information.

4.1.2. Frames of reference in vision for action

As described in chapter 1, during object-directed actions the brain implements sensorimotor transformation to translate sensory information of the target in further different frames of reference to accurately orchestrate the movement. A crucial question regarding such sensorimotor processes is related to how sensory information are re-coded in different frames

of reference. It is well known that a target's shape in the EVC is encoded in retinal coordinates. This information must be integrated with that on eye position to build a head-centered image and this is further integrated with head-, body- and hand-position in space to obtain an ultimate image in an egocentric frame of reference that is functional to hand-object interactions (Batista, 2002; Buneo et al., 2002; McGuire & Sabes, 2009; Pesaran et al., 2006). During visually-based actions, sensory information necessarily undergoes such process of subtraction of gaze position to reach the premotor cortex (Neggers & Bekkering, 2000). The more distal cortical nodes where retinotopic and eye-centered images are found along the dorsal visual stream are seemingly the lateral intraparietal area (LIP) and the frontal (FEF) and supplementary eye fields (SEF; Y. E. Cohen & Andersen, 2002; Martinez-trujillo et al., 2004; Vernet et al., 2014). The premotor cortex is generally considered to be "gaze-independent", at least for representations of objects for grasping (Gentilucci et al., 1983), though recent works indicated the presence of retinotopic coding in the monkey's premotor sector (Boussaoud et al., 1998; Lehmann & Scherberger, 2013; Mushiake et al., 1997). Further neuroimaging evidence in humans shows that gaze direction modulates the activity in the parieto-frontal network, which is known to be crucial for motor behavior, during reaching movements towards visual targets (Beurze et al., 2007; Beurze et al., 2010; Medendorp et al., 2003). Such an influence appears to be reflected on behavioral data as well, so that eccentric gaze directions induce larger grip aperture, consisting of the distance between the index finger and the thumb, during a reaching movement towards a visual target, presumably in order to facilitate contact with the target (Brown et al., 2005; Karl et al., 2012; Schlicht & Schrater, 2007). Note that investigations that examined sensorimotor transformations for grasping made use of the grip aperture as the index of hand shaping, namely the flexion of hand's fingers involved in the action that determines the distance between the fingertips. This index showed to be informative of many conditions under which the reach-to-grasp action is performed, first and foremost the target size (Berthier et al., 1996;

Santello & Soechting, 1998). When reaching for an object under visual guidance, the hand is pre-shaped to accommodate the object's geometry and maximal grip aperture during reach is a measure that is highly informative of the capacity of the brain to build a visual representation of the object for acting upon it (Jeannerod et al., 1995). Therefore, grip aperture seems to remain the most direct and appropriate behavioral output to study the hand shaping during sensorimotor transformations.

To sum up, haptic information on objects, acquired in a hand-centered frame of reference is stored in "visual" buffer in the EVC, and information in the EVC needs to integrate gaze position to be used in grasping movements. Such a "visual" storage, albeit temporary, could be useful for the genesis of movement towards objects, after appropriate integration of object information in a more complex spatial map that includes other coordinates systems, such as hand-, body- or head-centered ones.

4.1.3. Is haptic information remapped in eye-centered coordinates?

The concepts above introduced raise the question about whether gaze direction affects grasping movements towards haptically-explored objects, like it does for visually-explored objects. Indeed, while most behavioral studies have focused on how eye-position affects grasping movements towards visually-explored targets, the effects of gaze direction on movements towards haptically-explored targets has not been investigated yet; hence, this is the specific experimental hypothesis that we are addressing in this study. In other words, the question is: if the perceptual representation of a target is stored in a visual sketchpad, then is this mapped in eye-centered coordinates irrespective of the sensory modality initially used to explore the target? Specifically, is the memory-based perceptual representation of a target mapped in eye-centered coordinates even if the target is explored or located with senses other than vision, like proprioceptive or haptically-explored targets?

Neuroimaging evidence suggests that in sighted individuals, parietal areas code targets in gaze-centered coordinates for grasping actions, irrespective of whether the target to be grasped is visual or proprioceptive, i.e. a 3D real cube or one's own hand (Leoné et al., 2015). In addition, even in blind individuals spatial updating of proprioceptive target location for reaching movements depends on gaze direction (Reuschel et al., 2012). Therefore, we reasoned that if the perceptual representation of a target is encoded in eye-centered coordinates regardless of the modality in which the target has been perceived (or located), it is plausible that gaze direction affects grip aperture during grasping actions towards occulted objects that have been haptically explored. Alternatively, gaze direction could have no effect on delayed grasping actions towards haptically explored objects, which might be instead represented in hand-centered reference frames; thus, shifts in gaze position relative to a constant object location (and constant hand starting-position) should have no influence on subsequent movements.

To investigate whether grasping movements towards tactile stimuli are influenced by gaze direction, we conducted a behavioral investigation in which participants haptically explored a cylindrical object of three possible sizes aligned with body midline, and subsequently grasped it. The object was occluded from the participant's view throughout the duration of the experiment. We manipulated gaze direction so that participants fixated towards the object or away from it and measured fingers' extension during the haptically-guided reaching. We hypothesized that if an haptically explored object is mapped in eye-centered coordinates, then grip aperture would change when participants grasp the object while fixating peripheral as opposed to central locations. This would occur for two possible reasons: first, in the peripheral visual field, uncertainty about the properties (i.e., size) of the object to be grasped would increase the grip aperture (Burbeck, 1987; Burbeck & Yap, 1990; Levi & Klein, 1996; Whitaker, 1997); second, the remembered location of the object would conceivably also occupy

different eccentricities in retinotopic space and, therefore, be warped by the viewpoint (Clavagnier et al., 2007; Prado et al., 2005).

In this way we aim to highlight "configuration errors" (Wang, 2012), namely behavioral errors due to shifts of reference frames. These are generally evoked by changes in viewpoint or body part position and are widely employed in the cognitive neurosciences (as for example in Bisiach & Luzzatti, 1978). The finding of configuration errors is an indicator that a given behavioral function is actually based on a given reference frame. While previous studies have investigated the effect of gaze direction on maximum grip aperture of the thumb and index finger, as in a precision grip (Brown et al., 2005), we examined the influence of gaze on all fingers involved in a precision whole-hand grasp in order to provide a comprehensive view of the kinematics of all fingers that participate in hand actions. In addition, we performed a control experiment to test whether gaze direction affects non-goal-directed fingers movements, hence in the absence of an object or its mental representation.
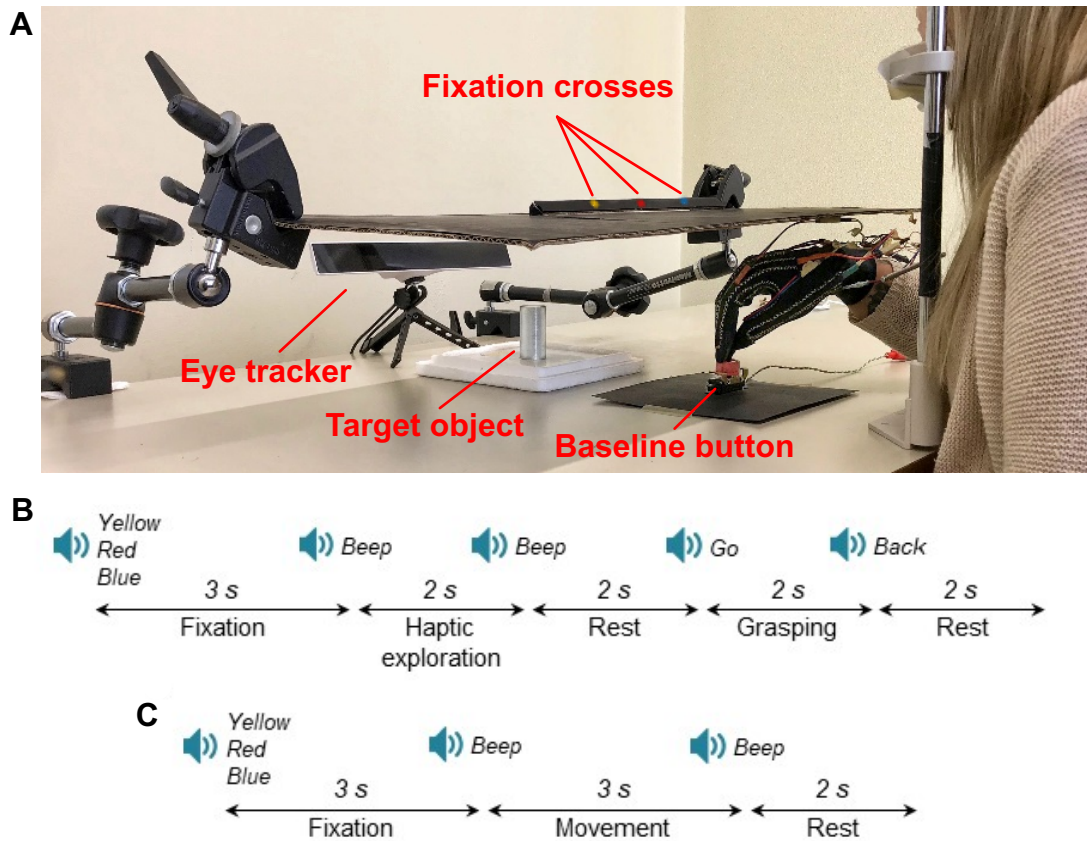
Figure 14. Image of the experimental setup and paradigms
(A) Experimental setup. Participants sat in front of a black panel with three fixation crosses (left, central and right). A button was placed in front of the subjects and served as the baseline position. Participants pressed the button with the fingers closed before and after each trial. In the main experiment, the panel hid one of the three differently sized objects. For each experimental session, the panel was set with a spirit level at a suitable distance for each participant so that gaze direction towards the central fixation cross coincided with the location of the object hid below the panel. The Gazepoint GP3 eye-tracker allowed us to control for participants' fixation and ensure that they could reliably fixate the instructed fixation point for the duration of each trial. The same setup was used for the control experiment, with the only exception that no object was used. (B) Timing of trials in the main experiment. At the beginning of each trial participants were instructed to direct their gaze towards the fixation cross whose color was cued by a recorded voice (yellow for left, red for center, blue for right). After 3 s, a "beep" sound marked the beginning of the haptic exploration phase and instructed participants to move the hand from the baseline position to reach and touch the object in order to find out which of the three object sizes was hidden beyond the panel. Participants haptically explored the object for 2 s, until a second beep occurred and instructed them to return the hand to the baseline position. After a 2 s rest, a "go" cue instructed participants to grasp the object they had touched seconds earlier, and after 2 s participants returned the hand to the baseline position upon a "back" cue. We manipulated gaze direction and object size in a 3 × 3 factorial design. (C) Timing of trials in the control experiment. At the beginning of each trial, participants fixated the cross whose color was cued by a recorded voice (yellow for left, red for center, blue for right). After 3 s, a "beep" sound instructed participants to move the hand forward and open it above the table (and below the panel). A second beep occurring 3 s later, cued the end of the trial and participants returned the hand to the home position. Only gaze direction was manipulated in the control experiment, leading to an experimental design with 3 trial types.

74

4.2. Materials and methods

4.2.1. Participants

Fifteen participants (8 females) with age ranging from 20 to 32 (mean age ± SD: 24.9 ± 4.5) took part in the main experiment. A control experiment was carried out with another set of 15 participants (12 females) with age ranging from 20 to 33 (mean age ± SD: 27 ± 3.9). All subjects were right-handed, had normal or corrected-to-normal visual acuity in both eyes and were naïve to the purposes of the experiment. Before the experimental session, each participant declared to have no neurological, psychiatric or other medical condition and gave his written informed consent. The experimental protocol was approved by the ethic committee of University of Verona and was carried out in accordance with the ethical standards of the Declaration of Helsinki.

4.2.2. Apparatus

Participants sat comfortably in front of a table where one of three differently sized metallic cylindric objects (height of 7 cm and radiuses of 1, 3 or 5 cm) was placed by the experimenter in between trials (mean distance ± SD from nasion: 51.8 ± 2.9 cm). The cylinders were the same that we used for the experiments described in chapters 2 and 3 (Figure 1A). As is the first experiment, each object was glued to a 15x15-cm plywood to facilitate its placement on a polystyrene base that was fixed on the table, in order to ensure that cylinders' position remained unchanged during the experimental sessions. The object was hidden from the participant's view by means of a black panel placed ~17 cm above a table (Figure 14A). During the experiment participants fixated one of three fixation crosses of different colors (blue on the left, red in the middle, yellow on the right) on the black panel. The central fixation cross and the hidden object were aligned with the participant's body midline, while the lateral fixation

marks were placed 8.5 cm to the left and to the right of the central cross. The distance of the participants' eyes from the central fixation cross was 30.9 ± 2.5 cm, while the distance from the lateral ones was 31.8 ± 2.8 cm; thus, the eccentric gaze directions were at $15.6 \pm 1.3°$ of visual angles from the central fixation. For each participant, the panel was installed using a pointer, so that the subject's gaze trajectory towards the central fixation cross coincided with the location of the cylindrical object hid below the panel. In other words, when looking at the central fixation participants would have been looking directly at the object if the panel had been removed. The panel was supported by two later mechanical arms; a spirit level was used to ensure that the surface of the panel was perfectly level on the horizontal plane. The subjects' head was fixed on a chin rest (mean height $\pm$ SD: 28.8 ± 2.9) to avoid head movements while looking at the lateral fixation crosses. Like in the previous experiments, we placed a button on the table between the participant (mean distance $\pm$ SD: 38.8 ± 3.3) and the object (mean distance $\pm$ SD: 24.8 ± 1.5) indicating the baseline position, during which participants rested the right hand with all fingers pointing down on the button (Figure 14A). Finally, a Gazepoint GP3 eye-tracker was placed in front of participants (mean distance from nasion $\pm$ SD in exp 1: 67.6 ± 1.82) to record the gaze coordinates. We set the distances between the elements of the experimental setting (the participant, the object's support base, the button, the panel and the chin rest) depending on the space of movement that each participant reported to find comfortable. Thus, we ensured that subjects had no discomfort due to the glove or its wire. The experimenter sat laterally to the table to change the objects before each trial. A screen pointed toward the experimenter informed him on which of the three objects had to be placed on the polystyrene support.

4.2.3. Procedure and experimental design

Each trial began with a recorded voice saying the color of one of the three fixation crosses ("blue" for left, "red" for center, "yellow" for right), and prompting the participants to fixate the cued cross for the whole duration of the trial. After 3 s, a "beep" sound indicated the beginning of the haptic exploration phase, during which subjects haptically explored the size of the cylindrical object placed beyond the panel. The haptic exploration phase lasted 2 s, after which a second "beep" sound cued participants to return the hand to the baseline position. After a delay of 2 s, a "go" cue indicated the beginning of the grasping phase, during which subject performed a reach-to-grasp action towards the object that was haptically explored moments earlier. Participants were instructed to grasp the object - without lifting it - from the top using all their fingers, and maintain the grip on the object until they heard a "back" sound 2 s later, which prompted them to bring the hand to the baseline position (Figure 14B).

In summary, we had a 3 × 3 factorial design, with factors SIZE (3 levels: small, medium, large) and GAZE (3 levels: left, center, right), which led to nine trial types: small object - left fixation, small object - central fixation, small object - right fixation, medium object - left fixation, medium object - center fixation, medium object - right fixation, large object - left fixation, large object - central fixation, and large object - right fixation. Each trial type was presented 20 times in randomized order; therefore, there were 180 trials in total, separated into 10 blocks.

Before starting the experiment, participants performed 3 training trials to get familiar with the task. In addition, participants underwent a preliminary procedure to validate the coordinates of eyes position for each fixation cross for off-line investigations of subjects' performance during the experiment. To this aim, participants were instructed to fixate each of the three crosses for 4 s in random order. This procedure was repeated 5 times, leading to 15 fixation trials.

4.2.4. Control experiment

We used the same set-up for a control experiment to determine whether a putative effect of gaze direction on fingers' movements occurs irrespectively of whether the action is object-directed or not. To this end, we asked our participants to perform intransitive movements, consisting of opening the hand approximately 7 cm above the table, while fixating central and peripheral fixations. The apparatus used for the control experiment was identical to the experimental session, with the exception that the cylindrical objects were not used in the control task. The distances between the elements of the experimental setting (the participant, the button, the panel and the chin rest) were based on what each participant reported to find comfortable to perform the movements. We placed the panel with the three fixation crosses ~17 cm above the table using two lateral mechanical arms; here too, a spirit level was used to ensure that the surface of the panel was perfectly level on the horizontal plane. The distance from subjects' nasion was 30.4 ± 2.1 cm from the central cross and 31.4 ± 2.1 cm from the lateral ones, leading to a visual angle of the eccentric gaze directions of $15.7 \pm 1.04°$ from the central fixation. Again, the participants' head was fixed on a chin rest (mean height $\pm$ SD: 28.03 ± 2.5 cm) to avoid head movements while looking laterally. The baseline button was placed on the table at 28.33 ± 3.2 cm from subject's nasion. Finally, the eye-tracker was placed at 68.5 ± 1.6 cm from participants' eyes to record the gaze coordinates.

As shown in Figure 14C, at the beginning of each trial participants fixated the cross instructed by the recorded voice ("blue" for left, "red" for center, "yellow" for right). After 3 s, a "beep" sound instructed participants to move the right hand forward, below the black panel, and open it approximately 7 cm above the table until a second "beep" occurred 3 s later and prompted the subjects to return the hand to the baseline position. The experimental design consisted of 3 levels of the factor GAZE (left, center, right). Each trial type was presented 20 times, for a total of 60 trials presented in 5 blocks. For each block, trials were presented in

random order and each condition was repeated 4 times. Before starting the control experiment, participants completed 3 training trials to get familiar with the task and underwent the preliminary procedure to validate the coordinates of eyes position for each fixation cross.
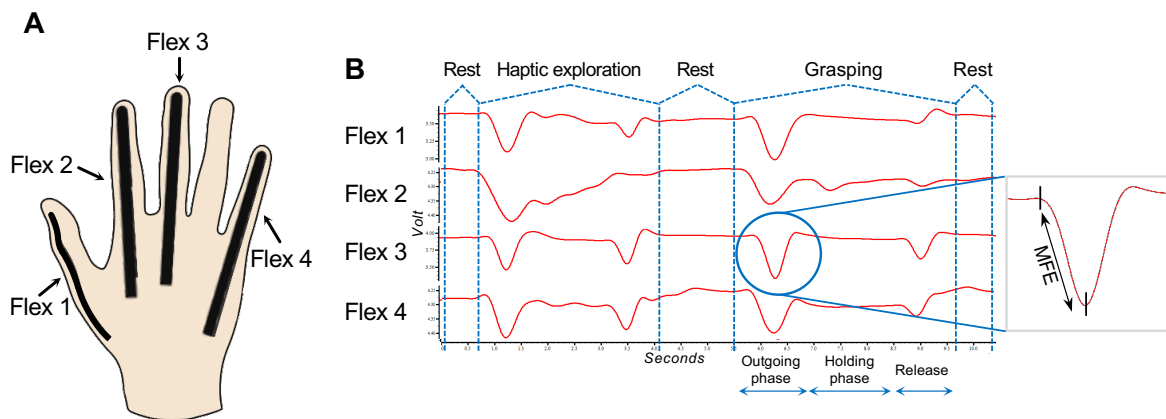
Figure 15. Glove used for acquisition of hand configuration and relative data
(A) Schema of the position of flexible sensors of the hand. Participants wore a glove equipped with flexible sensors that allowed us to measure MFE. There was a sensor for the thumb (flex 1), one for the index finger (flex 2), one for the middle finger (flex 3), and one for the little finger (flex 4). Each sensor consisted of a resistance variable to its own flexion. The sensors were connected to an analogical-digital converter so that we could quantify the voltage variations of each resistor for each movement of the fingers. (B) Example of signal generated by the voltage variations of each sensor for a whole trial recorded with Signal software from one of the participants. For each trial, the pattern was clear and consistent enough to allow us to recognize the phases of the ongoing trial (rest – haptic exploration – rest – grasping) and, more specifically, the reach-to-grasp action: outgoing phase, contact with the object (hold), return phase (release). In the reaching phase, MFE was calculated as the absolute value of the difference between the voltage recorded in the baseline position and the peak during the outgoing phase of the grasping movement, immediately before participants' fingers held the cylinder.

4.2.5. Grip aperture and eye movements measurement

Similarly to previous investigations of fingers dynamics (Dipietro et al., 2003; Fricke et al., 2017, 2019; Gentner & Classen, 2009; Kumar et al., 2012), we measured participants' right

hand pre-shaping during the whole-hand haptically-guided grasping by means of custom-built glove equipped with flexible sensors able to detect fingers' flexion. Here, we used the glove described and evaluated in chapter 2 and adopted in the TMS study described in chapter 3. As in the TMS study, we measured the signal from four 114-mm-long flexion sensors placed over the metacarpophalangeal and proximal interphalangeal joints of the thumb, index and little fingers (1 sensor for each finger, Figure 15A). As in both the experiments previously described, we used the analog-digital converter to connect the glove to the computer and in which the Signal software acquired the signal from each sensor. Also in this case, the signal recorded for each frame generated a pattern that allowed us to accurately recognize each phase of both the whole trial (rest – haptic exploration – rest – grasping) and, more importantly, the reach-to-grasp action: outgoing phase (i.e., the hand leaves the baseline position to head toward the object), the holding phase (contact with the object) and the release phase (i.e., the hand leaves the object to return to the starting position; Figure 15B). For more specific technical details on glove's assembly and setting, see the section "Grip aperture measurement" of the chapter 1.

To measure the maximum grip aperture of the participants' right hand we calculated the *maximum finger extension* (MFE) of all digits during the reach-to-grasp movement. MFE was calculated as the absolute value of the difference between the voltage recorded during the baseline position and the peak during the outgoing phase of the grasping movement, before the participant's fingers touched the object. We used the software OpenSesame (Mathôt et al., 2012) for the stimuli presentation, eye-tracker and fingers movements recording, as well as to trigger the analog-digital converter for the registration of fingers' movements from glove's sensors with Signal software.

4.3. Data analysis

For each participant, the ocular coordinates for each trial were compared with the ones recorded during the preliminary phase of fixation validation, in order to determine whether the fixation was in the correct spatial location, in both the exploration and the movement phases. We excluded trials in which participants moved their gaze away from the fixation point during the trial allowing a fixation of window of 3° of visual angles (eye movements > 3° of visual angles in horizontal and vertical dimension). We discarded 3% of total trials for fixation errors. To make the data from each finger comparable, we normalized the MFEs within each finger and within each participant by means of z-score normalization. For each experimental condition, we removed trials whose MFE deviated more than 2 standard deviations from the mean of each glove's sensor (4.4% in the main experiment, 4.1% in control experiment). In addition, we excluded trials whose kinematics pattern recorded by Signal software did not allow for a clear identification of the MFE (1% in the main experiment, 1.2% in control experiment).

We hypothesized that if the perceptual representation of a haptically-explored object is influenced by gaze direction, there would be a change of MFE when participants grasped each of the three sized objects while fixating peripheral directions (left and right) as compared to central fixation (corresponding to the occluded object location). In addition, we also examined MFE's standard deviation, as uncertainty about the target object might also be reflected in the variability of grip aperture besides than an increase in its mean value.

To test our hypothesis, we performed a repeated measures ANOVA with 3 within-subjects factors: FINGER (4 levels: thumb, index, middle finger, little finger) × GAZE (3 levels: Left, Centre, Right) × SIZE (3 levels: Small, Medium, Large). To get a comprehensive view of the kinematics of the whole hand during reach-to-grasp actions towards haptically explored objects, we analyzed data from all fingers involved in the precision whole-hand

grasps. In the control experiment, we conducted a repeated measures ANOVA with 2 within-subjects factors: FINGER (4 levels: thumb, index, middle finger, little finger) × GAZE (3 levels: Left, Centre, Right) to assess whether gaze direction influences hand shaping during non-object directed movements. Significance threshold was set at 0.05. Where interactions reached significance, we performed post-hoc tests with Tukey's Honestly Significant Difference (HSD) test. Effect sizes of significant results were reported as partial eta-squared (p-eta2) coefficients. All the analyses were conducted using SPSS (IBM Corp. Released 2012. IBM SPSS Statistics for Macintosh, Version 21.0. Armonk, NY: IBM Corp.).

Finger:	Thumb			Index			Middle			Little		
Object:	Small	Medium	Large	Small	Medium	Large	Small	Medium	Large	Small	Medium	Large
Left gaze	-0.22 (0.14)	0.05 (0.07)	0.22 (0.16)	-0.22 (0.09)	-0.07 (0.05)	0.37 (0.08)	-0.54 (0.09)	-0.03 (0.06)	0.33 (0.05)	-0.64 (0.07)	-0.11 (0.05)	0.54 (0.09)
Central gaze	-0.2 (0.12)	-0.12 (0.05)	0.3 (0.15)	-0.33 (0.09)	-0.05 (0.05)	0.3 (0.07)	-0.59 (0.08)	0.09 (0.05)	0.42 (0.08)	-0.65 (0.07)	-0.04 (0.05)	0.56 (0.07)
Right gaze	-0.25 (0.11)	-0.05 (0.07)	0.23 (0.14)	-0.31 (0.09)	0.0 (0.04)	0.3 (0.07)	-0.44 (0.09)	0.18 (0.06)	0.48 (0.07)	-0.48 (0.09)	0.11 (0.06)	0.69 (0.09)

Table 7
Z-score transformed Maximal Finger Extension (MFE) in all experimental conditions of the main experiment. Mean values (Standard Error) are given.

4.4. Results

4.4.1. Main experiment: FINGER × GAZE × SIZE ANOVA

The ANOVA with 3 within-subjects factors (FINGER × GAZE × SIZE) conducted on the average MFE in the main experiment revealed a main effect of GAZE ($F_{2,28} = 4.98$; $p = 0.01$; p-eta2 = 0.26), and a main effect of SIZE ($F_{2,28} = 47.77$; $p < 0.0000001$; p-eta2 = 0.77). In addition, we observed significant FINGER x SIZE ($F_{2,28} = 4.46$; $p < 0.0006$; p-eta2 = 0.24) and

FINGER x GAZE ($F_{2,28}$ = 3.22; p = 0.002; p-eta2 = 0.22) interactions. Nonsignificant results included the main effect of FINGER ($F_{3,42}$ = 1.16; p =0.34; p-eta2 = 0.07), the GAZE x SIZE interaction ($F_{2,28}$ = 0.60; p = 0.66; p-eta2 = 0.04) and the FINGER × GAZE × SIZE interaction ($F_{12,168}$ = 0.86; p = 0.58; p-eta2 = 0.06). Mean values of MFE for each experimental condition are given in Table 7.

Finger:	Thumb	Index	Middle	Little
Small cylinder	-0.22 (0.12)	-0.29 (0.08)	-0.52 (0.06)	-0.59 (0.06)
Medium cylinder	-0.04 (0.04)	-0.04 (0.02)	0.09 (0.03)	-0.01 (0.04)
Large cylinder	0.25 (0.14)	0.32 (0.07)	0.42 (0.06)	0.6 (0.07)
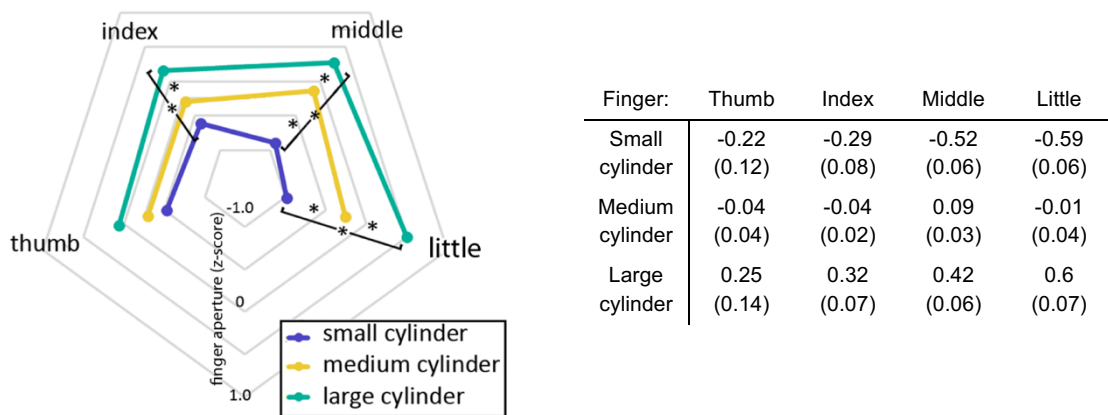
Figure 16. Finger × Size interaction (main experiment)
Mean z-scores transformed maximum finger extension (MFE). The diagram shows the individual finger excursions according to object size in the main experiment. Thumb and index finger failed to discriminate the object size, since thumb's flexion remains constant independently of the cylinder, and the index finger failed to distinguish the small and the medium cylinder. In contrast, MFE recorded from middle and little finger accurately scaled according to the object size. Asterisks indicate significant statistical differences for post-hoc comparisons ($p < 0.05$, corrected). The figure was processed by means of the GIMP (Gnu Image Manipulation Program) software.

Table 8
Z-scores transformed Maximal Finger Extension (MFE) in all experimental conditions of Finger × Size interaction. Mean values (Standard Error) are given.

4.4.2. Main experiment: FINGER × SIZE interaction

A significant FINGER × SIZE ($F_{2,28}$ = 4.46; $p < 0.0006$; p-eta2 = 0.24) was found, illustrated in Figure 16. We further investigated such interaction were by means of four separate 1-way ANOVAs, one for each of the four fingers. The 1-way ANOVA on the thumb data did not show any main effect of SIZE ($F_{2,28}$ = 3.13; p = 0.059). The 1-way ANOVA on the index

finger data showed a main effect of SIZE ($F_{2,28} = 17.44$; $p = 0.00001$). Post-hoc analyses with Tukey's Honestly Significant Test showed that MFEs to the small object were not different from those to the medium object ($p = 0.06$), but they were significantly different from those to the large object ($p = 0.0001$) and that MFEs to the medium object were significantly different from those to the large object ($p = 0.004$). The 1-way ANOVA on the middle finger data showed a main effect of SIZE ($F_{2,28} = 55.22$; $p < 0.000001$). Post-hoc analyses with Tukey's HSD showed that MFEs to the small object were different from those to the medium object ($p = 0.0001$) and from those to the large object ($p = 0.0001$) and that MFEs to the medium object were significantly different from those to the large object ($p = 0.003$). The 1-way ANOVA on the little finger data showed a main effect of SIZE ($F_{2,28} = 65.13$, $p < 0.000001$). Post-hoc analyses with Tukey's HSD showed that MFEs to the small object were different from those to the medium object ($p = 0.0001$) and from those to the large object ($p = 0.0001$) and that MFEs to the medium object were significantly different from those to the large object ($p = 0.001$). To summarize, the FINGER x SIZE interaction implied that not all fingers scaled accurately to object size. In fact, we found that there was a gradient of fingers mobility from the thumb to the little finger. The thumb's MFE failed to show significant modulation from object size. The index finger showed a weak and incomplete correlation with object size, while the middle and little fingers showed a clear linear correlation with object size, which was even more robust for the little finger than for the middle finger. This result confirms the accurate measurement of our glove and demonstrates that MFE scales with object size during memory-based grasping actions towards tactile stimuli. The mobility gradient observed here, from thumb to little finger is difficult to relate to the previous literature because the vast majority of studies investigating the effect of object size on grip aperture describe only the thumb-index pair, ignoring the remaining fingers. Thus, we cannot be sure whether this pattern is specific to our recording apparatus,

specific to our task or, possibly a general pattern. Mean values of MFE for FINGER × SIZE interaction are reported in Table 8.
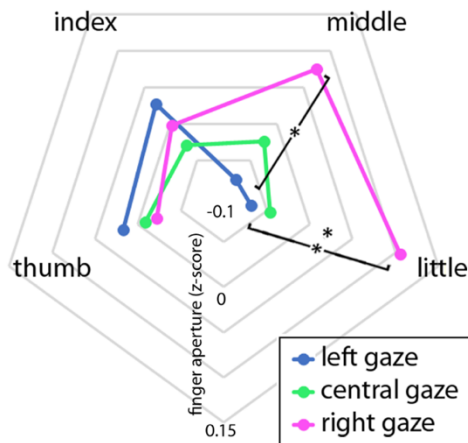
Finger:	Thumb	Index	Middle	Little
Left gaze	0.02 (0.03)	0.03 (0.03)	-0.06 (0.04)	-0.07 (0.03)
Central gaze	-0.01 (0.02)	-0.03 (0.02)	0.00 (0.04)	-0.05 (0.02)
Right gaze	-0.02 (0.02)	0.00 (0.02)	0.06 (0.03)	0.11 (0.02)

Figure 17. Finger × Gaze interaction (main experiment)
Mean z-scores transformed maximum finger extension (MFE). The diagram shows the individual finger excursions according to the gaze direction in the main experiment. Gaze direction did not affect flexion of the thumb and index finger. Instead, it modulated flexion of the middle finger (showing larger aperture while looking at right compared to left but not central gaze) and the little finger (showing wider aperture for right gaze compared to left and central gaze). Asterisks indicate significant statistical differences for post-hoc comparisons ($p < 0.05$, corrected). The figure was processed by means of the GIMP (Gnu Image Manipulation Program) software.

Table 9
Z-scores transformed Maximal Finger Extension (MFE) in all experimental conditions of Finger × Gaze interaction. Mean values (Standard Error) are given.

4.4.3. Main experiment: FINGER × GAZE interaction

We observed a significant FINGER × GAZE ($F_{2,28} = 3.22$; $p = 0.002$; p-eta2 = 0.22) interaction, that is illustrated in Figure 17. The 2-way interaction was further investigated by means of four separate 1-way ANOVAs, one for each of the four fingers. No significant effect of GAZE was found in the ANOVAs on the thumb ($F_{2,28} = 0.44$; $p = 0.65$) and index ($F_{2,28} = 0.97$; $p = 0.39$) MFEs. The ANOVA on the middle finger showed a significant main effect of

GAZE ($F_{2,28}$ = 4.37; p = 0.022). Post hoc tests using Tukey's HSD showed that MFEs with left gaze were significantly smaller than MFEs with right gaze (p = 0.018). MFEs in central position of gaze were not significantly different from the left and right gaze conditions. The ANOVA on the little finger showed a significant main effect of GAZE ($F_{2,28}$ =11.79; p = 0.00002). Post hoc tests using Tukey's HSD showed that MFEs with left gaze were significantly smaller than MFEs with right gaze (p = 0.0004). MSFEs in central position of gaze were significantly different from the right gaze condition (p = 0.0017), but not from MFEs in left gaze. Mean values of MFE for FINGER × GAZE interaction are reported in Table 9.

Object size:	Small	Medium	Large
	0.81 (0.03)	0.85 (0.02)	0.91 (0.01)
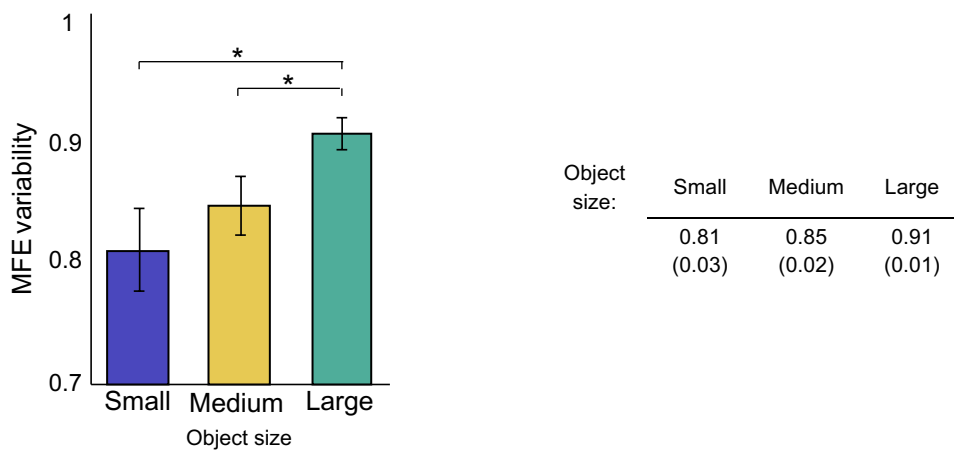
Figure 18. Variability (standard deviation) of MFE as a function of object size (main experiment)
Bars indicate the standard deviation of MFE for each object size. Analysis revealed more variability for grasping movements towards the Large than the small and medium object. Asterisks indicate significant statistical differences for post-hoc comparisons (p < 0.05, corrected). Error bars denote ± 1 standard error of the mean (SEM).

Table 10
Variability values of z-scores transformed Maximal Finger Extension (MFE) for the main effect of Size in the control experiment. Mean values (Standard Error) are given.

4.4.4. Main experiment: analysis on MFE variability

In addition to analyzing the MFE, we also explored whether eccentricity could affect hand shaping in terms of variability of fingers' movement, as uncertainty about object size might increase when participants fixate away from the object. Hence, we analyzed the standard deviation of MFE by means of an ANOVA with 3 within-subjects factors (FINGER × GAZE × SIZE) that showed a main effect of SIZE ($F_{2,28} = 7.49$; $p = 0.003$; p-eta2 = 0.19) with higher variability of MFE for the Large vs. Small ($p < 0.001$) and Large vs. Medium object ($p = 0.02$; Figure 18). Since no other significant effect or interaction was observed (all $p > 0.16$), this analysis showed no effect of eccentricity on grip aperture variability. Mean values of MFE variability for the main effect of SIZE are reported in Table 10.

Finger:	Thumb	Index	Middle	Little
Left gaze	-0.03 (0.04)	-0.07 (0.03)	-0.01 (0.03)	-0.03 (0.06)
Central gaze	0.03 (0.03)	0.09 (0.03)	0.03 (0.03)	-0.01 (0.05)
Right gaze	0.0 (0.05)	-0.02 (0.04)	-0.02 (0.04)	0.03 (0.06)
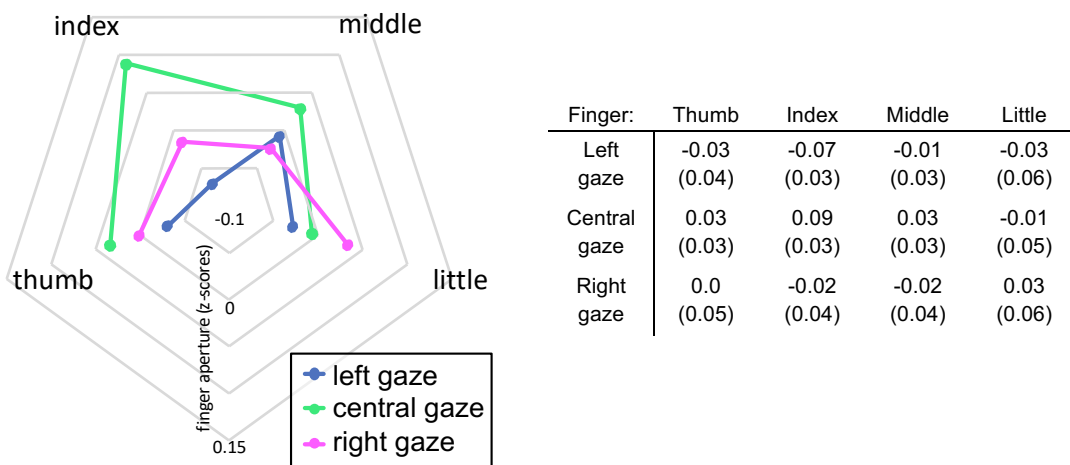
Figure 19. Finger extension in control experiment
Mean z-scores transformed maximum finger extension (MFEs). Gaze direction had no effect on fingers flexion while participants performed intransitive movements (all $p > 0.05$). The figure was processed by means of the GIMP (Gnu Image Manipulation Program) software.

Table 11
Z-scores transformed Maximal Finger Extension (MFE) in all experimental conditions of the control experiment. Mean values (Standard Error) are given.

4.4.5. Control experiment: FINGER × GAZE ANOVA

The FINGER × GAZE 2 within-subject factors ANOVA on MFEs of participants performing intransitive (non-object directed) movements failed to show any effect. The main effect of FINGER ($F_{3,42} = 0.62$, $p = 0.6$; p-eta2 = 0.04), the main effect of GAZE ($F_{2,28} = 1.19$; $p = 0.3$; p-eta2 = 0.08) and the FINGER × GAZE interaction ($F_{6,84} = 0.65$, $p = 0.7$; p-eta2 = 0.04; Figure 19) show non-significant results. We concluded that gaze direction did not affect fingers' movements during intransitive actions. The mean MFEs are shown in Table 11.

Finger:	Thumb	Index	Middle	Little
	1.0	0.99	1.0	0.96
	(0.0)	(0.0)	(0.0)	(0.01)
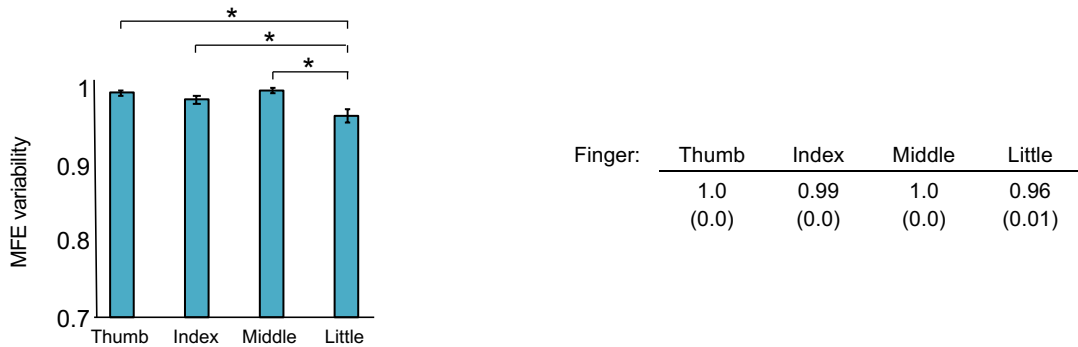
Figure 20. Variability (standard deviation) of MFE as a function of finger (control experiment)
Bars indicate the variability (standard deviation) of each finger's movement during non-object-directed actions in the control experiment. During intransitive movements, variability in the pinky finger was significantly lower than the other fingers (all $p < 0.003$). Asterisks indicate significant statistical differences for post-hoc comparisons ($p < 0.05$, corrected). Error bars denote ± 1 standard error of the mean (SEM).

Table 12
Variability values of z-scores transformed Maximal Finger Extension (MFE) for the main effect of Finger in the control experiment. Mean values (Standard Error) are given.

4.4.6. Control experiment: analysis on MFE variability

Like in the main experiment, we also analyzed the standard deviation of MFE recorded in the control experiment with an ANOVA with 2 within-subject factors (FINGER × GAZE)

to verify whether gaze direction influenced the variability of fingers' movement. As shown in figure 20, the ANOVA showed a main effect of FINGER ($F_{3,42} = 11.06$; $p < 0.0001$; p-eta2 = 0.44) resulting from lower variability for the little finger compared to all the other fingers (all $p < 0.003$). Since no other effect emerged from the analysis (all $p > 0.1$), we concluded that gaze direction did not affect the variability of fingers' movements during non-object-directed actions. Mean values of MFE variability for the main effect of FINGER are reported in Table 12.

4.5. Discussion

5.5.1. Main findings

Results of our investigation indicate that finger aperture is significantly modulated by gaze direction while grasping towards haptically explored objects. A control experiment in which participants performed intransitive non-object-directed hand movements failed to show any effect of gaze direction. Similar evidence showing gaze-dependency of reaching movements towards proprioceptive targets has been previously shown for spatial targets in blind and sighted individuals (Reuschel et al., 2012; Sathian, 2005). Here we show an effect of gaze in the dimension of grasping for the first time. Thus, our results suggest that object properties (such as size) that are perceived with touch are mapped in coordinates that are dependent of gaze direction.

The modulation was evident in the middle and, to a greater extent, in the little finger. The thumb and index finger failed to show any modulation from gaze. In both the index and middle fingers, the finger aperture was larger when the participant was looking right, and smaller when the participant was looking left. It is interesting to note that the thumb in the

present data failed to show modulation even by object size (Figure 5) and similarly, the index finger appeared to be less movable than the last two fingers. Grip aperture is expected to scale with object size. Indeed, we found a robust effect of object size on the average finger aperture, but deeper analysis showed a gradient of motility of the fingers, from the thumb, which stayed almost fixed, to the most mobile little finger. Such gradient in movement range and in adaptation to object size could explain why we found effects of gaze only in the middle and little fingers, namely in the ones that showed higher mobility and task-related flexibility.

In the control experiment we showed that in the absence of a target object, gaze direction failed to modulate hand shaping. The value of this control experiments is to be evaluated according to a subtraction logic: the features present in the control task include the gaze manipulation and the finger movement. The main task also contains the elements of haptic acquisition of the object geometry, its storage in memory and its recall. We can therefore capitalize on the null results of the experiment by hypothesizing that the effects of gaze are not systematically present whenever a movement is made away from fixation points, but rather are specific to transitive, goal-directed movements. In the absence of more control conditions we cannot state that the effects of gaze are exclusive to the task of keeping in memory and using a haptically-acquired object image.

The aim of the experiment was to find configuration errors (i.e., errors due to a reference frame shift) in haptically-guided grasping, when manipulating the eye-centered frame of reference. The main results here confirm that shifts in eye position produce configuration errors when grasping an unseen object, supposedly associated with gaze direction.

5.5.2. Comparison with the effects of gaze direction on visually-guided grasping

One possible explanation of the present data is comparing them to the effects of gaze direction on visually guided grasping. Behavioral studies have shown that several aspects of

grasping movements display more conservative grasping behaviors when there is higher visual uncertainty about the target object, and the uncertainty about an object's properties increases when the object is in peripheral vision (Burbeck, 1987; Burbeck & Yap, 1990; Levi & Klein, 1996; Sivak & MacKenzie, 1990; Whitaker, 1997). In particular, during grasping actions, uncertainty about the target object is reflected in wider grip apertures during the movement, as this behavior would avoid collisions with the object (Rand et al., 2007; Wing et al., 1986). Besides the effects of sensory uncertainty, it is possible that effects of eccentricity of vision are due to the fact that the central (foveal) and peripheral visual field may be supported by separated neural systems as shown by dissociations between central and peripheral grasping in neuropsychological research. For instance, eccentric grasping is typically impaired in optic ataxia (Prado et al., 2005) but also in putative ventral stream lesions as shown by Hesse and colleagues (2012).

In line with this, investigations about the kinematics of grasping movements have consistently shown wider grip apertures during actions directed at objects that are away from our gaze as opposed to within our central visual field (Brown et al., 2005; Hall et al., 2014; Schlicht & Schrater, 2007). Evidence about the influence of gaze direction on grasping behavior has been replicated in several visual conditions, including continuous visual information about the target and hand throughout the movement as well as during no online visual information about target and hand during the movement (Karl & Whishaw, 2013; Schlicht & Schrater, 2007). In addition, similar results have been found when the location of the gaze varied with respect to a fixed target location, as well as when the location of the target varied with respect to a fixed gaze direction, suggesting that the observed effects are indeed related to the increasing distance of the target relative to fixation rather than the body. Further, different studies have shown similar effects regardless of whether participants had their head fixed or not, indicating

that the effect is independent of the direction of the head (Brown et al., 2005; Hall et al., 2014; Schlicht & Schrater, 2007).

We also found no effect of gaze eccentricity on the variability of MFE, which is in line with previous findings on the effect of eccentricity on grip aperture variability during visually-guided movements (Brown et al., 2005). However, in our study participants showed higher variability when grasping the large as compared to the small and medium object independently of eye position. One possible explanation of this could reside on the Weber's law, according to which there is a relation of direct proportionality between each stimulus and the so-called just noticeable difference (JND); namely, the JND for a weaker intensity stimulus is minor than the JND for a stronger intensity stimulus (Ganel et al., 2008). Based on this, Ganel and colleagues (2008), showed that the variability of grip aperture during manual estimation of visually perceived objects increases proportionally with object size. The same effect was observed for delayed, memory-based grasping, but not for real time actions. Memory-based grasping is a condition in which performance has been shown to be driven by perceptual representations and which can be fully dissociated from real-time grasping (Goodale et al., 2004). In line with this, Pettypiece and colleagues (2010) demonstrated that the same phenomenon occurs also during the manual estimation of haptically perceived object, but not for real-time grasping actions, i.e., while participants had online feedback about the size of the target object by holding it with the non-grasping hand. Hence, both visual- and haptic-based manual estimation of objects, as well as delayed actions towards visual stimuli follow Weber's law. Here we extend these findings to delayed grasping actions towards haptically explored objects. Indeed, in our study, participants performed haptic exploration of the object and the subsequent action with the same hand, and therefore there was a delay between the exploration and action phase.

Summing up, during vision, the effect of gaze is symmetrical and depends on eccentricity of the target. In the present study we failed to show such a pattern; on the contrary,

92

we found an asymmetrical effect, with larger apertures when looking right compared to when looking left or centrally.

5.5.3. Gaze direction asymmetrically affects hand shaping during haptically-guided reaching

There are many possible explanations for the asymmetrical effects observed on hand shaping. First, it is possible that the asymmetry could be related to the use of the participants' right hand. However, previous studies showed no difference between left and right hand when comparing the kinematics of both hands for grasping in conditions of occluded vision (Grosskopf & Kuhtz-Buschbeck, 2006; Tretriluxana et al., 2008). Second, it is likely that the combination of the hand used and the visual field in which the action was performed caused the observed asymmetry (despite the lack of visual information about the object); in this case, further investigations are required to disambiguate this issue. Third, it is possible that gaze direction modulated the extension only of those fingers (i.e., middle and little finger) having a secondary role in whole-hand grasping actions as opposed to those ones typically involved in precision grasping (i.e. thumb and index finger). Indeed, evidence suggests that during a reach-to-grasp action, the first contact between the hand and the target object occurs with the thumb and the index (Bicchi et al., 2011; Gabiccini et al., 2011). Notably, the core role of these two fingers in grasping movements was previously highlighted by investigations of the grip force during grasping with multiple finger prehension. Specifically, Kinoshita and colleagues (1995) have shown that the sum of the grip force exerted by index, middle, ring and little finger is equal to the force exerted by the thumb. Bedsides, the authors pointed out that, excluding the thumb, the greatest force comes from the index finger (42%), followed by the middle (27%), ring (18%) and little finger (13%). In addition, when all the fingers were used in a prehension task, higher releasing times were recorded for thumb and index finger. More importantly, the

grip force exerted by the index finger remained equal also when participants were asked to use three or four fingers. Analogue results were later reported by Santello and Soechting (2000). In addition, Lukos and colleagues (2007) examined the contact points of whole-hand grasping of object whose center of mass (CM) could vary from central to lateral in either a predictable or unpredictable way. Here, authors highlighted that when the CM varied unpredictably participants adopted a default spatial distribution of contact points involving the thumb and index finger. The same default combination was used to grasp object with predictable central CM as well. Taken together, this evidence suggests that the thumb and the index finger are the core fingers in whole hand reach-to-grasp movements, while the other fingers could have a secondary role depending on the type of movement required and the context and intention of the action itself (Ansuini et al., 2006, 2008). In light of this, we can assert that in our experiment gaze direction had no significant influence on the core-fingers during the reaching; on the contrary, it modulated the middle and little finger, which showed lower MFE while looking at the peripheral left as compared to central or right fixation.

5.5.4. Dependency of haptically-acquired object geometry from eye position indirectly supports the EVC's role as a memory sketchpad buffer

Recent evidence shows that the EVC in sighted individuals is also involved in tactile perception of objects despite the lack of visual information (D. A. Cunningham et al., 2013; James et al., 2002; Merabet et al., 2007, 2008; Perini et al., 2020; Sathian, 2005, 2016; Snow et al., 2014) as well as during action execution towards haptically explored objects (Marangon et al., 2016; Monaco et al., 2017). In addition, the activity pattern in the EVC allows decoding action planning seconds before participants perform a movement towards a visible target (Monaco et al., 2020). These findings suggest that the EVC is involved in mechanisms that go

well beyond visual processing, and in line with this, a theory describing the EVC as an all-purpose cognitive and spatial blackboard has been proposed (Roelfsema & de Lange, 2016). Thus, it would seem plausible that haptically explored objects as well as subsequent action plans are represented and stored in eye-centered coordinates with similar mechanisms as engaged for actions towards visually explored objects. Our finding showing effects of eye position on haptic grasping indicate that haptic memory for objects could rely at some point on an eye-centered frame of reference. This finding fits extremely well with the idea that visual system activity in non-visual behavior is causally related to performance. However, this effect of gaze direction needs to be further examined in future investigations in which other frames of reference (i.e., head- or body-centered) will be considered.

5.5.5. Limitations and future directions

The present study has several limitations. First, here we kept object position constant and manipulated eye position. A full factorial design, testing also eccentric object position and shifts in head or body-centered frames of reference and the left hand could provide more complete information. Second, while we hypothesize that the observed effects are a distortion of the memory of haptically-obtained object geometry, we cannot clearly describe the way the object's representation changes. Testing different object shapes and different orientations could help in characterizing this feature. Third, it is possible that effects of gaze direction on grip aperture may be related to eccentricity of the peripheral gaze directions (about 15° of visual angle). Further studies should investigate different and larger eccentricities (up to ~50° as in other studies (Brown et al., 2005; Hall et al., 2014)). Finally, to investigate into the asymmetry of the effect of gaze observed here, further investigations are needed in which participants use the right or the left hand in the same task, and in which participants grasp objects with vision, using the same manipulations. This would allow the deflections and asymmetry (which would

presumably replicate in the new experiment) to be interpreted more adequately as departures of

one extent or another from typical performance.

Bibliography

Aguirre, G. K., & D'Esposito, M. (1999). Topographical disorientation: A
synthesis and taxonomy. *Brain*, *122*(9), 1613–1628.
https://doi.org/10.1093/brain/122.9.1613

Aleotti, A., & Caselli, S. (2006). Grasp recognition in virtual reality for robot
pregrasp planning by demonstration. *Proceedings - IEEE International
Conference on Robotics and Automation*, *2006*, 2801–2806.
https://doi.org/10.1109/ROBOT.2006.1642125

Andersen, R. A. (1997). Multimodal integration for the representation of space
in the posterior parietal cortex. *Philosophical Transactions of the Royal
Society B: Biological Sciences*, *352*(1360), 1421–1428.
https://doi.org/10.1098/rstb.1997.0128

Ansuini, C., Cavallo, A., Koul, A., D'Ausilio, A., Taverna, L., & Becchio, C.
(2016). Grasping others' movements: Rapid discrimination of object size
from observed hand movements. *Journal of Experimental Psychology:
Human Perception and Performance*, *42*(7), 918–929.
https://doi.org/10.1037/xhp0000169

Ansuini, C., Cavallo, A., Koul, A., Jacono, M., Yang, Y., & Becchio, C. (2015). Predicting object size from hand kinematics: A temporal perspective. *PLoS ONE*, *10*(3), 1–13. https://doi.org/10.1371/journal.pone.0120432

Ansuini, C., Giosa, L., Turella, L., Altoè, G., & Castiello, U. (2008). An object for an action, the same object for other actions: Effects on hand shaping. *Experimental Brain Research*, *185*(1), 111–119. https://doi.org/10.1007/s00221-007-1136-4

Ansuini, C., Santello, M., Massaccesi, S., Castiello, U., Santello, M., & Massaccesi, S. (2006). Effects of End-Goal on Hand Shaping. *Journal of Neurophysiology*, *95*, 2456–2465. https://doi.org/10.1152/jn.01107.2005.

Avanzini, P., Abdollahi, R. O., Sartori, I., Caruana, F., Pelliccia, V., Casaceli, G., Mai, R., Lo Russo, G., Rizzolatti, G., & Orban, G. A. (2016). Four-dimensional maps of the human somatosensory system. *Proceedings of the National Academy of Sciences of the United States of America*, *113*(13), E1936–E1943. https://doi.org/10.1073/pnas.1601889113

Avenanti, A., Paracampo, R., Annella, L., Tidoni, E., & Aglioti, S. M. (2017). Boosting and decreasing action prediction abilities through excitatory and inhibitory tDCS of inferior frontal cortex. *Cerebral Cortex*, 1–15. https://doi.org/10.1093/cercor/bhx041

Awiszus, F. (2003). TMS and threshold hunting. In *Supplements to Clinical Neurophysiology* (Vol. 56). Elsevier B.V. https://doi.org/10.1016/S1567-424X(09)70205-3

Balan, P. F., & Gottlieb, J. (2009). Functional significance of nonspatial information in monkey lateral intraparietal area. *Journal of Neuroscience*, *29*(25), 8166–8176. https://doi.org/10.1523/JNEUROSCI.0243-09.2009

Bartoli, E., Maffongelli, L., Jacono, M., & D'Ausilio, A. (2014). Representing tools as hand movements: Early and somatotopic visuomotor transformations. *Neuropsychologia*, *61*(1), 335–344. https://doi.org/10.1016/j.neuropsychologia.2014.06.025

Bates, D., Maechler, M., Bolker, B., & Walker, S. (2015). *lme4: Linear mixed-effect models using Eigen and S4. (R package version 1.1-7). R. November*.

Batista, A. P. (2002). Inner space: Reference frames. *Current Biology*, *12*(11), 380–383.

Battaglini, P., Muzur, A., Galletti, C., Skrap, M., Brovelli, A., & Fattori, P. (2002). Effects of lesions to area V6A in monkeys. *Experimental Brain Research*, *144*(3), 419–422. https://doi.org/10.1007/s00221-002-1099-4

Berthier, N. E., Clifton, R. K., Gullapalli, V., McCall, D. D., & Robin, D. J. (1996). Visual Information and Object Size in the Control of Reaching.

Journal of Motor Behavior, *28*(3), 187–197.

https://doi.org/10.1080/00222895.1996.9941744

Beurze, S. M., de Lange, F. P., Toni, I., & Medendorp, W. P. (2007). Integration

of Target and Effector Information in the Human Brain During Reach

Planning. *Journal of Neurophysiology*, *97*(1), 188–199.

https://doi.org/10.1152/jn.00456.2006

Beurze, S. M., de Lange, F. P., Toni, I., & Medendorp, W. P. (2009). Spatial and

Effector Processing in the Human Parietofrontal Network for Reaches and

Saccades. *Journal of Neurophysiology*, *101*(6), 3053–3062.

https://doi.org/10.1152/jn.91194.2008

Beurze, S. M., Toni, I., Pisella, L., & Medendorp, W. P. (2010). Reference

frames for reach planning in human parietofrontal cortex. *Journal of

Neurophysiology*, *104*(3), 1736–1745.

https://doi.org/10.1152/jn.01044.2009

Bianchi, M., Salaris, P., & Bicchi, A. (2013a). Synergy-based hand pose

sensing: Optimal glove design. *International Journal of Robotics Research*,

32(4), 407–424. https://doi.org/10.1177/0278364912474079

Bianchi, M., Salaris, P., & Bicchi, A. (2013b). Synergy-based hand pose

sensing: Reconstruction enhancement. *International Journal of Robotics*

Research, *32*(4), 396–406. https://doi.org/10.1177/0278364912474078

Bicchi, A., Gabiccini, M., & Santello, M. (2011). Modelling natural and artificial hands with synergies. *Philosophical Transactions of the Royal Society B: Biological Sciences*, *366*(1581), 3153–3161. https://doi.org/10.1098/rstb.2011.0152

Binkofski, F., & Buxbaum, L. J. (2013). Two action systems in the human brain. *Brain and Language*, *127*(2), 222–229. https://doi.org/10.1016/j.bandl.2012.07.007

Binkofski, F., Dohle, C., Posse, S., Stephan, K. M., Hefter, H., Seitz, R. J., & Freund, H.-J. (1998). Human anterior intraparietal area subserves prehension: a combined lesion and functional MRI activation study. *Neurology*, *50*(5), 1253–1259.

Bisiach, E., & Luzzatti, C. (1978). Unilateral Neglect of Representational Space. *Cortex*. https://doi.org/10.1016/S0010-9452(78)80016-1

Bonini, L. (2016). The Extended Mirror Neuron Network: Anatomy, Origin, and Functions. *The Neuroscientist*, *23*(1), 56–67. https://doi.org/10.1177/1073858415626400

Bonini, L., Maranesi, M., Livi, A., Fogassi, L., & Rizzolatti, G. (2014a). Space-Dependent Representation of Objects and Other's Action in Monkey

Ventral Premotor Grasping Neurons. *Journal of Neuroscience*, *34*(11), 4108–4119. https://doi.org/10.1523/JNEUROSCI.4187-13.2014

Bonini, L., Maranesi, M., Livi, A., Fogassi, L., & Rizzolatti, G. (2014b). Ventral premotor neurons encoding representations of action during self and others' inaction. *Current Biology*, *24*(14), 1611–1614. https://doi.org/10.1016/j.cub.2014.05.047

Borra, E., Belmalih, A., Calzavara, R., Gerbella, M., Murata, A., Rozzi, S., & Luppino, G. (2008). Cortical connections of the macaque anterior intraparietal (AIP) area. *Cerebral Cortex*, *18*(5), 1094–1111. https://doi.org/10.1093/cercor/bhm146

Borra, E., Gerbella, M., Rozzi, S., & Luppino, G. (2017). The macaque lateral grasping network: A neural substrate for generating purposeful hand actions. *Neuroscience and Biobehavioral Reviews*, *75*, 65–90. https://doi.org/10.1016/j.neubiorev.2017.01.017

Borra, E., & Luppino, G. (2017). Functional anatomy of the macaque temporo-parieto-frontal connectivity. *Cortex*, *97*, 306–326. https://doi.org/10.1016/j.cortex.2016.12.007

Boussaoud, D., Jouffrais, C., & Bremmer, F. (1998). Eye Position Effects on the Neuronal Activity of Dorsal Premotor Cortex in the Macaque Monkey.

Journal of Neurophysiology, *80*, 1132–1150.

Bracci, S., & Peelen, M. V. (2013). Body and object effectors: The organization of object representations in high-level visual cortex reflects body-object interactions. *Journal of Neuroscience*, *33*(46), 18247–18258. https://doi.org/10.1523/JNEUROSCI.1322-13.2013

Breiman, L. (2001). Random forests. *Machine Learning*, *45*, 5–32. https://doi.org/10.1201/9780367816377-11

Breveglieri, R., Bosco, A., Borgomaneri, S., Tessari, A., Galletti, C., Avenanti, A., & Fattori, P. (2020). Transcranial Magnetic Stimulation Over the Human Medial Posterior Parietal Cortex Disrupts Depth Encoding During Reach Planning. *Cerebral Cortex*, *February*, 1–14. https://doi.org/10.1093/cercor/bhaa224

Brochier, T., & Umiltà, M. A. (2007). Cortical control of grasp in non-human primates. *Current Opinion in Neurobiology*, *17*(6), 637–643. https://doi.org/10.1016/j.conb.2007.12.002

Brown, L. E., Halpert, B. A., & Goodale, M. A. (2005). Peripheral vision for perception and action. *Experimental Brain Research*, *165*(1), 97–106. https://doi.org/10.1007/s00221-005-2285-y

Buneo, C. A., Jarvis, M. R., Batista, A. P., & Andersen, R. A. (2002). Direct

visuomotor transformations for reaching. *Nature*, *416*(6881), 632–636.

Burbeck, C. A. (1987). Position and spatial frequency in large-scale localization judgments. *Vision Research*, *27*(3), 417–427. https://doi.org/10.1016/0042-6989(87)90090-3

Burbeck, C. A., & Yap, Y. L. (1990). Two mechanisms for localization? Evidence for separation-dependent and separation-independent processing of position information. *Vision Research*, *30*(5), 739–750. https://doi.org/10.1016/0042-6989(90)90099-7

Burton, H., McLaren, D. G., & Sinclair, R. J. (2006). Reading embossed capital letters: An fMRI study in blind and sighted individuals. *Human Brain Mapping*, *27*(4), 325–339. https://doi.org/10.1002/hbm.20188

Busan, P., Barbera, C., Semenic, M., Monti, F., Pizzolato, G., Pelamatti, G., & Battaglini, P. P. (2009). Effect of transcranial magnetic stimulation (TMS) on parietal and premotor cortex during planning of reaching movements. *PLoS ONE*, *4*(2), e4621. https://doi.org/10.1371/journal.pone.0004621

Byrnes, M. L., Thickbroom, G. W., Phillips, B. A., & Mastaglia, F. L. (2001). Long-term changes in motor cortical organisation after recovery from subcortical stroke. *Brain Research*, *889*, 278–287. https://doi.org/10.1016/S0006-8993(00)03089-4

Caminiti, R., Fet-rainat, S., & Battaglia, A. (1998). Visuomotor transformations: early cortical mechanisms of reaching. *Current Opinion in Neurobiology*, *8*, 753–761.

Caminiti, R, Innocenti, G. M., & Battaglia-Mayer, A. (2015). Organization and evolution of parieto-frontal processing streams in macaque monkeys and humans. *Neuroscience and Biobehavioral Reviews*, *56*, 73–96. https://doi.org/10.1016/j.neubiorev.2015.06.014

Camponogara, I., & Volcic, R. (2019). Grasping adjustments to haptic, visual, and visuo-haptic object perturbations are contingent on the sensory modality. *Journal of Neurophysiology*, *122*(6), 2614–2620. https://doi.org/10.1152/jn.00452.2019

Caselli, R. J. (1991). Rediscovering Tactile Agnosia. *Mayo Clinic Proceedings*, *66*(2), 129–142. https://doi.org/10.1016/S0025-6196(12)60484-4

Castellini, C., & Van Der Smagt, P. (2013). Evidence of muscle synergies during human grasping. *Biological Cybernetics*, *107*(2), 233–245. https://doi.org/10.1007/s00422-013-0548-4

Cattaneo, L. (2018). Fancies and fallacies of spatial sampling with transcranial magnetic stimulation (TMS). *Frontiers in Psychology*, *9*(JUL), 1–5. https://doi.org/10.3389/fpsyg.2018.01171

Cattaneo, L., & Barchiesi, G. (2011). Transcranial magnetic mapping of the short-latency modulations of corticospinal activity from the ipsilateral hemisphere during rest. *Frontiers in Neural Circuits*, *5*(14), 1–13. https://doi.org/10.3389/fncir.2011.00014

Cattaneo, L., Maule, F., Tabarelli, D., Brochier, T., & Barchiesi, G. (2015). Online repetitive transcranial magnetic stimulation (TMS) to the parietal operculum disrupts haptic memory for grasping. *Human Brain Mapping*, *36*(11), 4262–4271. https://doi.org/10.1002/hbm.22915

Cattaneo, L., & Parmigiani, S. (2021). Stimulation of Different Sectors of the Human Dorsal Premotor Cortex Induces a Shift from Reactive to Predictive Action Strategies and Changes in Motor Inhibition : A Dense Transcranial Magnetic Stimulation (TMS) Mapping Study. *Brain Science*, *11*(534), 1–16.

Cavina-Pratesi, C., Monaco, S., Fattori, P., Galletti, C., McAdam, T. D., Quinlan, D. J., Goodale, M. A., & Culham, J. C. (2010). Functional magnetic resonance imaging reveals the neural substrates of arm transport and grip formation in reach-to-grasp actions in humans. *Journal of Neuroscience*, *30*(31), 10306–10323. https://doi.org/10.1523/JNEUROSCI.2023-10.2010

Cheung, S. H., Fang, F., He, S., & Legge, G. E. (2009). Retinotopically Specific Reorganization of Visual Cortex for Tactile Pattern Recognition. *Current*

Biology, *19*(7), 596–601. https://doi.org/10.1016/j.cub.2009.02.063

Cisek, P. (2007). Cortical mechanisms of action selection: The affordance competition hypothesis. *Philosophical Transactions of the Royal Society B: Biological Sciences*, *362*(1485), 1585–1599. https://doi.org/10.1098/rstb.2007.2054

Cisek, P., & Kalaska, J. F. (2010). Neural mechanisms for interacting with a world full of action choices. *Annual Review of Neuroscience*, *33*, 269–298. https://doi.org/10.1146/annurev.neuro.051508.135409

Civarro, M., Ambrosini, E., Tosoni, A., Committeri, G., Fattori, P., & Galletti, C. (2013). rTMS of Medial Parieto-occipital Cortex Interferes with Attentional Reorienting during Attention and Reaching Tasks. *Journal of Cognitive Neuroscience*, *25*(9), 1453–1462. https://doi.org/10.1162/jocn_a_00409

Clavagnier, S., Prado, J., Kennedy, H., & Perenin, M. T. (2007). How humans reach: Distinct cortical systems for central and peripheral vision. *Neuroscientist*, *13*(1), 22–27. https://doi.org/10.1177/1073858406295688

Cohen, N. R., Cross, E. S., Tunik, E., Grafton, S. T., & Culham, J. C. (2009). Ventral and dorsal stream contributions to the online control of immediate and delayed grasping: A TMS approach. *Neuropsychologia*, *47*(6), 1553–

1562. https://doi.org/10.1016/j.neuropsychologia.2008.12.034

Cohen, Y. E., & Andersen, R. A. (2002). A common reference frame for movement plans in the posterior parietal cortex. *Nature Reviews Neuroscience*, *3*(7), 553–562. https://doi.org/10.1038/nrn873

Connolly, J. D., Andersen, R. A., & Goodale, M. A. (2003). FMRI evidence for a "parietal reach region" in the human brain. *Experimental Brain Research*, *153*(2), 140–145. https://doi.org/10.1007/s00221-003-1587-1

Crawford, J. D., Henriques, D. Y. P., & Medendorp, W. P. (2011). Three-dimensional transformations for goal-directed action. *Annual Review of Neuroscience*, *34*, 309–331. https://doi.org/10.1146/annurev-neuro-061010-113749

Criado, J. M., de la Fuente, A., Heredia, M., Riolobos, A. S., & Yajeya, J. (2008). Single-cell recordings: A method for investigating the brain's activation pattern during exercise. *Methods*, *45*(4), 262–270. https://doi.org/10.1016/j.ymeth.2008.05.007

Cuijpers, R. H., Smeets, J. B. J., & Brenner, E. (2004). On the relation between object shape and grasping kinematics. *Journal of Neurophysiology*, *91*(6), 2598–2606. https://doi.org/10.1152/jn.00644.2003

Culham, J. C., Cavina-Pratesi, C., & Singhal, A. (2006). The role of parietal

cortex in visuomotor control: What have we learned from neuroimaging?

Neuropsychologia, *44*(13), 2668–2684.

https://doi.org/10.1016/j.neuropsychologia.2005.11.003

Culham, J. C., Danckert, S. L., DeSouza, J. F. X., Gati, J. S., Menon, R. S., &

Goodale, M. A. (2003). Visually guided grasping produces fMRI activation

in dorsal but not ventral stream brain areas. *Experimental Brain Research*,

153(2), 180–189. https://doi.org/10.1007/s00221-003-1591-5

Culham, J. C., & Valyear, K. F. (2006). Human parietal cortex in action.

Current Opinion in Neurobiology, *16*(2), 205–212.

https://doi.org/10.1016/j.conb.2006.03.005

Cunningham, D. A., Machado, A., Yue, G. H., Carey, J. R., & Plow, E. B.

(2013). Functional somatotopy revealed across multiple cortical regions

using a model of complex motor task. *Brain Research*, *1531*, 25–36.

https://doi.org/10.1038/jid.2014.371

Cunningham, S. I., Weiland, J. D., Bao, P., Lopez-Jaime, G. R., & Tjan, B. S.

(2015). Correlation of vision loss with tactile-evoked V1 responses in

retinitis pigmentosa. *Vision Research*, *111*, 197–207.

https://doi.org/10.1016/j.visres.2014.10.015

Davare, M., Andres, M., Clerget, E., Thonnard, J. L., & Olivier, E. (2007).

Temporal dissociation between hand shaping and grip force scaling in the anterior intraparietal area. *Journal of Neuroscience*, *27*(15), 3974–3980. https://doi.org/10.1523/JNEUROSCI.0426-07.2007

Davare, M., Andres, M., Cosnard, G., Thonnard, J.-L., & Oliver, E. (2006). Dissociating the Role of Ventral and Dorsal Premotor Cortex in Precision Grasping. *Journal of Neuroscience*, *26*(8), 2260–2268. https://doi.org/10.1523/JNEUROSCI.3386-05.2006

Davare, M., Kraskov, A., Rothwell, J. C., & Lemon, R. N. (2011). Interactions between areas of the cortical grasping network. *Current Opinion in Neurobiology*, *21*(4), 565–570. https://doi.org/10.1016/j.conb.2011.05.021

Davare, M., Montague, K., Olivier, E., Rothwell, J. C., & Lemon, R. N. (2009). Ventral premotor to primary motor cortical interactions during object-driven grasp in humans. *Cortex*, *45*(9), 1050–1057. https://doi.org/10.1016/j.cortex.2009.02.011

Davare, M., Rothwell, J. C., & Lemon, R. N. (2010). Causal Connectivity between the Human Anterior Intraparietal Area and Premotor Cortex during Grasp. *Current Biology*, *20*(2), 176–181. https://doi.org/10.1016/j.cub.2009.11.063

Di Pellegrino, G., Fadiga, L., Fogassi, L., Gallese, V., & Rizzolatti, G. (1992).

Understanding motor events: a neurophysiological study. *Experimental Brain Research*, *91*, 176–180.

Dipietro, L., Sabatini, A. M., & Dario, P. (2003). Evaluation of an instrumented glove for hand-movement acquisition. *Journal of Rehabilitation Research and Development*, *40*(2), 179–189. https://doi.org/10.1682/jrrd.2003.03.0181

Donnarumma, F., Costantini, M., Ambrosini, E., Friston, K., & Pezzulo, G. (2017). Action perception as hypothesis testing. *Cortex*, *89*, 45–60. https://doi.org/10.1016/j.cortex.2017.01.016

Eickhoff, S. B., Grefkes, C., Zilles, K., & Fink, G. R. (2007). The somatotopic organization of cytoarchitectonic areas on the human parietal operculum. *Cerebral Cortex*, *17*(8), 1800–1811. https://doi.org/10.1093/cercor/bhl090

Ellison, A., Schindler, I., Pattison, L. L., & Milner, A. D. (2004). An exploration of the role of the superior temporal gyrus in visual search and spatial perception using TMS. *Brain*, *127*(10), 2307–2315. https://doi.org/10.1093/brain/awh244

Fabbri, S., Strnad, L., Caramazza, A., & Lingnau, A. (2014). Overlapping representations for grip type and reach direction. *NeuroImage*, *94*, 138–146. https://doi.org/10.1016/j.neuroimage.2014.03.017

Fattori, P., Breveglieri, R., Raos, V., Bosco, A., & Galletti, C. (2012). Vision for action in the macaque medial posterior parietal cortex. *Journal of Neuroscience*, *32*(9), 3221–3234. https://doi.org/10.1523/JNEUROSCI.5358-11.2012

Fattori, P., Raos, V., Breveglieri, R., Bosco, A., Marzocchi, N., & Galletti, C. (2010). The dorsomedial pathway is not just for reaching: Grasping neurons in the medial parieto-occipital cortex of the macaque monkey. *Journal of Neuroscience*, *30*(1), 342–349. https://doi.org/10.1523/JNEUROSCI.3800-09.2010

Faugier-Grimaud, S., Frenois, C., & Peronnet, F. (1985). Effects of posterior parietal lesions on visually guided movements in monkeys. *Experimental Brain Research*, *59*(1), 125–138. https://doi.org/10.1007/BF00237673

Filimon, F. (2010). Human cortical control of hand movements: Parietofrontal networks for reaching, grasping, and pointing. *Neuroscientist*, *16*(4), 388–407. https://doi.org/10.1177/1073858410375468

Filimon, F., Nelson, J. D., Hagler, D. J., & Sereno, M. I. (2007). Human cortical representations for reaching: Mirror neurons for execution, observation, and imagery. *NeuroImage*, *37*(4), 1315–1328. https://doi.org/10.1016/j.neuroimage.2007.06.008

Filimon, F., Nelson, J. D., Huang, R. S., & Sereno, M. I. (2009). Multiple

parietal reach regions in humans: Cortical representations for visual and

proprioceptive feedback during on-line reaching. *Journal of Neuroscience*,

29(9), 2961–2971. https://doi.org/10.1523/JNEUROSCI.3211-08.2009

Finocchiaro, C., Capasso, R., Cattaneo, L., Zuanazzi, A., & Miceli, G. (2015).

Thematic role assignment in the posterior parietal cortex: A TMS study.

Neuropsychologia, *77*, 223–232.

https://doi.org/10.1016/j.neuropsychologia.2015.08.025

Fluet, M. C., Baumann, M. A., & Scherberger, H. (2010). Context-specific grasp

movement representation in macaque ventral premotor cortex. *Journal of

Neuroscience*, *30*(45), 15175–15184.

https://doi.org/10.1523/JNEUROSCI.3343-10.2010

Fogassi, L., Gallese, V., Buccino, G., Craighero, L., Fadiga, L., & Rizzolatti, G.

(2001). Cortical mechanism for the visual guidance of hand grasping

movements in the monkey A reversible inactivation study. *Brain*, *124*, 571–

586.

Forster, M. T., Hattingen, E., Senft, C., Gasser, T., Seifert, V., & Szelényi, A.

(2011). Navigated transcranial magnetic stimulation and functional

magnetic resonance imaging: Advanced adjuncts in preoperative planning

for central region tumors. *Neurosurgery*, *68*(5), 1317–1324.

https://doi.org/10.1227/NEU.0b013e31820b528c

Fricke, C., Gentner, R., Alizadeh, J., & Classen, J. (2019). Linking Individual Movements to a Skilled Repertoire: Fast Modulation of Motor Synergies by Repetition of Stereotyped Movements. *Cerebral Cortex*, *00*, 1–14. https://doi.org/10.1093/cercor/bhz159

Fricke, C., Gentner, R., Rumpf, J. J., Weise, D., Saur, D., & Classen, J. (2017). Differential spatial representation of precision and power grasps in the human motor system. *NeuroImage*, *158*(June), 58–69. https://doi.org/10.1016/j.neuroimage.2017.06.080

Friston, K. J., Harrison, L., & Penny, W. (2003). Dynamic causal modelling. *NeuroImage*, *19*(4), 1273–1302. https://doi.org/10.1016/S1053-8119(03)00202-7

Gabiccini, M., Bicchi, A., Prattichizzo, D., & Malvezzi, M. (2011). On the role of hand synergies in the optimal choice of grasping forces. *Autonomous Robots*, *31*(2–3), 235–252. https://doi.org/10.1007/s10514-011-9244-1

Gail, A., & Andersen, R. A. (2006). Neural dynamics in monkey parietal reach region reflect context-specific sensorimotor transformations. *Journal of Neuroscience*, *26*(37), 9376–9384. https://doi.org/10.1523/JNEUROSCI.1570-06.2006

Gallese, V., Murata, A., Kaseda, M., Niki, N., & Sakata, H. (1994). Deficit of

hand preshaping after muscimol injection in monkey parietal cortex.

Neuroreport, *5*, 1525–1529.

Galletti, C., & Fattori, P. (2018). The dorsal visual stream revisited: Stable

circuits or dynamic pathways? *Cortex*, *98*, 203–217.

https://doi.org/10.1016/j.cortex.2017.01.009

Gallivan, J. P., Cant, J. S., Goodale, M. A., & Flanagan, J. R. (2014).

Representation of object weight in human ventral visual cortex. *Current

Biology*, *24*, 1866–1873. https://doi.org/10.1016/j.cub.2014.06.046

Gallivan, J. P., & Culham, J. C. (2015). Neural coding within human brain areas

involved in actions. *Current Opinion in Neurobiology*, *33*, 141–149.

https://doi.org/10.1016/j.conb.2015.03.012

Gallivan, J. P., McLean, D. A., Flanagan, J. R., & Culham, J. C. (2013). Where

One Hand Meets the Other: Limb-Specific and Action-Dependent

Movement Plans Decoded from Preparatory Signals in Single Human

Frontoparietal Brain Areas. *Journal of Neuroscience*, *33*(5), 1991–2008.

https://doi.org/10.1523/JNEUROSCI.0541-12.2013

Gallivan, J. P., McLean, D. A., Smith, F. W., & Culham, J. C. (2011). Decoding

Effector-Dependent and Effector-Independent Movement Intentions from

Human Parieto-Frontal Brain Activity. *Journal of Neuroscience*, *31*(47),

17149–17168. https://doi.org/10.1523/JNEUROSCI.1058-11.2011

Gamberini, M., Passarelli, L., Fattori, P., Zucchelli, M., Bakola, S., Luppino, G.,

& Galletti, C. (2009). Cortical Connections of the Visuomotor

Parietooccipital Area V6Ad of the Macaque Monkey. *The Journal of

Comparative Neurology*, *513*, 622–642. https://doi.org/10.1002/cne.21980

Ganel, T., Chajut, E., & Algom, D. (2008). Visual coding for action violates

fundamental psychophysical principles. *Current Biology*, *18*(14), 599–601.

https://doi.org/10.1016/j.cub.2008.04.052

Gentilucci, M., Scandolara, C., Pigarev, I. N., & Rizzolatti, G. (1983). Visual

responses in the postarcuate cortex (area 6) of the monkey that are

independent of eye position. *Experimental Brain Research*.

https://doi.org/10.1007/BF00239214

Gentner, R., & Classen, J. (2006). Modular Organization of Finger Movements

by the Human Central Nervous System. *Neuron*, *52*(4), 731–742.

https://doi.org/10.1016/j.neuron.2006.09.038

Gentner, R., & Classen, J. (2009). Development and evaluation of a low-cost

sensor glove for assessment of human finger movements in

neurophysiological settings. *W*, *178*(1), 138–147.

https://doi.org/10.1016/j.jneumeth.2008.11.005

Gerbella, M., Belmalih, A., Borra, E., Rozzi, S., & Luppino, G. (2011). Cortical

connections of the anterior (F5a) subdivision of the macaque ventral

premotor area F5. *Brain Structure and Function*, *216*, 43–65.

https://doi.org/10.1007/s00429-010-0293-6

Gerbella, M., Rozzi, S., & Rizzolatti, G. (2017). The extended object-grasping

network. *Experimental Brain Research*, *235*(10), 2903–2916.

https://doi.org/10.1007/s00221-017-5007-3

Glover, S., Miall, R. C., & Rushworth, M. F. S. (2005). Parietal rTMS disrupts

the initiation but not the execution of on-line adjustments to a perturbation

of object size. *Journal of Cognitive Neuroscience*, *17*(1), 124–136.

https://doi.org/10.1162/0898929052880066

Goodale, M. A., & Milner, A. D. (1992). Separate visual pathways for

perception and action. *Trends in Neurosciences*, *15*(1), 20–15.

https://doi.org/10.1093/litthe/11.1.80

Goodale, M. A., Westwood, D. A., & Milner, A. D. (2004). Two distinct modes

of control for object-directed action. *Progress in Brain Research*, *144*, 131–

144. https://doi.org/10.1016/S0079-6123(03)14409-3

Goodman, J. M., & Bensmaia, S. J. (2018). The Neural Basis of Haptic

Perception. In *Stevens' Handbook of Experimental Psychology and Cognitive Neuroscience*. https://doi.org/10.1002/9781119170174.epcn205

Grafton, S. T. (2010). The cognitive neuroscience of prehension: Recent developments. *Experimental Brain Research*, *204*(4), 475–491. https://doi.org/10.1007/s00221-010-2315-2

Grafton, S. T., Fagg, A. H., Woods, R. P., & Arbib, M. A. (1996). Functional anatomy of pointing and grasping in humans. *Cerebral Cortex*, *6*(2), 226–237. https://doi.org/10.1093/cercor/6.2.226

Grol, M. J., Majdandžić, J., Stephan, K. E., Verhagen, L., Dijkerman, H. C., Bekkering, H., Verstraten, F. A. J., & Toni, I. (2007). Parieto-frontal connectivity during visually guided grasping. *Journal of Neuroscience*, *27*(44), 11877–11887. https://doi.org/10.1523/JNEUROSCI.3923-07.2007

Grosskopf, A., & Kuhtz-Buschbeck, J. P. (2006). Grasping with the left and right hand: a kinematic study. *Experimental Brain Research*, *168*, 230–240. https://doi.org/10.1007/s00221-005-0083-1

Häger-Ross, C., & Schieber, M. H. (2000). Quantifying the Independence of Human Finger Movements: Comparisons of Digits, Hands, and Movement Frequencies. *The Journal of Neuroscience*, *20*(22), 8542–8550.

Hall, L. A., Karl, J. M., Thomas, B. L., & Whishaw, I. Q. (2014). Reach and

Grasp reconfigurations reveal that proprioception assists reaching and hapsis assists grasping in peripheral vision. *Experimental Brain Research*, *232*(9), 2807–2819. https://doi.org/10.1007/s00221-014-3945-6

Hepp-Reymond, M.-C., Hüsler, E. J., Maier, M. A., & Qi, H.-X. (1994). Force-related neuronal activity in two regions of the primate ventral premotor cortex. *Can. J. Physiol. Pharmacol.*, *72*(1919), 571–579.

Hesse, C., Ball, K., & Schenk, T. (2012). Neuropsychologia Visuomotor performance based on peripheral vision is impaired in the visual form agnostic patient DF. *Neuropsychologia*, *50*(1), 90–97. https://doi.org/10.1016/j.neuropsychologia.2011.11.002

Hoshi, E., & Tanji, J. (2000). Integration of target and body-part information in the premotor cortex when planning action. *Nature*, *408*, 466–470.

Hoshi, E., & Tanji, J. (2007). Distinctions between dorsal and ventral premotor areas: anatomical connectivity and functional properties. *Current Opinion in Neurobiology*, *17*(2), 234–242. https://doi.org/10.1016/j.conb.2007.02.003

Hsiao, S., & Yau, J. (2008). Neural basis of haptic perception. In M. Grunwald (Ed.), *Human Haptic Perception: Basics and Applications*. Springer Berlin Heidelberg. https://doi.org/10.1007/978-3-7643-7612-3

Huda, R., Goard, M. J., Pho, G. N., & Sur, M. (2019). Neural mechanisms of

sensorimotor transformation and action selection. *European Journal of Neuroscience*, *49*(8), 1055–1060. https://doi.org/10.1111/ejn.14069

Husain, M., & Nachev, P. (2006). Space and the parietal cortex. *Trends in Cognitive Sciences*, *11*(1), 30–36. https://doi.org/10.1016/j.tics.2006.10.011

Jakobson, L. S., Archibald, Y. M., Carey, D. P., & Goodale, M. A. (1991). A kinematic analysis of reaching and grasping movements in a patient recovering from optic ataxia. *Neuropsychologia*, *29*(8). https://doi.org/10.1016/0028-3932(91)90073-H

James, T. W., Humphrey, G. K., Gati, J. S., Servos, P., Menon, R. S., & Goodale, M. A. (2002). Haptic study of three-dimensional objects activates extrastriate visual areas. *Neuropsychologia*, *40*(10), 1706–1714. https://doi.org/10.1016/S0028-3932(02)00017-9

James, T. W., Kim, S., & Fisher, J. S. (2007). The neural basis of haptic object processing. *Canadian Journal of Experimental Psychology*, *61*(3), 219–229. https://doi.org/10.1037/cjep2007023

Jarque-Bou, N. J., Scano, A., Atzori, M., & Müller, H. (2019). Kinematic synergies of hand grasps: A comprehensive study on a large publicly available dataset. *Journal of NeuroEngineering and Rehabilitation*, *16*(1), 1–14. https://doi.org/10.1186/s12984-019-0536-6

Jeannerod, M., Arbib, M. A., Rizzolatti, G., & Sakata, H. (1995). Grasping

   objects: the cortical mechanisms of visuomotor transformation. In *Trends in*

   Neurosciences (Vol. 18, Issue 7, pp. 314–320).

   https://doi.org/10.1016/0166-2236(95)93921-J

Jerde, T. E., Soechting, J. F., & Flanders, M. (2003). Biological constraints

   simplify the recognition of hand shapes. *IEEE Transactions on Biomedical*

   Engineering, *50*(2), 265–269. https://doi.org/10.1109/TBME.2002.807640

Johnson, P. B., Ferraina, S., Bianchi, L., & Caminiti, R. (1996). Cortical

   networks for visual reaching: Physiological and anatomical organization of

   frontal and parietal lobe arm regions. *Cerebral Cortex*, *6*(2), 102–119.

   https://doi.org/10.1093/cercor/6.2.102

Karl, J. M., Sacrey, L. A. R., Doan, J. B., & Whishaw, I. Q. (2012). Hand

   shaping using hapsis resembles visually guided hand shaping. *Experimental*

   Brain Research, *219*(1), 59–74. https://doi.org/10.1007/s00221-012-3067-y

Karl, J. M., & Whishaw, I. Q. (2013). Different evolutionary origins for the

   Reach and the Grasp: An explanation for dual visuomotor channels in

   primate parietofrontal cortex. *Frontiers in Neurology*, *4 DEC*(December),

   1–13. https://doi.org/10.3389/fneur.2013.00208

Karnath, H. O., & Perenin, M. T. (2005). Cortical control of visually guided

reaching: Evidence from patients with optic ataxia. *Cerebral Cortex*, *15*(10), 1561–1569. https://doi.org/10.1093/cercor/bhi034

King, M., Rauch, H. G. L., Stein, D. J., & Brooks, S. J. (2014). NeuroImage The handyman's brain: A neuroimaging meta-analysis describing the similarities and differences between grip type and pattern in humans. *NeuroImage*, *102*(2), 923–937. https://doi.org/10.1016/j.neuroimage.2014.05.064

Kinoshita, H., Kawai, S., & Ikuta, K. (1995). Contributions and co-ordination of individual fingers in multiple finger prehension. *Ergonomics*, *38*(6), 1212–1230. https://doi.org/10.1080/00140139508925183

Könönen, M., Tamsi, N., Säisänen, L., Kemppainen, S., Määttä, S., Julkunen, P., Jutila, L., Äikiä, M., Kälviäinen, R., Niskanen, E., Vanninen, R., Karjalainen, P., & Mervaala, E. (2015). Non-invasive mapping of bilateral motor speech areas using navigated transcranial magnetic stimulation and functional magnetic resonance imaging. *Journal of Neuroscience Methods*, *248*, 32–40. https://doi.org/10.1016/j.jneumeth.2015.03.030

Krieg, S. M., Shiban, E., Buchmann, N., Gempt, J., Foerschler, A., Meyer, B., & Ringel, F. (2012). Utility of presurgical navigated transcranial magnetic brain stimulation for the resection of tumors in eloquent motor areas: Clinical article. *Journal of Neurosurgery*, *116*(5), 994–1001. https://doi.org/10.3171/2011.12.JNS111524

Krubitzer, L., Clarey, J., Tweedale, R., Elston, G., & Calford, M. (1995). A

   redefinition of somatosensory areas in the lateral sulcus of macaque

   monkeys. *Journal of Neuroscience*, *15*(5 II), 3821–3839.

   https://doi.org/10.1523/jneurosci.15-05-03821.1995

Kumar, P., Verma, J., & Prasad, S. (2012). Hand Data Glove: A Wearable Real-

   Time Device for Human- Computer Interaction. *International Journal of*

   Advanced Science and Technology, *43*(June), 15–26.

Lang, C. E., & Schieber, M. H. (2003). Differential Impairment of Individuated

   Finger Movements in Humans After Damage to the Motor Cortex or the

   Corticospinal Tract. *Journal of Neurophysiology*, *90*(4), 1160–1170.

   https://doi.org/10.1152/jn.00805.2003

Lang, C. E., & Schieber, M. H. (2004a). Human finger independence:

   Limitations due to passive mechanical coupling versus active

   neuromuscular control. *Journal of Neurophysiology*, *92*(5), 2802–2810.

   https://doi.org/10.1152/jn.00480.2004

Lang, C. E., & Schieber, M. H. (2004b). Reduced Muscle Selectivity during

   Individuated Finger Movements in Humans after Damage to the Motor

   Cortex or Corticospinal Tract. *Journal of Neurophysiology*, *91*(4), 1722–

   1733. https://doi.org/10.1152/jn.00805.2003

Lanzilotto, M., Livi, A., Maranesi, M., Gerbella, M., Barz, F., Ruther, P., Fogassi, L., Rizzolatti, G., & Bonini, L. (2016). Extending the cortical grasping network: Pre-supplementary motor neuron activity during vision and grasping of objects. *Cerebral Cortex*, *26*(12), 4435–4449. https://doi.org/10.1093/cercor/bhw315

Lee Masson, H., Bulthé, J., Op De Beeck, H. P., & Wallraven, C. (2016). Visual and Haptic Shape Processing in the Human Brain: Unisensory Processing, Multisensory Convergence, and Top-Down Influences. *Cerebral Cortex*, *26*(8), 3402–3412. https://doi.org/10.1093/cercor/bhv170

Lee Masson, H., Kang, H. mook, Petit, L., & Wallraven, C. (2018). Neuroanatomical correlates of haptic object processing: combined evidence from tractography and functional neuroimaging. *Brain Structure and Function*, *223*(2), 619–633. https://doi.org/10.1007/s00429-017-1510-3

Lega, C., Chelazzi, L., & Cattaneo, L. (2019). Two distinct systems represent contralateral and ipsilateral sensorimotor processes in the human premotor cortex: A dense tms mapping study. *Cerebral Cortex*, *00*, 1–17. https://doi.org/10.1093/cercor/bhz237

Lehmann, S. J., & Scherberger, H. (2013). Reach and Gaze Representations in Macaque Parietal and Premotor Grasp Areas. *The Journal of Neuroscience*, *33*(16), 7038–7049. https://doi.org/10.1523/JNEUROSCI.5568-12.2013

Leoné, F. T. M., Monaco, S., Henriques, D. Y. P., Toni, I., & Medendorp, W. P. (2015). Flexible reference frames for grasp planning in human parietofrontal cortex. *ENeuro*, *2*(3), 1–15. https://doi.org/10.1523/ENEURO.0008-15.2015

Levi, D. M., & Klein, S. A. (1996). Limitations on position coding imposed by undersampling and univariance. *Vision Research*, *36*(14), 2111–2120. https://doi.org/10.1016/0042-6989(95)00264-2

Li, N., Daie, K., Svoboda, K., & Druckmann, S. (2016). Robust neuronal dynamics in premotor cortex during motor planning. *Nature*, *532*(7600), 459–464. https://doi.org/10.1038/nature17643

Lisanby, S. H., Gutman, D., Luber, B., Schroeder, C., & Sackeim, H. (2001). Sham TMS: Intracerebral Measurement of the Induced Electrical Field and the Induction of Motor-Evoked Potentials. *Biological Psychiatry*, *49*, 460–463. https://doi.org/10.1016/S1571-5078(08)00412-1

Livi, A., Lanzilotto, M., Maranesi, M., Fogassi, L., Rizzolatti, G., & Bonini, L. (2019). Agent-based representations of objects and actions in the monkey pre-supplementary motor area. *Proceedings of the National Academy of Sciences of the United States of America*, *116*(7), 2691–2700. https://doi.org/10.1073/pnas.1810890116

Lukos, J., Ansuini, C., & Santello, M. (2007). Choice of contact points during

multidigit grasping: Effect of predictability of object center of mass location. *Journal of Neuroscience*, *27*(14), 3894–3903. https://doi.org/10.1523/JNEUROSCI.4693-06.2007

Luppino, G., Matelli, M., & Camarda, R. (1993). Corticocortical Connections of Area F3 in the Macaque Monkey. *The Journal of Comparative Neurology*, *338*, 114–140.

Luppino, G., Rozzi, S., Calzavara, R., & Matelli, M. (2003). Prefrontal and agranular cingulate projections to the dorsal premotor areas F2 and F7 in the macaque monkey. *European Journal of Neuroscience*, *17*, 559–578. https://doi.org/10.1046/j.1460-9568.2003.02476.x

Mahon, B. Z., Milleville, S. C., Negri, G. A. L., Rumiati, R. I., Caramazza, A., & Martin, A. (2007). Action-Related Properties Shape Object Representations in the Ventral Stream. *Neuron*, *55*(3), 507–520. https://doi.org/10.1016/j.neuron.2007.07.011

Mantini, D., Hasson, U., Betti, V., Perrucci, M. G., Romani, G. L., Corbetta, M., Orban, G. A., & Vanduffel, W. (2012). Interspecies activity correlations reveal functional correspondence between monkey and human brain areas. *Nature Methods*, *9*(3), 277–282. https://doi.org/10.1038/nmeth.1868

Marangon, M., Kubiak, A., & Króliczak, G. (2016). Haptically Guided

Grasping. fMRI Shows Right-Hemisphere Parietal Stimulus Encoding, and Bilateral Dorso-Ventral Parietal Gradients of Object- and Action-Related Processing during Grasp Execution. *Frontiers in Human Neuroscience*, *9*(January), 1–19. https://doi.org/10.3389/fnhum.2015.00691

Martinez-trujillo, J. C., Medendorp, W. P., Wang, H., & Crawford, J. D. (2004). *Frames of Reference for Eye-Head Gaze Commands in Primate Supplementary Eye Fields*. *44*, 1057–1066.

Mathôt, S., Schreij, D., & Theeuwes, J. (2012). OpenSesame: An open-source, graphical experiment builder for the social sciences. *Behavior Research Methods*, *44*(2), 314–324. https://doi.org/10.3758/s13428-011-0168-7

Matsumura, M., Sawaguchi, T., Oishi, T., Ueki, K., & Kubota, K. (1991). Behavioral deficits induced by local injection of bicuculline and muscimol into the primate motor and premotor cortex. *Journal of Neurophysiology*, *65*(6), 1542–1553. https://doi.org/10.1152/jn.1991.65.6.1542

Maule, F., Barchiesi, G., Brochier, T., & Cattaneo, L. (2015). Haptic working memory for grasping: The role of the parietal operculum. *Cerebral Cortex*, *25*(2), 528–537. https://doi.org/10.1093/cercor/bht252

Mazzola, L., Faillenot, I., Barral, F. G., Mauguière, F., & Peyron, R. (2012). Spatial segregation of somato-sensory and pain activations in the human

operculo-insular cortex. *NeuroImage*, *60*(1), 409–418.

https://doi.org/10.1016/j.neuroimage.2011.12.072

McGuire, L. M. M., & Sabes, P. N. (2009). Sensory transformations and the use

of multiple reference frames for reach planning. *Nature Neuroscience*,

12(8), 1056–1061. https://doi.org/10.1038/nn.2357

Medendorp, W. P., Goltz, H. C., Vilis, T., & Crawford, J. D. (2003). Gaze-

Centered Updating of Visual Space in Human Parietal Cortex. *The Journal

of Neuroscience*, *23*(15), 6209–6214. https://doi.org/10.1523/jneurosci.23-

15-06209.2003

Merabet, L. B., Hamilton, R., Schlaug, G., Swisher, J. D., Kiriakopoulos, E. T.,

Pitskel, N. B., Kauffman, T., & Pascual-Leone, A. (2008). Rapid and

reversible recruitment of early visual cortex for touch. *PLoS ONE*, *3*(8),

e3046. https://doi.org/10.1371/journal.pone.0003046

Merabet, L. B., Swisher, J. D., McMains, S. A., Halko, M. A., Amedi, A.,

Pascual-Leone, A., & Somers, D. C. (2007). Combined activation and

deactivation of visual cortex during tactile sensory processing. *Journal of

Neurophysiology*, *97*(2), 1633–1641. https://doi.org/10.1152/jn.00806.2006

Mesulam, M. M. (1999). Spatial attention and neglect: Parietal, frontal and

cingulate contributions to the mental representation and attentional targeting

of salient extrapersonal events. *Philosophical Transactions of the Royal Society B: Biological Sciences*, *354*(1387), 1325–1346. https://doi.org/10.1098/rstb.1999.0482

Milner, A. D., & Goodale, M. A. (2008). Two visual systems re-viewed. *Neuropsychologia*, *46*(3), 774–785. https://doi.org/10.1016/j.neuropsychologia.2007.10.005

Mirabella, G., Pani, P., & Ferraina, S. (2011). Neural correlates of cognitive control of reaching movements in the dorsal premotor cortex of rhesus monkeys. *Journal of Neurophysiology*, *106*(3), 1454–1466. https://doi.org/10.1152/jn.00995.2010

Monaco, S., Gallivan, J. P., Figley, T. D., Singhal, A., & Culham, J. C. (2017). Recruitment of Foveal Retinotopic Cortex During Haptic Exploration of Shapes and Actions in the Dark. *The Journal of Neuroscience*, *37*(48), 11572–11591. https://doi.org/10.1523/JNEUROSCI.2428-16.2017

Monaco, S., Malfatti, G., Culham, J. C., Cattaneo, L., & Turella, L. (2020). Decoding motor imagery and action planning in the early visual cortex : Overlapping but distinct neural mechanisms. *NeuroImage*, *218*, 116981. https://doi.org/10.1016/j.neuroimage.2020.116981

Monaco, S., Sedda, A., Cavina-Pratesi, C., & Culham, J. C. (2015). Neural

correlates of object size and object location during grasping actions. *European Journal of Neuroscience*, *41*(4), 454–465. https://doi.org/10.1111/ejn.12786

Murata, A., Fadiga, L., Fogassi, L., Gallese, V., Raos, V., & Rizzolatti, G. (1997). Object representation in the ventral premotor cortex (Area F5) of the monkey. *Journal of Neurophysiology*, *78*(4), 2226–2230. https://doi.org/10.1152/jn.1997.78.4.2226

Murata, A., Gallese, V., Luppino, G., Kaseda, M., & Sakata, H. (2000). Selectivity for the shape, size, and orientation of objects for grasping in neurons of monkey parietal area AIP. *Journal of Neurophysiology*, *83*(5), 2580–2601. https://doi.org/10.1152/jn.2000.83.5.2580

Mushiake, H., Tanatsugu, Y., & Tanji, J. (1997). Neuronal Activity in the Ventral Part of Premotor Cortex During Target-Reach Movement is Modulated by Direction of Gaze. *Journal of Neurophysiology*, *78*(1), 567–571. https://doi.org/10.1152/jn.1997.78.1.567

Nachev, P., Kennard, C., & Husain, M. (2008). Functional role of the supplementary and pre-supplementary motor areas. *Nature Reviews*, *9*, 856–869. https://doi.org/10.1038/nrn2478

Nakayama, Y., Yamagata, T., Tanji, J., & Hoshi, E. (2008). Transformation of a

Virtual Action Plan into a Motor Plan in the Premotor Cortex. *Journal of Neuroscience*, *28*(41), 10287–10297. https://doi.org/10.1523/JNEUROSCI.2372-08.2008

Neggers, S. F. W., & Bekkering, H. (2000). Ocular gaze is anchored to the target of an ongoing pointing movement. *Journal of Neurophysiology*, *83*(2), 639–651. https://doi.org/https://doi.org/10.1152/jn.2000.83.2.639

Oliver, R., Bjoertomt, O., Driver, J., Greenwood, R., & Rothwell, J. C. (2009). Novel "hunting" method using transcranial magnetic stimulation over parietal cortex disrupts visuospatial sensitivity in relation to motor thresholds. *Neuropsychologia*, *47*(14), 3152–3161. https://doi.org/10.1016/j.neuropsychologia.2009.07.017

Olivier, E., Davare, M., Andres, M., & Fadiga, L. (2007). Precision grasping in humans: from motor control to cognition. *Current Opinion in Neurobiology*, *17*(6), 644–648. https://doi.org/10.1016/j.conb.2008.01.008

Orban, G. A. (2016). Functional definitions of parietal areas in human and non-human primates. *Proceedings of the Royal Society B: Biological Sciences*, *283*(1828). https://doi.org/10.1098/rspb.2016.0118

Padberg, J., Recanzone, G., Engle, J., Cooke, D., Goldring, A., & Krubitzer, L. (2010). Lesions in posterior parietal area 5 in monkeys result in rapid

behavioral and cortical plasticity. *Journal of Neuroscience*, *30*(39), 12918–12935. https://doi.org/10.1523/JNEUROSCI.1806-10.2010

Parmigiani, S., Barchiesi, G., & Cattaneo, L. (2015). The dorsal premotor cortex exerts a powerful and specific inhibitory effect on the ipsilateral corticofacial system: a dual-coil transcranial magnetic stimulation study. *Experimental Brain Research*, *233*(11), 3253–3260. https://doi.org/10.1007/s00221-015-4393-7

Peltier, S., Stilla, R., Mariola, E., Laconte, S., Hu, X., & Sathian, K. (2007). Activity and effective connectivity of parietal and occipital cortical regions during haptic shape perception. *Neuropsy*, *45*, 476–483. https://doi.org/10.1016/j.neuropsychologia.2006.03.003

Perini, F., Powell, T., Watt, S., & Downing, P. E. (2020). Neural representations of haptic object size in the human brain revealed by multivoxel fMRI patterns Francesca. *Journal of Neurophysiology*. https://doi.org/https://doi.org/10.1152/jn.00160.2020

Pesaran, B., Nelson, M. J., & Andersen, R. A. (2006). Dorsal Premotor Neurons Encode the Relative Position of the Hand, Eye, and Goal during Reach Planning. *Neuron*, *51*(1), 125–134. https://doi.org/10.1016/j.neuron.2006.05.025

Pettypiece, C. E., Goodale, M. A., & Culham, J. C. (2010). Integration of haptic and visual size cues in perception and action revealed through cross-modal conflict. *Experimental Brain Research*, *201*(4), 863–873. https://doi.org/10.1007/s00221-009-2101-1

Picht, T., Krieg, S. M., Sollmann, N., Rösler, J., Niraula, B., Neuvonen, T., Savolainen, P., Lioumis, P., Mäkelä, J. P., Deletis, V., Meyer, B., Vajkoczy, P., & Ringel, F. (2013). A comparison of language mapping by preoperative navigated transcranial magnetic stimulation and direct cortical stimulation during awake surgery. *Neurosurgery*, *72*(5), 808–819. https://doi.org/10.1227/NEU.0b013e3182889e01

Picht, T., Mularski, S., Kuehn, B., Vajkoczy, P., Kombos, T., & Suess, O. (2009). Navigated transcranial magnetic stimulation for preoperative functional diagnostics in brain tumor surgery. *Neurosurgery*, *65*(ONS Suppl 1), ons93–ons99. https://doi.org/10.1227/01.NEU.0000348009.22750.59

Picht, T., Schmidt, S., Brandt, S., Frey, D., Hannula, H., Neuvonen, T., Karhu, J., Vajkoczy, P., & Suess, O. (2011). Preoperative functional mapping for rolandic brain tumor surgery: Comparison of navigated transcranial magnetic stimulation to direct cortical stimulation. *Neurosurgery*, *69*(3), 581–588. https://doi.org/10.1227/NEU.0b013e3182181b89

Pietrini, P., Furey, M. L., Ricciardi, E., Gobbini, M. I., Wu, W. H. C., Cohen, L.

G., Guazzelli, M., & Haxby, J. V. (2004). Beyond sensory images: Object-based representation in the human ventral pathway. *Proceedings of the National Academy of Sciences of the United States of America*, *101*(15), 5658–5663. https://doi.org/10.1073/pnas.0400707101

Prado, J., Clavagnier, S., Otzenberger, H., Scheiber, C., Kennedy, H., & Perenin, M. T. (2005). Two Cortical Systems for Reaching in Central and Peripheral Vision. *Neuron*, *48*, 849–858. https://doi.org/10.1016/j.neuron.2005.10.010

Ptito, M., Fumal, A., Martens De Noordhout, A., Schoenen, J., Gjedde, A., & Kupers, R. (2008). TMS of the occipital cortex induces tactile sensations in the fingers of blind Braille readers. *Experimental Brain Research*, *184*(2), 193–200. https://doi.org/10.1007/s00221-007-1091-0

Rajkomar, A., Dean, J., & Kohane, I. (2019). Machine learning in medicine. *New England Journal of Medicine*, *380*(14), 1347–1358. https://doi.org/10.1056/NEJMra1814259

Rand, M. K., Lemay, M., Squire, L. M., Shimansky, Y. P., & Stelmach, G. E. (2007). Role of vision in aperture closure control during reach-to-grasp movements. *Experimental Brain Research*, *181*(3), 447–460. https://doi.org/10.1007/s00221-007-0945-9

Raos, V., Umilta, M., Murata, A., Fogassi, L., & Gallese, V. (2005). Functional Properties of Grasping-Related Neurons in the Ventral Premotor Area F5 of the Macaque Monkey. *Journal of Neurophysiology*, *95*, 709–729. https://doi.org/10.1152/jn.00463.2005.

Rauch, H. G. L., Schönbächler, G., & Noakes, T. D. (2013). Neural Correlates of Motor Vigour and Motor Urgency During Exercise. *Sports Med*, *43*, 227–241. https://doi.org/10.1007/s40279-013-0025-1

Reuschel, J., Rösler, F., Henriques, D. Y. P., & Fiehler, K. (2012). Spatial updating depends on gaze direction even after loss of vision. *Journal of Neuroscience*, *32*(7), 2422–2429. https://doi.org/10.1523/JNEUROSCI.2714-11.2012

Rice, N. J., Tunik, E., & Grafton, S. T. (2006). The anterior intraparietal sulcus mediates grasp execution, independent of requirement to update: New insights from transcranial magnetic stimulation. *Journal of Neuroscience*, *26*(31), 8176–8182. https://doi.org/10.1523/JNEUROSCI.1641-06.2006

Rizzolatti, G., Camarda, R., Fogassi, L., Gentilucci, M., Luppino, G., & Matelli, M. (1988). Functional organization of inferior area 6 in the macaque monkey - II. Area F5 and the control of distal movements. *Experimental Brain Research*, *71*(3), 491–507. https://doi.org/10.1007/BF00248742

Rizzolatti, Giacomo, Cattaneo, L., Fabbri-Destro, M., & Rozzi, S. (2014).

Cortical Mechanisms Underlying the Organization of Goal-Directed Actions

and Mirror Neuron-Based Action Understanding. *Physiological Reviews*,

94(2), 655–706. https://doi.org/10.1152/physrev.00009.2013

Rizzolatti, Giacomo, Gentilucci, M., Camarda, R. M., Gallese, V., Luppino, G.,

Matelli, M., & Fogassi, L. (1990). Neurons related to reaching-grasping arm

movements in the rostral part of area 6 (area 6aβ). *Experimental Brain*

Research, *82*(2), 337–350. https://doi.org/10.1007/BF00231253

Rizzolatti, Giacomo, & Luppino, G. (2001). The Cortical Motor System.

Neuron, *31*, 889–901.

Rizzolatti, Giacomo, Luppino, G., & Matelli, M. (1998). The Orgnaization of

the Cortical Motor System: New Concepts. *Electroencephalography and*

Clinical Neurophysiology, *106*, 283–296.

Rizzolatti, Giacomo, & Matelli, M. (2003). Two different streams form the

dorsal visual system: Anatomy and functions. *Experimental Brain Research*,

153(2), 146–157. https://doi.org/10.1007/s00221-003-1588-0

Roelfsema, P. R., & de Lange, F. P. (2016). Early Visual Cortex as a Multiscale

Cognitive Blackboard. *Annual Review of Vision Science*, *2*(1), 131–151.

https://doi.org/10.1146/annurev-vision-111815-114443

Rossi, S., Hallettb, M., Rossini, P. M., Pascual-Leone, A., & Group, T. S. of T.

    C. (2009). Safety, ethical considerations, and application guidelines for the

    use of transcranial magnetic stimulation in clinical practice and research.

    Clinical Neurophysiology, *120*(12), 2008–2039.

    https://doi.org/10.1016/j.clinph.2009.08.016.Rossi

Rossini, P. M., Burke, D., Chen, R., Cohen, L. G., Daskalakis, Z., Di Iorio, R.,

    Di Lazzaro, V., Ferreri, F., Fitzgerald, P. B., George, M. S., Hallett, M.,

    Lefaucheur, J. P., Langguth, B., Matsumoto, H., Miniussi, C., Nitsche, M.

    A., Pascual-Leone, A., Paulus, W., Rossi, S., … Ziemann, U. (2015). Non-

    invasive electrical and magnetic stimulation of the brain, spinal cord, roots

    and peripheral nerves: Basic principles and procedures for routine clinical

    and research application: An updated report from an I.F.C.N. Committee.

    Clinical Neurophysiology, *126*(6), 1071–1107.

    https://doi.org/10.1016/j.clinph.2015.02.001

Rozzi, S., Calzavara, R., Belmalih, A., Borra, E., Gregoriou, G. G., Matelli, M.,

    & Luppino, G. (2006). Cortical Connections of the Inferior Parietal Cortical

    Convexity of the Macaque Monkey. *Cerebral Cortex*, *16*, 1389–1417.

    https://doi.org/10.1093/cercor/bhj076

Rozzi, S., Ferrari, P. F., Bonini, L., Rizzolatti, G., & Fogassi, L. (2008).

    Functional organization of inferior parietal lobule convexity in the macaque

monkey: Electrophysiological characterization of motor, sensory and mirror responses and their correlation with cytoarchitectonic areas. *European Journal of Neuroscience*, *28*(8), 1569–1588. https://doi.org/10.1111/j.1460-9568.2008.06395.x

Ruben, J., Schwiemann, J., Deuchert, M., Meyer, R., Krause, T., Curio, G., Villringer, K., Kurth, R., & Villringer, A. (2001). Somatotopic organization of human secondary somatosensory cortex. *Cerebral Cortex*, *11*(5), 463–473. https://doi.org/10.1093/cercor/11.5.463

Sack, A. T., Cohen Kadosh, R., Schuhmann, T., Moerel, M., Walsh, V., & Goebel, R. (2008). Optimizing Functional Accuracy of TMS in Cognitive Studies: A Comparison of Methods. *Journal of Cognitive Neuroscience*, *21*(2), 207–221. https://doi.org/10.1162/jocn.2009.21126

Sadato, N., Okada, T., Honda, M., & Yonekura, Y. (2002). Critical period for cross-modal plasticity in blind humans: A functional MRI study. *NeuroImage*, *16*(2), 389–400. https://doi.org/10.1006/nimg.2002.1111

Sadato, N., Pascual-Leone, A., Grafman, J., Ibañez, V., Deiber, M. P., Dold, G., & Hallett, M. (1996). Activation of the primary visual cortex by Braille reading in blind subjects. In *Nature* (Vol. 380, Issue 6574, pp. 526–528). https://doi.org/10.1038/380526a0

Sakai, K., Hikosaka, O., Miyauchi, S., Sasaki, Y., Fujimaki, N., & Pütz, B.

(1999). Presupplementary Motor Area Activation during Sequence Learning

Reflects Visuo-Motor Association. *The Journal of Neuroscience*, *19*, 1–6.

Sakata, H., Taira, M., Murata, A., & Mine, S. (1995). Neural Mechanisms of

Visual Guidance of Hand Action in the Parietal Cortex of the Monkey.

Cerebral Cortex, *5*(5), 429–438. https://doi.org/10.1093/cercor/5.5.429

Salatino, A., Poncini, M., George, M. S., & Ricci, R. (2014). Hunting for right

and left parietal hot spots using single-pulse TMS: Modulation of

visuospatial perception during line bisection judgment in the healthy brain.

Frontiers in Psychology, *5*, 1–7. https://doi.org/10.3389/fpsyg.2014.01238

Santandrea, E., Breveglieri, R., Bosco, A., Galletti, C., & Fattori, P. (2018).

Preparatory activity for purposeful arm movements in the dorsomedial

parietal area V6A: Beyond the online guidance of movement. *Scientific

Reports*, *8*(1), 1–16. https://doi.org/10.1038/s41598-018-25117-0

Santello, M., Bianchi, M., Gabiccini, M., Ricciardi, E., Salvietti, G.,

Prattichizzo, D., Ernst, M., Moscatelli, A., Jörntell, H., Kappers, A. M. L.,

Kyriakopoulos, K., Albu-Schäffer, A., Castellini, C., & Bicchi, A. (2016).

Hand synergies: Integration of robotics and neuroscience for understanding

the control of biological and artificial hands. *Physics of Life Reviews*, *17*, 1–

23. https://doi.org/10.1016/j.plrev.2016.02.001

Santello, M., Flanders, M., & Soechting, J. F. (1998). Postural hand synergies

for tool use. *Journal of Neuroscience*, *18*(23), 10105–10115.

https://doi.org/10.1523/jneurosci.18-23-10105.1998

Santello, M., & Soechting, J. F. (1997). Matching object size by controlling

finger span and hand shape. *Somatosensory and Motor Research*, *14*(3),

203–212. https://doi.org/10.1080/08990229771060

Santello, M., & Soechting, J. F. (1998). Gradual Molding of the Hand to Object

Contours. *Journal of Neurophysiology*, *79*, 1307–1320.

Santello, M., & Soechting, J. F. (2000). Force synergies for multifingered

grasping. *Experimental Brain Research*, *133*(4), 457–467.

https://doi.org/10.1007/s002210000420

Sartori, L., Camperio Ciani, A., Bulgheroni, M., & Castiello, U. (2013).

Reaching and grasping behavior in Macaca fascicularis: A kinematic study.

Experimental Brain Research, *224*(1), 119–124.

https://doi.org/10.1007/s00221-012-3294-2

Sathian, K. (2005). Visual cortical activity during tactile perception in the

sighted and the visually deprived. *Developmental Psychobiology*, *46*(3),

279–286. https://doi.org/10.1002/dev.20056

Sathian, K. (2016). Analysis of haptic information in the cerebral cortex.

Journal of Neurophysiology, *116*, 1795–1806.

https://doi.org/10.1152/jn.00546.2015

Schaeffner, L. F., & Welchman, A. E. (2017). Mapping the visual brain areas
susceptible to phosphene induction through brain stimulation. *Experimental
Brain Research*, *235*(1), 205–217. https://doi.org/10.1007/s00221-016-
4784-4

Schettino, L. F., Adamovich, S. V., & Poizner, H. (2003). Effects of object
shape and visual feedback on hand configuration during grasping.
Experimental Brain Research, *151*(2), 158–166.
https://doi.org/10.1007/s00221-003-1435-3

Schlicht, E. J., & Schrater, P. R. (2007). Effects of visual uncertainty on
grasping movements. *Experimental Brain Research*, *182*, 47–57.
https://doi.org/10.1007/s00221-007-0970-8

Schubotz, R. I., & Von Cramon, D. Y. (2003). Functional-anatomical concepts
of human premotor cortex: Evidence from fMRI and PET studies.
NeuroImage, *20*(SUPPL. 1), 120–131.
https://doi.org/10.1016/j.neuroimage.2003.09.014

Sereno, M. I., & Tootell, R. B. H. (2005). From monkeys to humans: What do
we now know about brain homologies? *Current Opinion in Neurobiology*,

15(2), 135–144. https://doi.org/10.1016/j.conb.2005.03.014

Shinoura, N., Suzuki, Y., Yamada, R., Tabei, Y., Saito, K., & Yagi, K. (2009).

Damage to the right superior longitudinal fasciculus in the inferior parietal

lobe plays a role in spatial neglect. *Neuropsychologia*, *47*(12), 2600–2603.

https://doi.org/10.1016/j.neuropsychologia.2009.05.010

Silverstein, J. (2012). Mapping the motor and sensory cortices: A historical look

and a current case study in sensorimotor localization and direct cortical

motor stimulation. *Neurodiagnostic Journal*, *52*(1), 54–68.

https://doi.org/10.1080/21646821.2012.11079843

Simone, L. K., Sundarrajan, N., Luo, X., Jia, Y., & Kamper, D. G. (2007). A

low cost instrumented glove for extended monitoring and functional hand

assessment. *Journal of Neuroscience Methods*, *160*(2), 335–348.

https://doi.org/10.1016/j.jneumeth.2006.09.021

Sivak, B., & MacKenzie, C. L. (1990). Integration of visual information and

motor output in the reaching and grasping: the contributions of peripheral

and central vision. *Neuropsychologia*, *28*(10), 1095–1116.

Snow, J. C., Strother, L., & Humphreys, G. W. (2014). Haptic Shape Processing

in Visual Cortex. *Journal of Cognitive Neuroscience*, *26*(5), 1154–1167.

https://doi.org/10.1162/jocn

Stoeckel, C., Gough, P. M., Watkins, K. E., & Devlin, J. T. (2009).

  Supramarginal gyrus involvement in visual word recognition. *Cortex*, *45*(9),

  1091–1096. https://doi.org/10.1016/j.cortex.2008.12.004.Supramarginal

Styrkowiec, P. P., Nowik, A. M., & Króliczak, G. (2019). The neural

  underpinnings of haptically guided functional grasping of tools: An fMRI

  study. *NeuroImage*, *194*(March), 149–162.

  https://doi.org/10.1016/j.neuroimage.2019.03.043

Tanné-Gariépy, J., Rouiller, E. M., & Boussaoud, D. (2002). Parietal inputs to

  dorsal versus ventral premotor areas in the macaque monkey: Evidence for

  largely segregated visuomotor pathways. *Experimental Brain Research*,

  145(1), 91–103. https://doi.org/10.1007/s00221-002-1078-9

Tarapore, P. E., Picht, T., Bulubas, L., Shin, Y., Kulchytska, N., Meyer, B.,

  Berger, M. S., Nagarajan, S. S., & Krieg, S. M. (2016). Safety and

  tolerability of navigated TMS for preoperative mapping in neurosurgical

  patients. *Clinical Neurophysiology*, *127*(3), 1895–1900.

  https://doi.org/10.1016/j.clinph.2015.11.042

Tarapore, P. E., Picht, T., Bulubas, L., Shin, Y., Kulchytska, N., Meyer, B.,

  Nagarajan, S. S., & Krieg, S. M. (2016). Safety and tolerability of navigated

  TMS in healthy volunteers. *Clinical Neurophysiology*, *127*(3), 1916–1918.

  https://doi.org/10.1016/j.clinph.2015.11.043

Thickbroom, G. W., Byrnes, M. L., Archer, S. A., & Mastaglia, F. L. (2004). Motor outcome after subcortical stroke correlates with the degree of cortical reorganization. *Clinical Neurophysiology*, *115*(9), 2144–2150. https://doi.org/10.1016/j.clinph.2004.04.001

Tretriluxana, J., Gordon, J., & Winstein, C. J. (2008). Manual asymmetries in grasp pre-shaping and transport – grasp coordination. *Experimental Brain Research*, *188*, 305–315. https://doi.org/10.1007/s00221-008-1364-2

Tunik, E., Frey, S. H., & Grafton, S. T. (2005). Virtual lesions of the anterior intraparietal area disrupt goal-dependent on-line adjustments of grasp. *Nature Neuroscience*, *8*(4), 505–511. https://doi.org/10.1038/nn1430

Turella, L., & Lingnau, A. (2014). Neural correlates of grasping. *Frontiers in Human Neuroscience*, *8*, 1–8. https://doi.org/10.3389/fnhum.2014.00686

Turella, L., Tucciarelli, R., Oosterhof, N. N., Weisz, N., Rumiati, R., & Lingnau, A. (2016). Beta band modulations underlie action representations for movement planning. *NeuroImage*, *136*, 197–207. https://doi.org/10.1016/j.neuroimage.2016.05.027

Van Donkelaar, P., & Adams, J. (2005). Gaze-dependent deviation in pointing induced by transcranial magnetic stimulation over the human posterior parietal cortex. *Journal of Motor Behavior*, *37*(2), 157–163.

https://doi.org/10.3200/JMBR.37.2.157-163

van Ede, F., Chekroud, S. R., Stokes, M. G., & Nobre, A. C. (2019). Concurrent visual and motor selection during visual working memory guided action. *Nature Neuroscience*, *22*(3), 477–483. https://doi.org/10.1038/s41593-018-0335-6

Verhagen, L., Chris Dijkerman, H., Pieter Medendorp, W., & Toni, I. (2012). Cortical dynamics of sensorimotor integration during grasp planning. *Journal of Neuroscience*, *32*(13), 4508–4519. https://doi.org/10.1523/JNEUROSCI.5451-11.2012

Verhagen, L., Dijkerman, H. C., Grol, M. J., & Toni, I. (2008). Perceptuo-motor interactions during prehension movements. *Journal of Neuroscience*, *28*(18), 4726–4735. https://doi.org/10.1523/JNEUROSCI.0057-08.2008

Vernet, M., Quentin, R., Chanes, L., Mitsumasu, A., & Valero-cabré, A. (2014). Frontal eye field , where art thou ? Anatomy , function , and non-invasive manipulation of frontal regions involved in eye movements and associated cognitive operations. *Frontiers in Integrative Neuroscience*, *8*, 1–24. https://doi.org/10.3389/fnint.2014.00066

Vesia, M., Barnett-Cowan, M., Elahi, B., Jegatheeswaran, G., Isayama, R., Neva, J. L., Davare, M., Staines, W. R., Culham, J. C., & Chen, R. (2017).

Human dorsomedial parieto-motor circuit specifies grasp during the planning of goal-directed hand actions. *Cortex*, *92*, 175–186. https://doi.org/10.1016/j.cortex.2017.04.007

Vesia, M., Culham, J. C., Jegatheeswaran, G., Isayama, R., Le, A., Davare, M., & Chen, R. (2018). Functional interaction between human dorsal premotor cortex and the ipsilateral primary motor cortex for grasp plans: A dual-site TMS study. *NeuroReport*, *29*(16), 1355–1359. https://doi.org/10.1097/WNR.0000000000001117

Vesia, M., Prime, S. L., Yan, X., Sergio, L. E., & Crawford, J. D. (2010). Specificity of human parietal saccade and reach regions during transcranial magnetic stimulation. *Journal of Neuroscience*, *30*(39), 13053–13065. https://doi.org/10.1523/JNEUROSCI.1644-10.2010

Vuilleumier, P. (2013). Mapping the functional neuroanatomy of spatial neglect and human parietal lobe functions: Progress and challenges. *Annals of the New York Academy of Sciences*, *1296*(1), 50–74. https://doi.org/10.1111/nyas.12161

Wang, R. F. (2012). Theories of spatial representations and reference frames: What can configuration errors tell us ? *Psychonomic Bulletin and Review*, *19*, 575–587. https://doi.org/10.3758/s13423-012-0258-2

Whitaker, D. (1997). Disentangling theRoleof Spatial Scale, Separation and

    Eccentricityin Weber's Law for Position. *Vision Research*, *37*(5), 515–524.

Wilson, B. A., Berry, E., Gracey, F., Harrison, C., Stow, I., Macniven, J.,

    Weatherley, J., & Young, A. W. (2005). Egocentric disorientation following

    bilateral parietal lobe damage. *Cortex*, *41*(4), 547–554.

    https://doi.org/10.1016/S0010-9452(08)70194-1

Wing, A. M., Turton, A., & Fraser, C. (1986). Grasp Size and Accuracy of

    Approach in Reaching. *Journal of Motor Behavior*, *18*(3), 245–260.

    https://doi.org/10.1080/00222895.1986.10735380

Winges, S. A., Weber, D. J., & Santello, M. (2003). The role of vision on hand

    preshaping during reach to grasp. *Experimental Brain Research*, *152*(4),

    489–498. https://doi.org/10.1007/s00221-003-1571-9

Wise, S. P., Boussaoud, D., Johnson, P. B., & Caminiti, R. (1997). Premotor and

    parietal cortex: Corticocortical connectivity and combinatorial

    computations. *Annual Review of Neuroscience*, *20*, 25–42.

    https://doi.org/10.1146/annurev.neuro.20.1.25

Wong, T. T. (2015). Performance evaluation of classification algorithms by k-

    fold and leave-one-out cross validation. *Pattern Recognition*, *48*(9), 2839–

    2846. https://doi.org/10.1016/j.patcog.2015.03.009

Yau, J. M., Kim, S. S., Thakur, P. H., & Bensmaia, S. J. (2016). Feeling form:

The neural basis of haptic shape perception. *Journal of Neurophysiology*,

115(2), 631–642. https://doi.org/10.1152/jn.00598.2015

Zoia, S., Pezzetta, E., Blason, L., SCabar, A., Carrozzi, M., Bulgheroni, M., &

Castiello, U. (2006). A Comparison of the Reach-To-Grasp Movement

Between Children and Adults: A Kinematic Study. *Developmental*

Neuropsychology, *30*(2), 719–738.

https://doi.org/10.1207/s15326942dn3002